BENZOYLFORMATE DECARBOXYLASE FROM *PSEUDOMONAS STUTZERI* ST-201: GENE CLONING, ENZYME CHARACTERIZATION AND ROLE IN D-PHENYLGLYCINE DEGRADATION

CHOEDCHAI SAEHUAN

A THESIS SUBMITTED IN PARTIAL FULFILLMENT
OF THE REQUIREMENTS FOR
THE DEGREE OF DOCTOR OF PHILOSOPHY
(MICROBIOLOGY)
FACULTY OF GRADUATE STUDIES
MAHIDOL UNIVERSITY
2007

Thesis

Entitled

BENZOYLFORMATE DECARBOXYLASE FROM PSEUDOMONAS STUTZERI ST-201: GENE CLONING, ENZYME CHARACTERIZATION AND ROLE IN D-PHENYLGLYCINE DEGRADATION

……
Mr. Choedchai Saehuan
Candidate

……
Prof. Vithaya Meevootisom, Ph.D.
Major-Advisor

……
Assoc. Prof. Pimchai Chaiyen, Ph.D.
Co-Advisor

……
Assoc. Prof. Sarawut Jitrapakdee, Ph.D.
Co-Advisor

……
Assist. Prof. Suthep Wiyakrutta, Ph.D.
Co-Advisor

……..
Prof. Banchong Mahaisavariya, M.D.
Dean
Faculty of Graduate Studies

……
Prof. Vithaya Meevootisom, Ph.D.
Chair
Doctor of Philosophy
Programme in Microbiology
Faculty of Science

Thesis

Entitled

BENZOYLFORMATE DECARBOXYLASE FROM PSEUDOMONAS STUTZERI ST-201: GENE CLONING, ENZYME CHARACTERIZATION AND ROLE IN D-PHENYLGLYCINE DEGRADATION

was submitted to the Faculty of Graduate Studies, Mahidol University

for the degree of Doctor of Philosophy (Microbiology)

on

December 20, 2007

……
Mr. Choedchai Saehuan
Candidate

……
Prof. Vithaya Meevootisom, Ph.D.
Member

……
Assoc. Prof. Nongluksna Sriubolmas
Chair

……
Assoc. Prof. Pimchai Chaiyen, Ph.D.
Member

……
Assoc. Prof. Sarawut Jitrapakdee, Ph.D.
Member

……
Assist. Prof. Suthep Wiyakrutta, Ph.D.
Member

……
Michael J. McLeish, Ph.D.
Member

……..
Prof. Banchong Mahaisavariya, M.D.
Dean
Faculty of Graduate Studies
Mahidol University

……
Prof. Skorn Mongkolsuk, Ph.D.
Dean
Faculty of Science
Mahidol University

ACKNOWLEDGEMENTS

I would like to express my sincere gratitude and deep appreciation to Prof. Vithaya Meevootisom, my major advisor for invaluable guidance, supervision and encouragement throughout this study. Equally, I am grateful attitude to Assist. Prof. Suthep Wiyakrutta, my co-advisor, for his guidance, comments, suggestions and discussion.

I also would like to thank Dr. Michael J. McLeish and Prof. George L. Kenyon (University of Michigan, USA) for their creative guidance, continuous discussion and especially for their support and kindness while I was doing a part of the thesis in USA.

I also wish to sincerely thank Assist. Prof. Theerasak Rojanarata and Duangnate Isarangkul Na Ayudhaya for their endless kindness and helpful guidance. My thankfulness is to Dr. Poramaet Laowanapiban, all of B600 and B601 members and other people who have not been mentioned here for their kind help and friendship during my study.

Of the most importance, I greatly appreciate my mother, my sister and my brother for their loves, understanding, support and encouragement in every way possible to enable me to succeed in my education.

Lastly, I am particularly indebted to Institutional Strengthening Programme of Faculty of Science, Mahidol University (2000-2002), Thesis Scholarship from the Commission on Higher Education and Faculty of Graduate Studies, Mahidol University (2004) and the Royal Golden Jubilee Ph.D. Programme, Thailand Research Fund (2005-2007) that enabled me to have a wonderful opportunity for my study.

Choedchai Saehuan

BENZOYLFORMATE DECARBOXYLASE FROM PSEUDOMONAS STUTZERI ST-201: GENE CLONING, ENZYME CHARACTERIZATION AND ROLE IN D-PHENYLGLYCINE DEGRADATION

CHOEDCHAI SAEHUAN 4336653 SCMI/D

Ph.D. (MICROBIOLOGY)

THESIS ADVISORS: VITHAYA MEEVOOTISOM, Ph.D.,
SUTHEP WIYAKRUTTA, Ph.D., PIMCHAI CHAIYEN, Ph.D.,
SARAWUT JITRAPAKDEE, Ph.D.

ABSTRACT

In this study, the role in D-phenylglycine degradation, gene cloning, expression, purification and characterization of a benzoylformate decarboxylase from *Pseudomonas stutzeri* ST-201 (*Ps*BFDC) were investigated. Following induction with D-phenylglycine, both D-phenylglycine aminotransferase and then BFDC activity were detected in cultures of *P. stutzeri* ST-201. Induction with benzoylformate, on the other hand, induced only BFDC activity. Sequential expression of the enzymes demonstrated the role of BFDC in the pathway in a step following D-phenylglycine degradation. Purification and N-terminal sequencing of *Ps*BFDC enabled the design of probes for hybridization in gene cloning. Sequencing of one genomic DNA restriction fragment revealed an open reading frame designated as *dpgB* which encoded *Ps*BFDC. Sequence alignment also suggested that the gene encoded a thiamin-diphosphate dependent enzyme. A *dpgB* gene which consisted of 1,581 bps of nucleotides and encoded a polypeptide of 526 amino acids was expressed with pET17b in *Escherichia coli* BL21 (DE3) and purified to homogeneity in a series of steps including ammonium sulfate fractionation, followed by Phenyl Sepharose FF hydrophobic interaction chromatography, ultrafiltration and Q-Sepharose FF anion-exchange chromatography with specific activity of 243 U mg^{-1}. Molecular weight (M_r) of the native *Ps*BFDC was estimated to be 224 kDa whereas M_r of the enzyme subunit was approximately 56 kDa. This indicated that the enzyme associated as a homotetramer. The isoelectric point (p*I*) of the enzyme was 5.2. The temperature and pH for maximal activity were 35-50 ^{o}C and 6.0, respectively. K_m value for benzoylformate was 0.69 mM and k_{cat} value was 222 s^{-1}. In addition to *Ps*BFDC, in this study a gene encoding a NAD^+/$NADP^+$-dependent benzaldehyde dehydrogenase (*Ps*BADH) denoted *dpgC* was cloned and expressed. Both *Ps*BFDC and *Ps*BADH had high sequence identities (both greater than 85%) and kinetic properties similar to those of the homologous enzymes in the mandelate pathway of *P. putida* ATCC 12633. However, *P. stutzeri* ST-201 was unable to grow on either isomer of mandelate, and sequencing indicated that the *dpgB* gene did not form part of an operon. Thus it appears that the two enzymes form part of a D-phenylglycine, rather than mandelate, degradation pathway.

KEY WORDS: BENZOYLFORMATE DECARBOXYLASE/ PSEUDOMONAS STUTZERI ST-201/ GENE CLONING/ CHARACTERIZATION/ D-PHENYLGLYCINE DEGRADATION PATHWAY

103 pp.

เอนไซม์เบนโซอิลฟอร์เมต ดีคาร์บอกซิเลส จาก Pseudomonas stutzeri ST-201: การโคลนยีน การศึกษาคุณสมบัติของเอนไซม์ และบทบาทของเอนไซม์ในการย่อยสลายดี-ฟีนิลกลัยซีน
(BENZOYLFORMATE DECARBOXYLASE FROM PSEUDOMONAS STUTZERI ST-201: GENE CLONING, ENZYME CHARACTERIZATION AND ROLE IN D-PHENYLGLYCINE DEGRADATION)

เชิดชาย แซ่ฮ่วน 4336653 SCMI/D

ปร.ด. (จุลชีววิทยา)

คณะกรรมการควบคุมวิทยานิพนธ์: วิทยา มีวุฒิสม, Ph.D., สุเทพ ไวยครุฑธา, Ph.D., พิมพ์ใจ ใจเย็น, Ph.D., ศราวุฒิ จิตรภักดี, Ph.D.,

บทคัดย่อ

การศึกษานี้รายงานบทบาทของเอนไซม์เบนโซอิลฟอร์เมต ดีคาร์บอกซิเลส (*Ps*BFDC) ใน *Pseudomonas stutzeri* ST-201 ในการย่อยสลายดี-ฟีนิลกลัยซีน รวมถึงการโคลนยีน การทำให้ยีนแสดงออก การทำเอนไซม์ให้บริสุทธิ์ และการศึกษาคุณสมบัติของเอนไซม์ โดยพบว่า *P. stutzeri* ST-201 สร้างเอนไซม์ดี-ฟีนิลกลัยซีน อะมิโนทรานสเฟอเรส และตามด้วย *Ps*BFDC ในเวลาต่อมาเมื่อถูกชักนำด้วยดี-ฟีนิลกลัยซีน แต่แบคทีเรียชนิดนี้สร้างเพียง *Ps*BFDC เท่านั้นเมื่อถูกชักนำด้วยเบนโซอิลฟอร์เมต ผลที่ได้แสดงให้เห็นว่า *Ps*BFDC มีบทบาทในขั้นตอนต่อจากการย่อยสลายดี-ฟีนิลกลัยซีน เมื่อแยก *Ps*BFDC จาก *P. stutzeri* ST-201 และทำให้บริสุทธิ์แล้ว นำไปหาลำดับของกรดอะมิโนด้านปลาย N เพื่อใช้ออกแบบ probe สำหรับทำ hybridization ในการโคลนยีน ได้ชิ้นดีเอนเอที่มี open reading frame ให้ชื่อว่า *dpgB* เป็นรหัสสำหรับเอนไซม์ *Ps*BFDC ซึ่งเมื่อทำ sequence alignment พบว่ามีความคล้ายคลึงกับยีนในกลุ่ม thiamin-diphosphate dependent enzymes ยีน *dpgB* นี้ประกอบด้วยนิวคลีโอไทด์ 1,581 คู่เบส และสร้างโพลีเปปไทด์ที่ประกอบด้วยกรดอะมิโน 526 ตัว เมื่อนำยีนนี้ซึ่งโคลนอยู่ในเวกเตอร์ pET17b ไปทำให้เกิดแสดงออกใน *Escherichia coli* BL21 (DE3) แล้วนำเอนไซม์ที่ได้ไปผ่านกระบวนการทำให้บริสุทธิ์ซึ่งประกอบด้วยการตกตะกอนโปรตีนด้วย ammonium sulfate ต่อด้วย Phenyl Sepharose FF hydrophobic interaction chromatography, ultrafiltration และ Q-Sepharose FF anion-exchange chromatography ในที่สุดได้เอนไซม์บริสุทธิ์ที่มี specific activity เท่ากับ 243 U mg^{-1} น้ำหนักโมเลกุลของ native *Ps*BFDC มีค่าประมาณ 224 kDa และหน่วยย่อยของเอนไซม์มีน้ำหนัก 56 kDa นั่นคือเอนไซม์ชนิดนี้ประกอบด้วยหน่วยย่อยที่เหมือนกัน 4 หน่วย เอนไซม์มี isoelectric point (p*I*) ที่ 5.2 ทำงานได้ดีที่สุดในช่วง 35-50 ^{o}C pH 6.0 ค่า K_m สำหรับเบนโซอิลฟอร์เมตคือ 0.69 mM และค่า k_{cat} คือ 222 s^{-1} การศึกษาครั้งนี้ยังสามารถโคลนยีนสำหรับ NAD^+/$NADP^+$-dependent benzaldehyde dehydrogenase จาก *P. stutzeri* ST-201(*Ps*BADH) ซึ่งให้ชื่อว่ายีน *dpgC* และทำให้เกิดการแสดงออกของยีนได้ เมื่อเปรียบเทียบกับเอนไซม์ในวิถีการย่อยสลายแมนดีเลต พบว่าทั้งเอนไซม์ *Ps*BFDC และ *Ps*BADH มีความคล้ายคลึงทั้งในแง่ลำดับกรดอะมิโน (มากกว่า 85% identity) และคุณสมบัติทางจลนศาสตร์กับ homologous enzymes ที่พบใน *P. putida* ATCC 12633 อย่างไรก็ตามเนื่องจาก *P. stutzeri* ST-201 ไม่สามารถเจริญเติบโตได้โดยใช้แมนดีเลต อีกทั้งยีน *dpgB* ก็มิได้เป็นส่วนหนึ่งของโอเปอรอน ดังนั้นเอนไซม์ *Ps*BFDC และ *Ps*BADH ใน *P. stutzeri* ST-201 น่าจะทำหน้าที่ในวิถีการย่อยสลายดี-ฟีนิลกลัยซีน แทนที่จะเป็นวิถีการย่อยสลายแมนดีเลต

103 หน้า

CONTENTS

CONTENTS (CONTINUED)

CONTENTS (CONTINUED)

Page

CONTENTS (CONTINUED)

Page

CONTENTS (CONTINUED)

Page

CONTENTS (CONTINUED)

Page

LIST OF TABLES

Page

LIST OF FIGURES

LIST OF FIGURES (CONTINUED)

Page

LIST OF FIGURES (CONTINUED)

Page

LIST OF FIGURES (CONTINUED)

Page

LIST OF ABBREVIATIONS

A, G, C, T	adenine, guanine, cytocine, thymine
BADH	benzaldehyde dehydrogenase
BFDC	benzoylformate decarboxylase
bp	base pair
°C	degree Celsius
CFE	cell-free extract
Da	Dalton
dpgA	gene encoding for D-phenylglycine aminotransferase in *Pseudomonas stutzeri* ST-201
dpgB	gene encoding for benzoylformate decarboxylase in *Pseudomonas stutzeri* ST-201
dpgC	gene encoding for benzaldehyde dehydrogenase in *Pseudomonas stutzeri* ST-201
D-PhgAT	D-phenylglycine aminotransferase
DNA	deoxyribonucleic acid
DTT	dithiothreitol
e.g.	for example
et al.	et alii (latin), and others
g	gram
h	hour
HIC	hydrophobic interaction chromatography
i.e.	id est (latin), that is
k_{cat}	catalytic constant, turnover number
K_m	Michaelis-Menten constant
l	liter
M	Molar (concentration)
ml	milliliter
min	minute
NAD	nicotinamide adenine dinucleotide

LIST OF ABBREVIATIONS (CONTINUED)

NADP	nicotinamide adenine dinucleotide phosphate
nt	nucleotide
PCR	polymerase chain reaction
*Pa*BFDC	benzoylformate decarboxylase from *Pseudomonas aeruginosa* PAO1
PDC	pyruvate decarboxylase
PLP	pyridoxal-5′-phosphate
*Pp*BADH	benzaldehyde dehydrogenase from *Pseudomonas putida* ATCC 12633
*Pp*BFDC	benzoylformate decarboxylase from *Pseudomonas putida* ATCC 12633
*Ps*BADH	benzaldehyde dehydrogenase from *Pseudomonas stutzeri* ST-201
*Ps*BFDC	benzoylformate decarboxylase from *Pseudomonas stutzeri* ST-201
rpm	round/revolution per minute
SDS-PAGE	sodium dodecyl sulfate polyacrylamide gel electrophoresis
sec	second
ThDP	thiamin diphosphate
UV	ultraviolet
µl	microliter
wt	wild type

CHAPTER 1
INTRODUCTION

1. Introduction

Benzoylformate decarboxylase (BFDC; EC 4.1.1.7) is a thiamin diphosphate (ThDP)-dependent enzyme that catalyzes both non-oxidative decarboxylation of benzoylformate forming benzaldehyde and carbon dioxide (1) (Figure 1A) and carboligation (C-C bond formation) enabling the conversion of aldehydes to chiral 2-hydroxy ketones, which are versatile building blocks for a variety of different fine chemicals (Figure 1B).

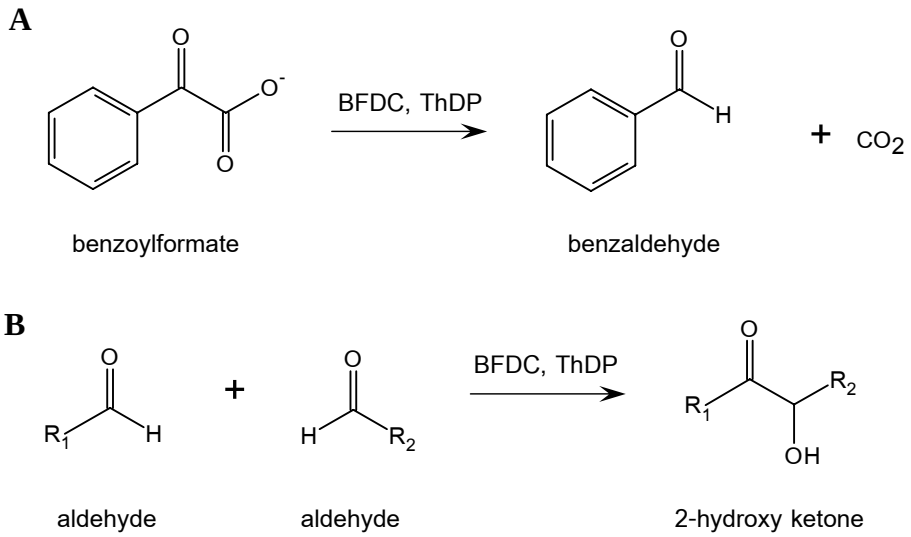

Figure 1. Decarboxylation (A) and carboligation (B) reactions catalyzed by BFDC.

BFDC was initially identified as one of the enzymes in the mandelate pathway, which enables bacteria to utilize mandelate as a sole carbon source by converting it to benzoic acid, which is then metabolized via the β-ketoadipate pathway and the citric acid cycle. In this pathway, benzoylformate is formed via the oxidation of *S*-mandelate (Figure 2) (2-4). To date, the enzyme has been found in *Pseudomonas, Acinetobacter*

species (5, 6), and *Neurospora crassa* (7), with the most detailed studies being carried out on the BFDC from *Pseudomonas putida* ATCC 12633 (*Pp*BFDC). These include enzyme purification and characterization (3, 4), gene cloning (8), kinetic and mechanistic studies (9-11), and X-ray crystallography (12, 13). Over the past few years *Pp*BFDC has become increasingly useful for the synthesis of enantiomerically pure pharmaceutical and chemical compounds (14-16). Consequently, there is a commercial interest in identifying BFDCs with an expanded substrate range whether by protein engineering (17-19) or from alternative sources such as metagenomic libraries (20).

Benzoylformate was reported as a product of the reaction catalyzed by D-phenylglycine aminotransferase (D-PhgAT) in *P. stutzeri* ST-201, a soil bacterium isolated in Thailand (21). Later, the gene encoding D-phgAT (*dpgA*) was cloned and expressed in *E. coli*. In those studies, *P. stutzeri* ST-201 had not been reported to possess BFDC, however, it had been shown to release both benzoylformate and benzoate into the culture medium during the early stages of D-phenylglycine degradation (21). Therefore it was reasonable to hypothesize that this strain probably produce not only BFDC, but also another related enzyme namely benzaldehyde dehydrogenase (BADH) for subsequent metabolism of benzoylformate and benzaldehyde, respectively. Here, we successfully prove the presence of BFDC in *P. stutzeri* ST-201 (*Ps*BFDC) and the role of *Ps*BFDC in D-phenylglycine degradation. Not only the gene encoding *Ps*BFDC (*dpgB*) but also the gene for *Ps*BADH *(dpgC)* have been cloned and expressed in *E. coli* and their gene products have been characterized. Moreover, we suggest that both enzymes form part of a catabolic pathway, which was termed the D-phenylglycine degradation pathway (Figure 2).

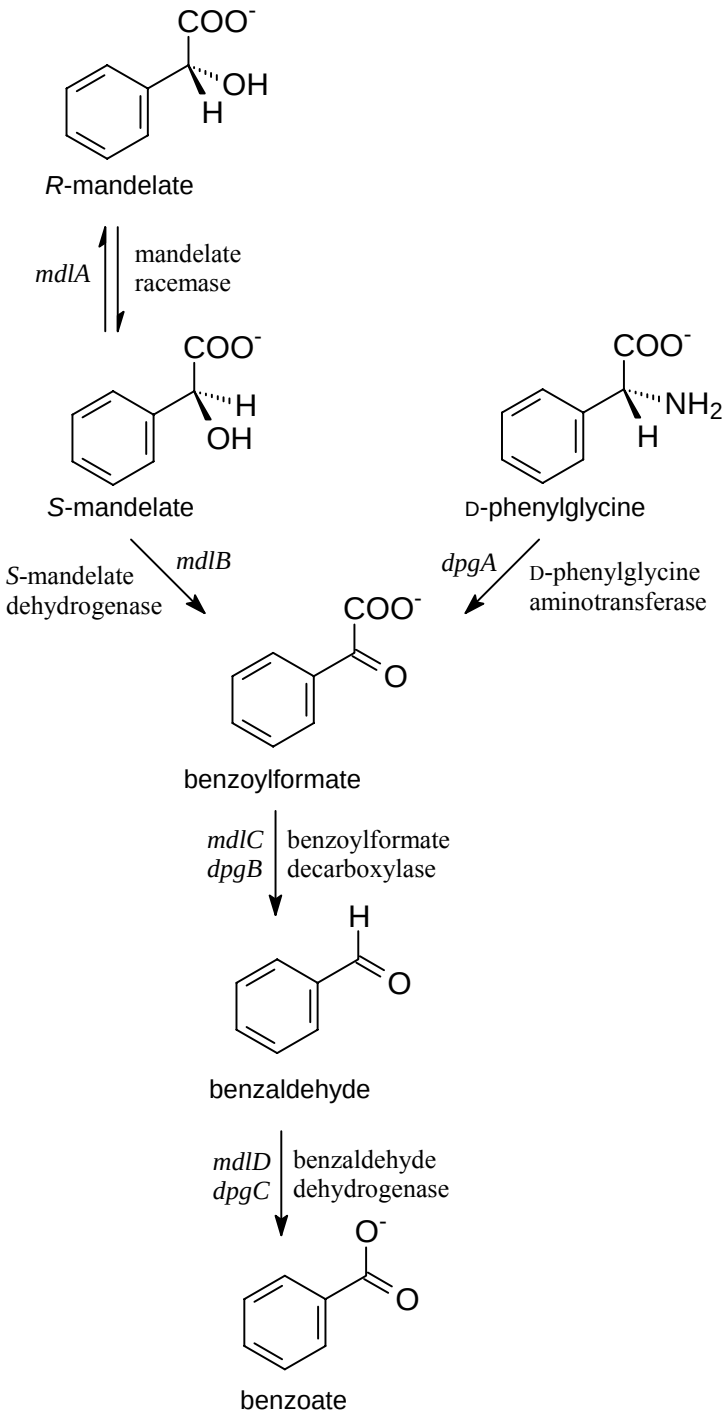

Figure 2. The mandelate pathway in *P. putida* ATCC 12633 and the proposed pathway for D-phenylglycine degradation in *P. stutzeri* ST-201.

2. Objectives

1. To study the role of *Ps*BFDC in D-phenylglycine degradation pathway of *P. stutzeri* ST-201.
2. To isolate and purify *Ps*BFDC from *P. stutzeri* ST-201.
3. To clone the gene encoding *Ps*BFDC (*dpgB)* and express in *E.coli.*
4. To characterize recombinant *Ps*BFDC.
5. To express and characterize histidine-tagged *Ps*BFDC.
6. To clone the gene encoding *Ps*BADH (*dpgC)*, express and characterize histidine-tagged *Ps*BADH.

CHAPTER 2
LITERATURE REVIEW

1. Thiamin diphosphate (ThDP)-dependent enzymes

1.1 Thiamin diphosphate

Thiamin diphosphate serves as a versatile cofactor in a number of enzymatic processes found in almost all major metabolic pathways. ThDP (Figure 3) consists of a pyrimidine ring, a thiazolium ring and a diphosphate group.

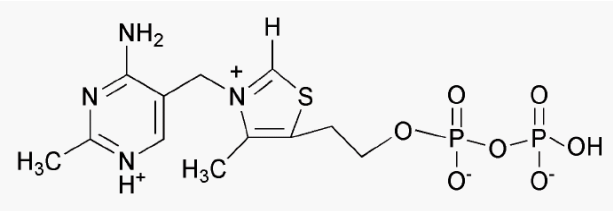

Figure 3. Chemical structure of thiamin diphosphate.

1.2 Thiamin diphosphate-dependent enzymes

ThDP-dependent enzymes include those having the potential reactions of both breaking and forming C-C bonds (22-24). The spectrum of reactions catalyzed by ThDP-enzymes encompasses non-oxidative decarboxylation of α-keto acid (α-keto acid decarboxylases), oxidative decarboxylation of α-keto acid (pyruvate oxidase), carboligation [transketolases (TKT), α-keto acid decarboxylases, acetoacetate syntase] as well as the cleavage of C-C bonds (TKT, benzaldehyde lyase).

A common feature of ThDP-dependent enzymes is the formation of a ThDP-bound carbanionic intermediate upon cleavage of a C-C bond (e.g. decarboxylation). The resulting intermediate was named “active aldehyde” (22).

The enzymes of this family differ widely, however, with regard to the fate of the ThDP-bound active aldehyde. α-Keto acid decarboxylases allow protonation of the intermediate, and their main products are the respective aldehydes.

However, these enzymes are also capable of performing an acyloin-type condensation reaction leading to chiral α-hydroxy ketones (Figure 4). This makes them interesting as catalysts for biotransformations.

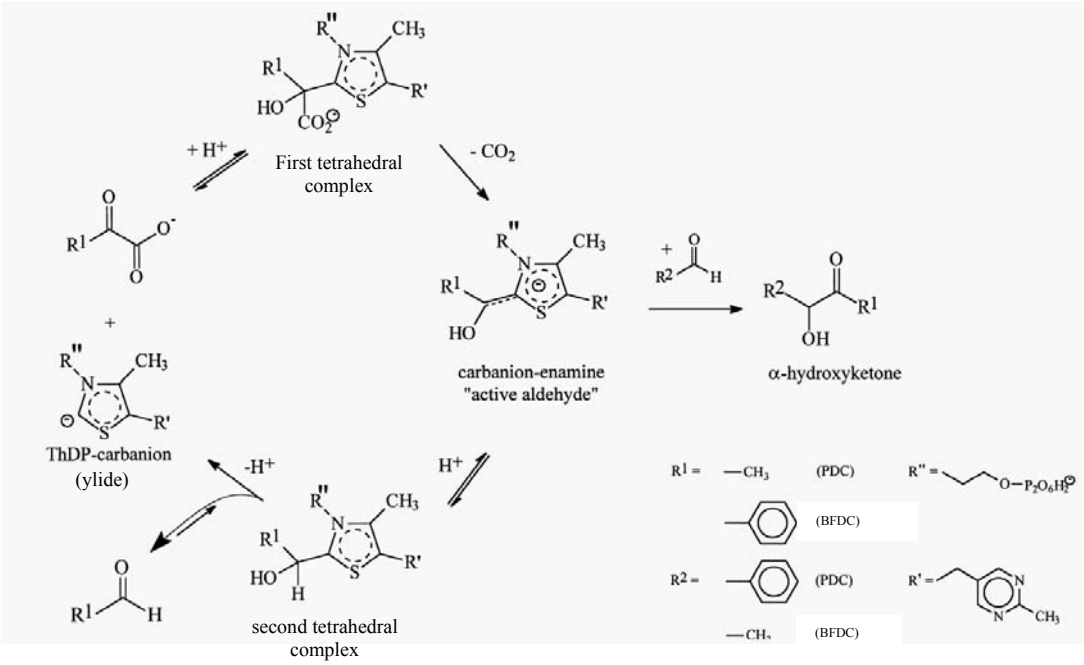

Figure 4. Reaction pathway of enzymatic α-keto acid decarboxylases and formation of α-hydroxy ketones by pyruvate decarboxylase (PDC) and benzoylformate decarboxyalse (BFDC). (25)

Chiral α-hydroxy ketones are versatile building blocks for the organic and pharmaceutical chemistry, e.g. for the synthesis of vitamin E and antifungals. Another well known example is the synthesis of (*R*)-phenylacetyl carbinol (PAC). For many decades, this pre-step for the synthesis of (1*R*,2*S*)-ephedrine has been obtained by biotransformation of benzaldehyde using a fermenting yeast. The optimization of this process is still a matter of research (Figure 5).

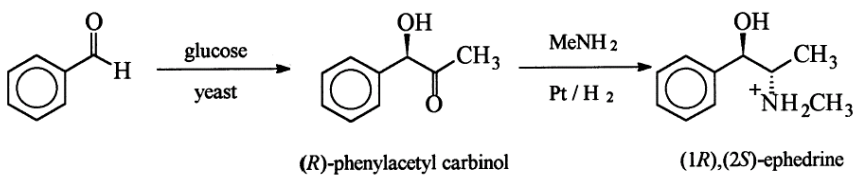

Figure 5. Synthesis of (1*R*,2*S*)-ephedrine. (25)

1.3 α-Keto acid decarboxylases

Among the ThDP-dependent α-keto acid decarboxylases, which catalyze the decarboxylation of α-keto acids as the main reaction, pyruvate decarboxylases (PDC), benzoylformate decarboxylases (BFDC), phenylpyruvate decarboxylases (PhePDC) and indole-3-pyruvate decarboxylases (InPDC) are the examples shown in Table 1. Whereas the formation of C-C bonds has been observed as a side-reaction of some of these enzymes, other α-keto acid decarboxylases like acetolactate synthase (EC 4.1.3.18) or α-keto glutarate synthase (EC 4.1.1.71) have both decarboxylation and carboligation in their main reaction paths.

Table 1. ThDP-dependent α-keto acid decarboxylases.

Enzyme	EC number	SwissProt accession number	Species	References
*Sc*PDC	4.1.1.1	P 06169	*Saccharomyces cerevisae*	25
*Zm*PDC	4.1.1.1	P 06627	*Zymomonas mobilis*	25
*Pp*BFDC	4.1.1.7	P 20906	*Pseudomonas putida*	3, 4, 8
*Ac*BFDC	4.1.1.7	not cloned	*Acinetobacter calcoaceticus*	5
*Ac*PhePDC	4.1.1.43	not cloned	*Acinetobacter calcoaceticus*	5
*Ec*InPDC	4.1.1.74	P 23234	*Enterobacter cloacae*	25
*Ab*InPDC	4.1.1.74	P 51852	*Azospirillium brasiliense*	25

1.4 Mechanism of decarboxylation and carboligation

The capability of ThDP to catalyze the decarboxylation of α-keto acids depends mainly on two properties of the thiazolium ring of ThDP: (a) its capacity to ionize to form an anion (ylide) and attack the α-carbonyl group of α-keto acids, and (b) its ability to stabilize the negative charge upon cleavage of the carbon dioxide. Different steps, which are relevant for thiamin-catalyzed decarboxylation and the formation of α-hydroxy ketones, are summarized in Figure 4.

The reaction cycle is started with activation of ThDP by the enzyme. This initial deprotonation step has recently been elucidated for PDCs and transketolase by Kern et al. (26). Subsequently, the negatively charged C2-ThDP, ThDP-carbanion (ylide) performs a nucleophilic attack on the α-carbonyl group of the α-keto acid. The resulting double negatively charged species is stabilized by proton transfer to the

former carbonyl group to give first tetrahedral complex. The decarboxylation of this complex results in the formation of an α-carbanion-enamine. This step has been intensively studied with PDC from yeast using conjugated α-keto acids with strong electron-withdrawing substituents on the phenyl ring. PDC converts such compounds to an α-carbanion-enamine that is a visible chromophore with a discrete life-time. A series of [*p*-(halomethyl)]benzoylformates have been investigated as substrates for BFDC. These analogues vary from acting as normal substrates to acting as competitive inhibitors (27, 28).

The carbanionic intermediate, carbanion-enamine is probably present in the mechanism of all ThDP-dependent enzymes, which decarboxylate α-keto acids as the first step. The main reaction path of α-keto acid decarboxylases is the generation of the respective aldehydes.

Alternatively, the formation of α-hydroxy ketones has been described for PDCs and BFDC. The last step of the reaction cycle is reversible in PDC. Thus carbanion-enamine may also be generated by addition of an aldehyde to give a second tetrahedral complex and with subsequent deprotonation. The latter reaction path allows the formation of α-hydroxy ketones from aldehydes as precursors.

2. Benzoylformate decarboxylases (BFDC)

Benzoylformate decarboxylase (BFDC) (E.C. 4.1.1.7) catalyzes the formation of benzaldehyde from benzoylformate by decarboxylation, and carboligation, side reaction. BFDC has been found in *Pseudomonas putida* ATCC 12633 (*Pp*BFDC) (3, 4), *Pseudomonas aeruginosa* (*Pa*BFDC) (29), *Acinetobacter calcoaceticus* (*Ac*BFDC) (5) and *Neurospora crassa* (*Nc*BFDC) (7) (Table 1). The properties of BFDCs are shown in Table 2.

Table 2. Enzyme properties of BFDCs.

Enzyme	Specific activity (U mg^{-1})	Native molecular weight (Da)	Temperature optimum (^oC)	pH optimum	pH stability	*p*I	K_m (mM)	Refenences
wt *Pp*BFDC	193	80000	ND	6.2	ND	ND	1	4
rec *Pp*BFDC	138	248000	ND	ND	5.5-7.5	6.5	0.37	11, 12
*Ac*BFDC	70	232000	ND	5.9	ND	ND	ND	5
*Nc*BFDC	1	ND	40	6.0	ND	ND	ND	7

wt = wild type

rec = recombinant

ND = not determined

3. Benzoylformate decarboxylase from *Pseudomonas putida* ATCC 12633 (*Pp*BFDC)

3.1 As a component of mandelate pathway

*Pp*BFDC is a component of the mandelate pathway, which allows *P. putida* to utilize *R*-mandelic acid as a sole carbon source by converting it finally to benzoic acid, which is then metabolized further via the β-ketoadipate pathway to the tricarboxylic acid cycle intermediates succinyl-coenzyme A (CoA) and acetyl-CoA (Figure 6).

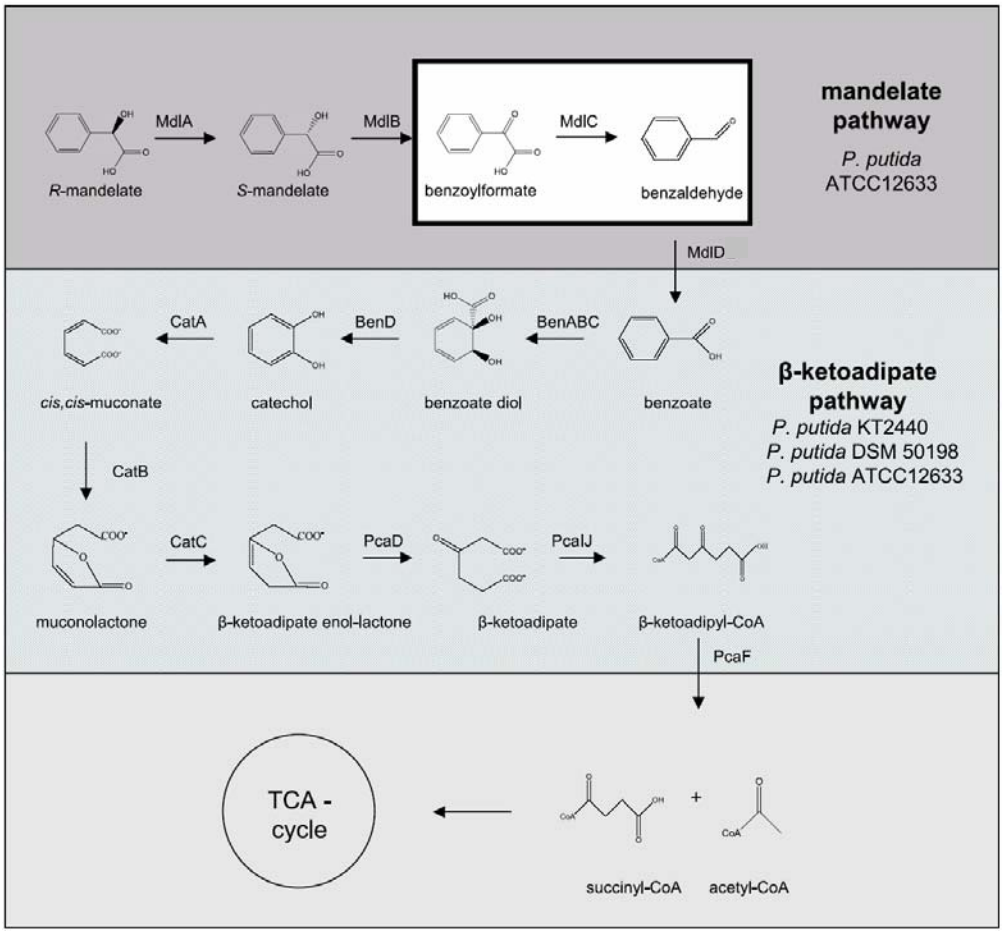

Figure 6. Mandelate and β-ketoadipate pathways in *P. putida*. The mandelate pathway in *Pseudomonas putida* ATCC 12633 is shown in dark gray, and the conversion of benzoylformate to benzaldehyde by a benzoylformate decarboxylase (MdlC or BFDC) is highlighted. The β-ketoadipate pathway (gray) also exists in the majority of all pseudomonads. Additionally, *P. putida* KT2440 and *P. putida* DSM50198 possess a benzaldehyde dehydrogenase. The metabolization of succinyl-CoA and acetyl-CoA via the tricarboxylic acid cycle is shown in light gray. MdlA, mandelate racemase; MdlB, *S*-mandelate dehydrogenase; MdlD (BADH), NAD^+- and $NADP^+$-benzaldehyde dehydrogenases; BenABC, benzoate dioxygenase; BenD, 2-hydro-1,2-dihydroxybenzoate dehydrogenase; CatA, catechol-1,2-dioxygenase; CatB, *cis,cis*-muconate lactonizing enzyme (cycloisomerase); CatC, muconolactone isomerase; PcaD, β-ketoadipate enolactone hydrolase I; PcaIJ, β-ketoadipate succinyl-CoA transferase subunit; PcaF, β-ketoadipyl CoA thiolase; TCA, tricarboxylic acid. (20)

Only *Pp*BFDC has been cloned so far (8), and its crystal structure was solved in the absence (13) and the presence (11) of mandelic acid as an inhibitor. The X-ray data suggested that the enzyme acted as a tetrameric enzyme of 240 kDa and the active site residues of *Pp*BFDC were elucidated by using site-directed mutants (11, 19) and directed evolution studies (17, 19).

3.2 Organization of genes involved in the mandelate pathway

Genetic experiments indicated that the genes for the mandelate pathway were all closely clustered on the chromosome (30, 31) and subsequently, it was reported that the mandelate pathway genes for *P. putida* ATCC 12633 resided on a single 10.5-kb restriction fragment as shown in Figure 7 (8). Sequencing of part of that fragment showed that three of the genes - those encoding mandelate racemase (*mdlA*), *S*-mandelate dehydrogenase (*mdlB*), and benzoylformate decarboxylase (*mdlC*) were arranged in an operon (8, 32). Furthermore, it appeared that the *mdlD* gene encoding for the $NAD(P)^+$-dependent benzaldehyde dehydrogenases (BADH) located upstream of the *mdlC* gene (33) and was transcribed independently. Currently, the *mdlY* gene has been cloned and expressed in *E. coli*, the gene product was purified and identified as a mandelamide hydrolase (MAH) (34). The *mdlX* encoded for a transcriptional regulatory protein which was revealed by the analysis of the deduced amino acid sequence from the open reading frame.

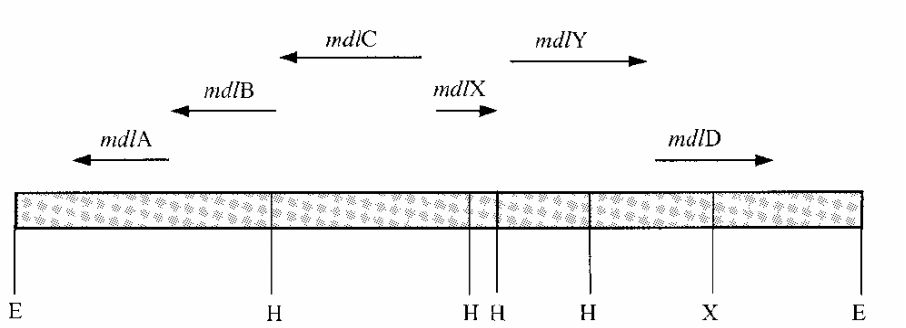

Figure 7. Schematic representation of the 10.5-kb *Eco*RI restriction fragment carrying genes of the mandelate pathway of *P. putida* ATCC 12633. The arrows show the position and orientation of the genes, and relevant restriction sites are indicated: E, *Eco*RI; H, *Hin*dIII; and X, *Xba*I. (34)

3.3 Structural and kinetic analysis of catalysis in decarboxylation by *Pp*BFDC (11)

The mechanism of non-oxidative decarboxylation suggested for ThDP-dependent catalysis by *Pp*BFDC binding with *R*-mandelate, a competitive inhibitor, similar to that of other related enzymes, is shown in Figure 8. In the initial step, the C4′ imino group of ThDP abstracts a proton from the C2 atom of the thiazolium ring, resulting in the formation of an ylide. The ylide attacks the carbonyl of the substrate to form the first tetrahedral intermediate, 2-α-mandelyl-ThDP. Decarboxylation of 2-α-mandelyl-ThDP results in the enamine intermediate. Protonation of the enamine provides a second tetrahedral intermediate, 2-α-hydroxybenzyl-ThDP. Finally, benzaldehyde is eliminated with the assistance of an enzymic base.

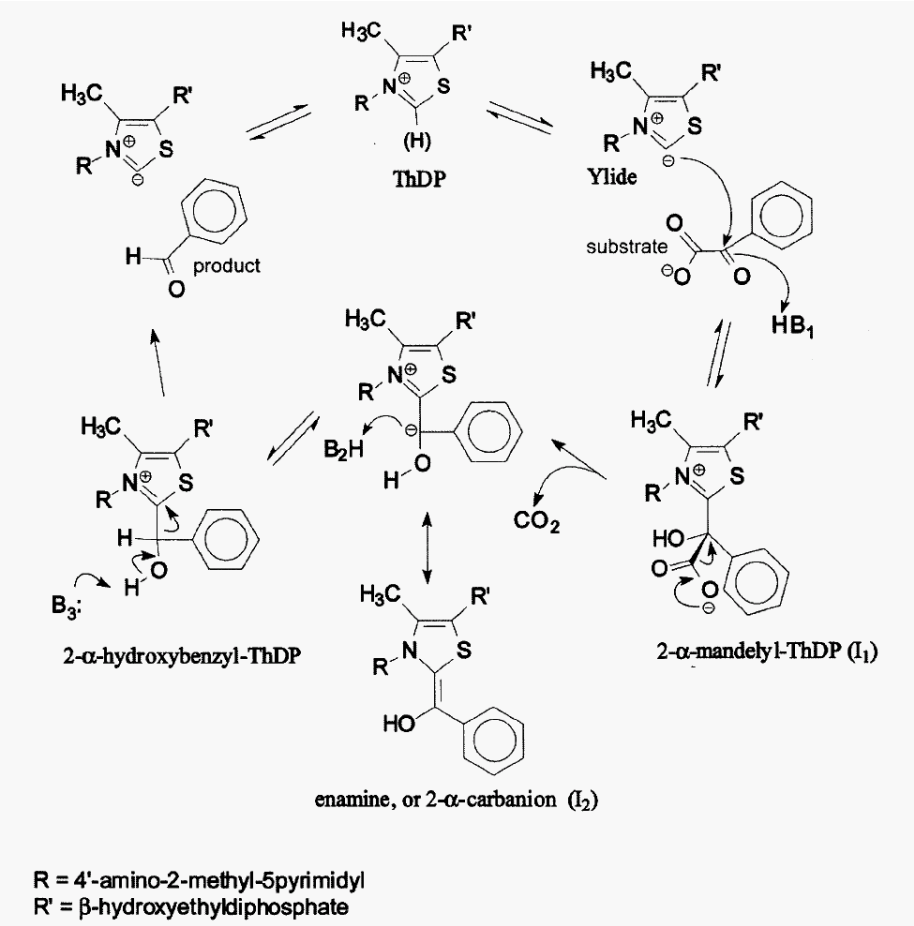

Figure 8. Postulated chemical mechanism for the *Pp*BFDC-catalyzed decarboxylation of benzoylformate. (11)

A structure of this enzyme binding *R*-mandelate, a competitive inhibitor, suggests that at least two hydrogen bonds are formed between the substrate, benzoylformate, and the active site side chains. The first one is between the carboxylate group of benzoylformate and the hydroxyl group of S26, and the second one is between carbonyl group of the substrate and an imidazole nitrogen of H70. Both steady state kinetic studies and stopped-flow experiments suggest the following roles for residues in the active site. The residue H70 is important for the protonation of the 2-α-mandelyl-ThDP intermediate, thereby assisting in decarboxylation, and for the deprotonation of the 2-α-hydroxybenzyl-ThDP intermediate, aiding product release. The residue H281 is involved in protonation of the enamine. Surprisingly, the residue S26 appears to be involved not only in substrate binding but also in other steps of the reaction.

3.4 Carboligation mediated by *Pp*BFDC

The formation of α-hydroxyketones by *Pp*BFDC was first described by Wilcocks et al. (35) using whole cells and cell extracts of *P. putida*, which formed *S*-2-hydroxypropiophenone (2-HPP) from benzoylformate and acetaldehyde as shown in Figure 9. The enantiomeric excess of 2-HPP was determined by ^{1}H-NMR spectroscopy and was found to be 91 - 92%.

Factors affecting 2-HPP formation by *Pp*BFDC were investigated by Wilcocks and Ward (36) and were found to be a broad pH optimum (pH 5-8) and temperature optimum (20-40^{o}C). Recently, *Pp*BFDC did also produce *R*-benzoin with high enantiomeric excess.

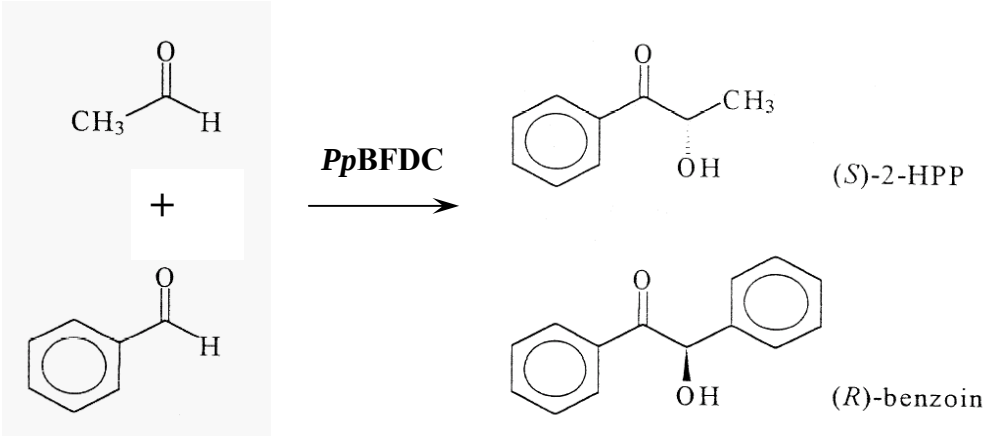

Figure 9. Reaction products of the biotransformation of benzoylformate and acetaldehyde with *Pp*BFDC. (25)

3.5 Substrate specificity of *Pp*BFDC

The substrate spectrum of *Pp*BFDC is limited to aromatic substrates. *Pp*BFDC requires substrates with an aromatic ring directly connected to the α-carbonyl group. Only benzoylformate or *para*-substituted benzoylformate (methylbenzoylformate, fluoromethylbenzoylformate, hydroxymethylbenzoylformate) have been shown as substrates, whereas pyruvate, α-ketobutyrate or α-ketoglutarate are not substrates (27). Recently, expanded substrate range of *Pp*BFDC was also studies (19).

3.6 Crystal structure of *Pp*BFDC

3.6.1 Description of the overall structure

*Pp*BFDC is composed of three domains, each is built around a central β-sheet. The α- and γ- domains are topologically equivalent, while the β-domain has a slightly different fold. Residues that make contact with the cofactor ThDP are located at the C-terminal ends of strands in the α- and γ-domain sheets. A detailed schematic diagram of the structure of PpBFDC is presented in Figure 10, and a ribbon diagram of the monomer is shown in Figure 11.

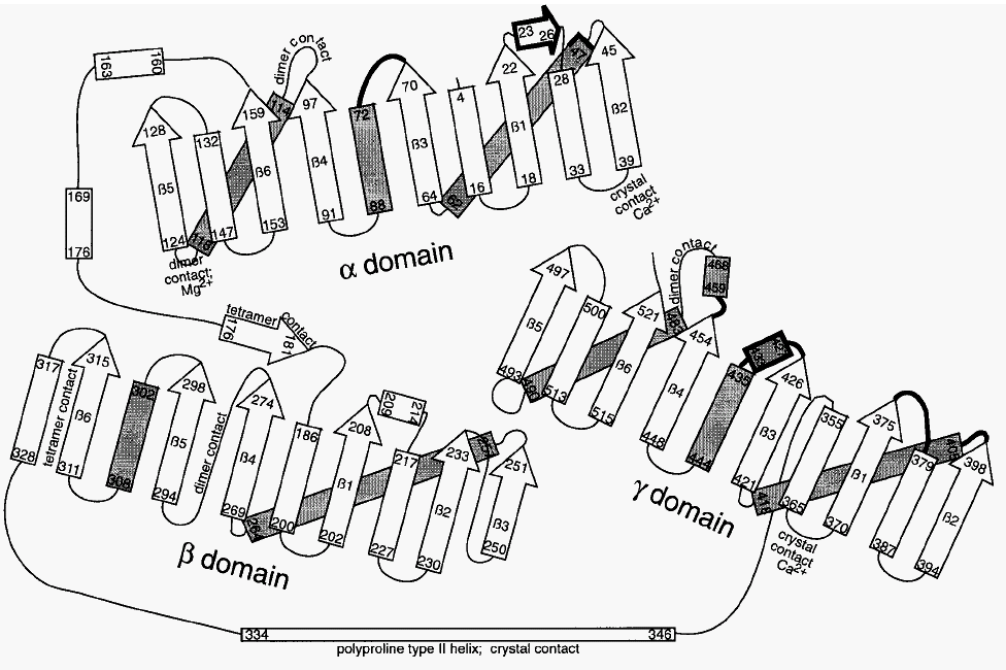

Figure 10. Schematic diagram of the *Pp*BFDC structure. Arrows indicate β-strands; rectangles indicate helices. Beginning and ending residues for each element of secondary structure are indicated. Major contacts (between monomers in the dimer and tetramer and crystal contacts) are indicated. Contacts with the cofactor ThDP are indicated in bold. Helices in white are in front of the β-sheets; shaded helices are behind the sheet. (13)

Figure 11. Ribbon diagram of the structure of a monomer of *Pp*BFDC. This stereo diagram is the same orientation as the schematic diagram in figure 10, with the α-domain on top, the β-domain at lower left, and the γ-domain at lower right. (13)

The architecture of *Pp*BFDC is shared by the other enzymes of known structure that utilize the cofactor ThDP: pyruvate decarboxylase, pyruvate oxidase, and transketolase. Consequently, the structure of *Pp*BFDC was able to superimpose on each of the other three ThDP-containing structures.

3.6.2 Quaternary structure

The native enzymes *Pp*BFDC, PDC, and pyruvate oxidase exist as tetramers, while transketolase as a dimer. ThDP is bound at a dimer interface in *Pp*BFDC, as with the other three enzymes. The binding site is formed by the α-domain of one monomer and the γ-domain of the other. Thus, it is useful to consider the *Pp*BFDC tetramer as a dimer of dimers as shown in Figure 12. The two dimers that make up the *Pp*BFDC tetramer are much more intimately associated than those that make up the PDC tetramer; in this sense, *Pp*BFDC is much more similar to pyruvate oxidase.

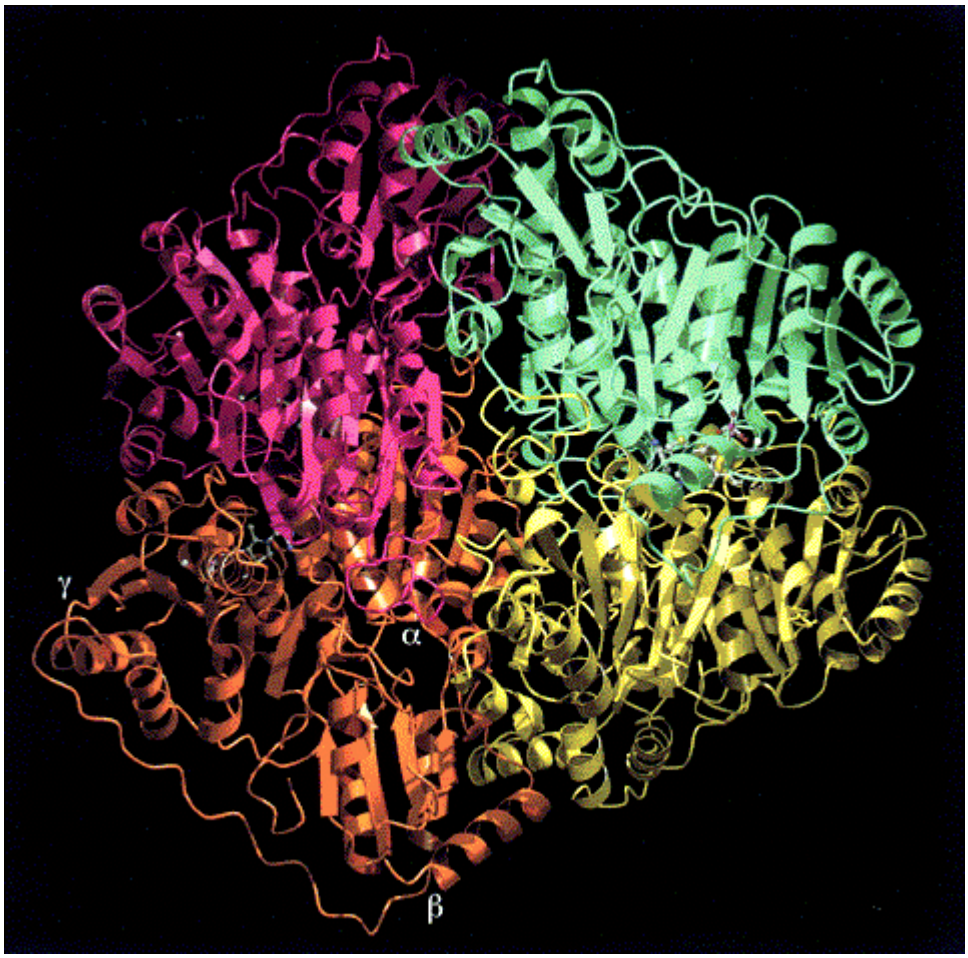

Figure 12. Ribbon diagram of the structure of a tetramer of *Pp*BFDC. Two active sites are at the interface between the red and purple monomers, and two are at the interface between the yellow and green monomers. The cofactor ThDP and its associated metal ion are shown as a ball-and-stick representation. Domains are labeled in the red monomer. (13)

3.6.3 Cofactor properties of *Pp*BFDC

In *Pp*BFDC, the ThDP and Mg^{2+}cofactors are located in the interface between two identical subunits. Each tetramer contains four ThDP molecules and four Mg^{2+}ions. Moreover, two additional metal ions are present, a Mg^{2+} which is located in the interface between two subunits and a Ca^{2+} ion at a crystal contact. The cofactors are buried deep in the enzyme.

The binding properties of the cofactors and the possible catalytic role of the residues located in the active center of the enzyme *Pp*BFDC are presented in Table 3. The metal ion Mg(II) is octahedrally coordinated with the carboxyl/carbonyl oxygen atoms of the conserved residues Asp, Asn, Gly, Gln and the diphosphate group of ThDP. Other conserved residues (Table 3) interact through hydrogen bonds with N(1′) and N(4′α)H_2 of the pyrimidine ring and the N(3) of the thiazole.

Table 3. Cofactor properties and temporary groups of residues involved in catalysis of the enzyme *Pp*BFDC (37) as revealed by crystal structure analysis (13) and site directed mutagenesis studies (11).

	***Pp*BFDC**
Cofactors	ThDP, Mg^{2+}, Ca^{2+}
Metal binding residues	D428, Q455, T457, H_2O, diphosphate
Cofactor's aminopyrimidine and thiazole moiety binding residues	N23, P24, E47, G401, L403,Y433
Imino tautomeric form stabilization and ylide formation	E47,G401
Carboxyalkyl-ThDP formation , decarboxylation	S26, H70, H281
Product release	H70
V-conformation stabilization	L403

4. Benzaldehyde dehydrogenase (BADH)

Benzaldehyde dehydrogenase catalyzes the generally irreversible conversion of benzaldehyde to benzoate by oxidation as shown in Figure 13. BADH has been found in *Pseudomonas putida* ATCC 12633 (*Pp*BADH) (34). Additionally, chromosomes of *P. putida* KT 2440 and *P. putida* DSM 50198 possess DNA sequences of putative BADH (20).

Figure 13. Reaction catalyzed by benzaldehyde dehydrogenase (BADH).

5. Benzaldehyde dehydrogenase from *Pseudomonas putida* ATCC 12633 (*Pp*BADH)

5.1 As a component of mandelate pathway

*Pp*BADH is a component of the mandelate pathway, which allows *P. putida* to utilize *R*-mandelic acid as a sole carbon source by converting benzaldehyde to benzoic acid, which is then metabolized by the β-ketoadipate pathway to the tricarboxylic acid cycle intermediates, succinyl-coenzyme A (CoA) and acetyl-CoA (Figure 6). *Pp*BADH is an $NAD(P)^+$-dependent enzyme having the molecular weight, as determined by electrospray mass spectroscopy, of 47,425 kDa which is consistent with the 47,431 kDa deduced from the amino acid sequence (34). *Pp*BADH is transcribed from the *mdlD* gene which consists of 1,311 base pairs. The enzyme is a homodimeric enzyme. It exhibits greater affinity for NAD^+ than $NADP^+$ and it is classified as a class 3 aldehyde dehydrogenase (38). It is similar to the rat class 3 aldehyde dehydrogenase, but unlike the *P. aeruginosa* enzymes betaine aldehyde dehydrogenase and glucose-6-phosphate dehydrogenase, in that both of which have greater affinity for $NADP^+$.

Aldehyde dehydrogenases are classified into at least 13 distinct families. Most are specific for NAD^+ and a few are specific for $NADP^+$. The class 3 aldehyde dehydrogenases are characterized by an ability to use NAD^+ or $NADP^+$.

5.2 Kinetic parameters for *Pp*BADH

Kinetic parameters for *Pp*BADH are shown in Table 4.

Table 4. Kinetic parameters for *Pp*BADH. (34)

Cofactor	K_m for benzaldehyde (μM)	k_{cat} (min^{-1})	k_{cat}/K_m (min^{-1} M^{-1})
NAD^+	63.4 ± 1.5	$(8.24 \pm 0.32) \times 10^3$	1.3×10^8
$NADP^+$	39.9 ± 4.4	$(2.55 \pm 0.10) \times 10^3$	6.39×10^7

6. *Pseudomonas stutzeri* ST-201

6.1 Definition of species (39)

Pseudomonas stutzeri is a member of the genus *Pseudomonas* sensu stricto. It is in group I of Palleroni's DNA-rRNA homology group within the phylum *Proteobacteria*. *P. stutzeri* is now recognized as those belonging to the class *Gammaproteobacteria*. Phylogenetic studies of *P. stutzeri* strains' 16S rRNA sequences and other phylogenetic markers demonstrate that they belong to the same branch, together with related species within the genus, such as *P. mendocina*, *P. alcaligenes*, *P. pseudoalcaligenes*, and *P. balearica*.

Typically, cells are rod shaped, 1 to 3 μm in length and 0.5 μm in width, and have a single polar flagellum. Under certain conditions, one or two lateral flagella may be produced. Phenotypic traits of the genus include a negative Gram stain, positive catalase and oxidase tests, and a strictly respiratory metabolism. In addition, *P. stutzeri* strains are defined as denitrifiers. They can grow on starch and maltose and have a negative reaction in arginine dihydrolase and glycogen hydrolysis tests.

The G+C content of their genomic DNA lies between 60 and 66 mol %. DNA-DNA hybridizations enable at least 17 genomic groups, called genomovars, to be distinguished. Members of the same genomovar have more than 70% similarity in DNA-DNA hybridizations. Members of different genomovars usually have similarity values below 50%.

6.2 Differentiation from other species (39)

No fluorescent pigments are produced, which differentiates *P. stutzeri* from other members of the fluorescent group of *Pseudomonas* spp. Before the use of genomic approaches to identifying bacteria became widespread, *P. stutzeri* strains were misidentified with other species. This was due to the intrinsic limitations of exclusively phenotypic identification procedures within the former genus *Pseudomonas*. *P. stutzeri* was most commonly confused with other *Pseudomonas* species (*P. mendocina*, *P. pseudoalcaligenes*, and *P. putida*); with species actually in other genera (such as *Delftia acidovorans* and *Ralstonia pickettii*); or even with the flavobacteria, *Alcaligenes* or *Achromobacter*.

Mandel proposed the species "*Pseudomonas stanieri*" for *P. stutzeri* strains with a low G+C content, around 62%; however, G+C content alone is a weak parameter for species differentiation (39).

The phylogenies of genes of the *rrn* operon, considered individually or with other housekeeping genes, demonstrate that all *P. stutzeri* strains are monophyletic. Such phylogenetic studies are currently another good tool for discriminating *P. stutzeri* from the rest of the bacterial species. *P. xanthomarina* has recently been described as a new species with only one representative strain. It is located in the same 16S rRNA phylogenetic branch as *P. stutzeri* and *P. balearica*, with sequence similarities above 98%. *P. stutzeri* can be differentiated phenotypically from both species.

6.3 Phenotypic characterization and identification of strain ST-201 (21, 40)

Pseudomonas stutzeri strain ST-201 was a gram-negative, motile, polar monotrichous flagellated rod, strictly aerobic, non-fermentative, non-spore forming, nonfluorescent, non-pigment producing and denitrifying. The strain formed medium, smooth, opaque colonies on LB agar and colonies became dull pink upon aging. The strain grew well at 30-35°C, but not above 42°C or below 8°C (21, 40).

7. D-Phenylglycine aminotransferase (D-PhgAT)

In 1997, an enzyme namely D-phenylglycine aminotransferase, D-PhgAT (EC 2.6.1.72) was isolated from a soil bacterium *Pseudomonas stutzeri* strain ST-201 and characterized (21). Subsequently, the gene encoding the enzyme, *dpgA*, was successfully cloned, sequenced, and overexpressed in *E. coli* (41). In 2003, the crystallization and preliminary X-ray crystallographic analysis of the enzyme was determined (42).

D-PhgAT, a vitamin B6-dependent enzyme, catalyzes the stereospecific amino-group transfer of D-phenylglycine to 2-oxoglutarate to yield benzoylformate and L-glutamate (Figure 14) by a reversible ping-pong kinetic mechanism (21). The enzyme requires pyridoxal-5′-phosphate (PLP) as a coenzyme and has substrate specificity for D-phenylglycine and D-4-hydroxyphenylglycine. However, neither D-

nor L-aromatic nor branch-chained amino acids can be utilized as substrates. Using the `stereo-inverting' transamination property of D-PhgAT, the amino nitrogen can be channeled directly between D-phenylglycine and L-glutamate, a central molecule in cellular nitrogen metabolism, without the need for additional amino-acid racemases for phenylglycine or glutamate.

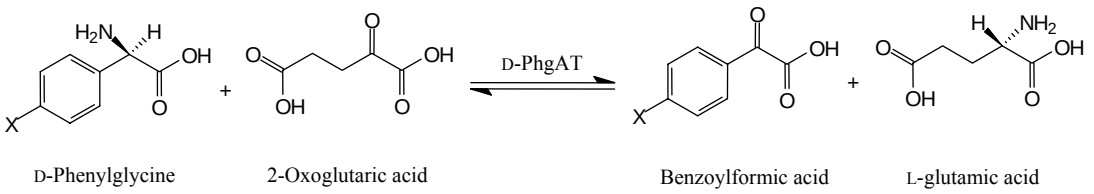

Figure 14. Stereo-inverting aminotransferase reaction catalysed by D-phenylglycine aminotransferase (D-PhgAT).

Native D-PhgAT was found as a homodimer of molecular mass 92 kDa. The enzyme was most active at alkaline pH with maximum activity at pH 9-10. The temperature for maximum activity was 35-45 ^{o}C. The apparent K_m value for D-phenylglycine and for 2-oxoglutarate at 35 ^{o}C, pH 9.5 were 1.1 and 2.4 mM, respectively. The enzyme was strongly inhibited by typical inhibitors of pyridoxal phosphate-dependent enzymes (21).

The *dpgA* gene consisted of 1,362 bps which encoded 453 amino acids of D-PhgAT. The recombinant D-PhgAT exhibited catalytic activity as expected similar to that of the native D-PhgAT including the stereo-inverting enzyme activity, the amino acid substrate specificity and kinetic properties (41).

CHAPTER 3
MATERIALS AND METHODS

1. Bacterial strains and plasmids

Pseudomonas stutzeri ST-201 was used as a wild type (wt) strain and it was available from a previous study (21). The pBluscript II SK (Stratagene) and pGEM-T Easy (Promega) were used as a cloning vector for genomic DNA restriction fragments and PCR products, respectively. The plasmids pET-17b, pET-19b and pET-24b (Novagen) were used as expression vectors of the enzyme genes. For plasmid amplification, *E. coli* JM 109 (Promega) was used as a host, whereas for gene expression, *E. coli* BL21 (DE3) and *E. coli* BL21 (DE3) pLysS (Promega) were employed.

2. Chemicals and reagents

Restriction endonuclease enzymes, DNA polymerase, DNA ligase and other molecular biology reagents were from New England Biolabs, Promega, Stratagene, Novagen or Roche Diagnostics. All other chemicals were of the highest quality commercially available from Amersham Biosciences, Sigma, Fluka, Fisher Biotech, Qiagen or other companies.

3. Determining for existence of enzymes involved in mandelate and D-phenylglycine degradation in *P. stutzeri* ST-201

To verify the existence of enzymes catabolizing substrates of interest, *P. stutzeri* ST-201 was tested for growth on minimal medium (MM) agar containing (in 1 l): 15 g agar, 3.4 g KH_2PO_4, 3.6 g Na_2HPO_4, 0.2 g $MgSO_4$, 8 mg $CaCl_2$, 10 mg yeast extract, 1 ml trace metals solution (43) and supplemented with an appropriate carbon source at a concentration of 10 mM: The carbon sources used were *R*-mandelate, *S*-mandelate, D-phenyglycine, benzoylformate and benzoate. For growth on

benzaldehyde which was immiscible with media at such concentration, a disk containing benzaldehyde (10 µl) was placed on agar instead. With the exception of MM containing D-phenyglycine, 0.4 g $NaNO_3$ was also included as a nitrogen source. The plates were examined for evidence of growth after incubation for 48 h at 30 ^oC

4. Study on the role of *Ps*BFDC in D-phenylglycine degradation

To study the involvement of *Ps*BFDC in D-phenylglycine degradation, the enzyme activity of BFDC as well as D-PhgAT were monitored after the induction with different substrates. *P. stutzeri* ST-201 was grown under a shaking condition at 200 rpm in 200 ml Luria-Bertani (LB) medium at 30 ^oC until the culture reached an OD_{600} of 2.8. Then, the cells were collected by centrifugation, washed with 200 ml 50 mM potassium phosphate buffer, pH 7.0 and the washed cells were added with 200 ml MM containing either glucose, D-phenyglycine or benzoylformate (10 mM). Incubation was continued under the same conditions for a further 160 min with samples being harvested every 20 min. Enzyme activity in crude cell extracts was then determined using standard assays.

5. Study of wt *Ps*BFDC

5.1 Purification of wt *Ps*BFDC

P. stutzeri ST-201 was grown in LB (200 ml x 16 of 500 ml flasks) at 30 ^oC under a shaking condition at 200 rpm until the culture reached an OD_{600} of ~2.8**.** Then, the cells were collected by centrifugation, washed with 50 mM potassium phosphate buffer, pH 7.0 and the washed cells were added with 200 ml MM containing 10 mM benzoylformate. Shaking was continued at 30 ^oC for 9 h after which time the cells were harvested by centrifugation (Sorvall RC 5C, Dupont) and the pellet was resuspended in a 9X volume lysis buffer comprising 50 mM potassium phosphate buffer, pH 6.0, 0.1 mM ThDP and 0.1 mM phenylmethylsulphonyl fluoride (PMSF). Following ultrasonication (Vibra cell, Sonics & Materials Inc.) on ice in cycle of 20-s burst with 20-s cooling and centrifugation (10,000 g , 20 min 4 ^oC) the cell-free extract (CFE) was subjected to stepwise ammonium sulfate fractionation. The ammonium sulfate fraction containing BFDC was dissolved in buffer A (25 mM potassium phosphate buffer, pH 6.0, 0.1 mM ThDP, 0.1 mM $MgCl_2$, 10 % glycerol)

and applied to a Phenyl Sepharose FF column (Amersham Biosciences) which had been connected to Biologic FPLC system (Bio-Rad) and equilibrated with buffer B (0.1 M sodium phosphate buffer, pH 6.0 and 0.1 mM ThDP) containing 1 M $(NH_4)_2SO_4$. The BFDC was then eluted with buffer B at a flow rate of 2 ml min^{-1}. The active fractions were pooled, concentrated and exchanged into buffer C (25 mM Tris·HCl buffer, pH 7.5, 0.1 mM ThDP) using centricon Plus-20 filtration unit cut off at 100,000 Daltons (Amicon). The concentrate was loaded onto a Q-Sepharose FF column (Amersham Biosciences) equilibrated with buffer C, and the enzyme was eluted with buffer C containing NaCl (0.75 M) at a flow rate of 2 ml min^{-1}. The purity of the active fractions was checked by SDS-PAGE using Mini-PROTEAN III system (Bio-Rad).

5.2 N-terminal sequencing of wt *Ps*BFDC

After the purity of the purified enzyme was confirmed, the enzyme sample was blotted onto a polyvinylidine difluoride membrane (Immobilon-P) using TransBlot SD semidry transfer cell (Bio-Rad) and subjected to N-terminal sequencing by Edman degradation at Biomolecular Research Facility (BRF), University of Newcastle, Australia.

6. Study of recombinant *Ps*BFDC

6.1 Construction of subgenomic library and cloning of *dpgB* gene

The degenerate forward primer, BFDC_F (Table 5), was designed based on the N-terminal amino acid sequence of wt *Ps*BFDC. The reverse primer, BFDC_R, was designed using the conserved amino acid sequences of BFDCs from *P. putida* ATCC 12633 (gi:3915757) and *P. aeruginosa* PAO1 (gi:15600094). Both primers were synthesized at Bio Basic Inc., Canada. With these primers, a 1.28-kb DNA fragment containing part of the gene encoding BFDC (*dpgB*) was amplified by polymerase chain reaction (PCR) using iNtRON's i-Taq^{TM} DNA polymerase protocol (annealing temperature at 55 ^{o}C) from the genomic DNA of *P. stutzeri* ST-201. The PCR products were cloned into pGEM-T Easy (Promega), subjected to sequencing and used to generate a digoxigenin-11-dUTP (DIG-11-dUTP)-labeled *dpgB* specific

probe (Roche Diagnostics) using for southern hybridization with genomic DNA and colony hybridization with subgenomic library.

For subgenomic library construction, briefly, genomic DNA isolated from *P. stutzeri* ST-201 with the method of Sambrook et al. (44) was subjected to digestion with various restriction enzymes, followed by agarose gel electrophoresis and southern hybridization (45) using hybridization temperature at 42 ^{o}C and detection kit (Roche Diagnostics). Positive DNA fragments were eluted from 0.75% Saekem-GTG agarose gel electrophoresis by using a GFX DNA and Gel Band Purification (Amersham Biosciences) and ligated into pBluescript II SK which had been digested with the corresponding restriction enzyme(s). The ligation products were transformed into *E. coli* JM 109 by electroporation and plated on LB agar containing 50 μg ml^{-1} ampicillin, 20 mM isopropyl-β-D-thiogalactopyranoside (IPTG) and 80 μg ml^{-1} 5-bromo-4-chloro-3-indolyl-β-D-galactopyranoside (X-gal). White colonies containing a DNA insert were screened by colony hybridization (46) with hybridization temperature at 42 ^{o}C using Hybond-N^{+} nylon membrane (Amersham Biosciences) and detection kit (Roche Diagnostics) to identify individual colonies carrying a plasmid containing the *dpgB* gene. The two plasmids identified in this step were designated pBCH1 and pBCH2.

Table 5. Primers used in this study.

Primer	Sequence
BFDC_F[a]	5′-GGCATHGAYACCGTITTCGG-3′
BFDC_R	5′-TAGTTGGCCGAGCCGTCG-3′
BFDC_N[b]	5′-ATATCC**CATATG**GCATCGGTACACAGC-3′
BFDC_C[b]	5′-AAATC**AAGCTT**CACAGGCTGACCGTGCTGAC-3′
BFDC_X[c]	5′-GCACGGTCAGC**CTcgag**AGCTTGGTACCGAGCTCGG-3′
BADH_F[b]	5′-CCGAATAGAGGGATTG**CATATG**AATTATCTGTCCCC-3′
BADH_R[b]	5′-GCGCGCTCCGCGT**CTCGAG**TTACGGCACAATCC-3′

[a]Degenerate primer where H = A, C or T; Y = C or T; I = inosine.

[b]Introduced restriction sites are in bold.

[c]The new *Xho*I site is in bold and the lowercase letters indicate the change of bases from the wild type sequence.

6.2 DNA sequencing and gene analysis

The nucleotide sequences of both strands of the DNA fragment in pBCH1 and pBCH2 were determined at the BioService Unit (BSU), National Science and Technology Development Agency (NSTDA), Thailand. The open reading frames (ORFs), DNA and protein alignment were analyzed using either VectorNTI (Invitrogen) or Bioedit (http://www.mbio.ncsu.edu/BioEdit/bioedit.html). The nucleotide and deduced amino acid sequences were compared to the sequences in the GenBank and SwissProt databases at the National Center for Biotechnology Information (Bethesda, MD) using the BLAST network server. Both programs i.e. Pattern Recognition of SeqWeb version 2.0 of Wisconsin Package (Genetics Complete Group; GCG) and Neural Network Promoter Prediction (NNPP) were used to search for the putative promoter sequence. The GCG was also used for searching the putative ribosome binding site. The putative transcriptional terminator was determined by web-based engine at www.bioinfo.rpi.edu/applications/mfold.

The nucleotide sequences determined in this work have been deposited under GenBank accession no EF419244.

6.3 Expression of *P. stutzeri* ST-201 *dpgB* gene in *E.coli* and purification of recombinant *Ps*BFDC

The *dpgB* gene was PCR amplified using high fidelity *Pfu* DNA polymerase protocol (Stratagene) with annealing temperature at 55 ^{o}C and pBCH1 as the template. The forward and reverse primers, BFDC_N and BFDC_C (Table 5) introduced *Nde*I and *Hin*dIII restriction sites, respectively and were synthesized at BSU, NSTDA, Thailand. The PCR product was digested with *Nde*I and *Hin*dIII and ligated into pET17b. The resulting plasmid pET17b*Ps*BFDC was verified for the fidelity of the amplification by sequencing at BSU, NSTDA, Thailand, and it was transformed into *E. coli* strain BL21 (DE3**)** (Promega).

For expression of the recombinant *Ps*BFDC, the transformants were grown at 37 ^{o}C, under a shaking condition at 200 rpm, in 200 ml x 6 of 500 ml flasks of LB containing 50 μg ml^{-1} ampicillin to an A_{600} of 0.8 and then induced by addition of 0.4 mM IPTG. After 6 h incubation at 25 ^{o}C, the cells were harvested by centrifugation. Purification of the recombinant *Ps*BFDC was accomplished using the

protocol described above for the wt *Ps*BFDC enzyme. The purified enzyme, which showed a single band on SDS-PAGE was stored at 4 °C in a storage buffer containing 50 mM sodium phosphate buffer, pH 6.0, 0.2 mM ThDP and 0.1 mM $MgCl_2$. The protein concentration was determined by the Bradford method using bovine serum albumin as the standard (47).

6.4 Characterization of recombinant *Ps*BFDC

6.4.1 Molecular weight determination

Native molecular weight of the recombinant *Ps*BFDC was estimated after gel filtration chromatography with Superdex 200 HR 10/30 column (Amersham Biosciences). Purified enzyme (100 µl) was injected onto the column which was previously equilibrated with 50 mM sodium phosphate buffer, pH 7.0 containing 0.15 M NaCl at a flow rate of 0.5 ml min^{-1}. Elution was performed with the same buffer and protein molecular weight markers including cytochrome C (12.4 kDa), carbonic anhydrase (29 kDa), albumin (66 kDa), alcohol dehydrogenase (150 kDa) and catalase (250 kDa) (Sigma) were used as the standards.

Molecular weight of the recombinant *Ps*BFDC subunits was also determined by SDS-PAGE. The enzyme was electrophoresed along with the standard markers in 4% (w/v) acrylamide for the stacking gel (pH 6.8) and 12% (w/v) acrylamide for the separating gel (pH 8.8). Protein bands were stained with Coomassie Blue.

6.4.2 Effect of temperature and pH on enzyme activity and stability

The effect of temperature on the recombinant *Ps*BFDC activity was determined at temperatures ranging from 10 to 80 ^{o}C at pH 6.0. For temperature stability, the enzyme was pre-incubated between 15 and 70 ^{o}C for 20 min, after which the remaining activity was determined under the standard direct continuous assay condition described in 9.2 at 35 ^{o}C. The effect of pH on the activity was investigated using sodium citrate buffer (pH 3-6), sodium phosphate buffer (pH 6-8), Tris-HCl buffer (pH 8-9), glycine-NaOH buffer (pH 9-10) and 3-[cyclohexylamino]-1-propanesulfonic acid (CAPS) buffer (pH 10-12), each at 66 mM in the standard direct continuous assay condition at 35 ^{o}C. For pH stability, the enzyme was pre-incubated in

different buffers with varying pH at 25 ^{o}C for 20 min, after which the remaining activity was determined under the standard direct continuous assay condition at 35 ^{o}C.

6.4.3 Isoelectric point (p*I*) estimation

p*I* of the recombinant *Ps*BFDC was determined by isoelectric focusing (IEF) with the two-dimensional polyacrylamide gel electrophoresis from Immobiline dry strip kit (Amersham Biosciences). Briefly**,** the enzyme was dissolved in rehydration solution, loaded on 7-cm immobilized non-linear pH 3-10 gradient strip, rehydrated and isoelectrically focused in an automated run, IPGphor Isoelectric Focusing system. The second-dimension SDS gel was carried out in a Mini PROTEAN III cell system. Coomassie Blue staining was used to locate the protein.

6.4.4 Kinetic parameters study

The kinetic parameters K_m and k_{cat} were determined by assaying the enzyme activity using the standard spectrophotometric direct method at 35 ^{o}C. Benzoylformate concentrations were varied appropriately and the reactions were started by the addition of BFDC. Initial velocity data were fitted to the Michaelis-Menten equation using the Enzyme Kinetics module of SigmaPlot® (SPSS Inc.). Kinetic parameters were determined per monomer using molecular mass of 56,302 Da for *Ps*BFDC.

7. Study of histidine-tagged *Ps*BFDC

7.1 Cloning and expression of histidine-tagged *Ps*BFDC

Using pET17b*Ps*BFDC as a template**,** the QuikChange (Stratagene) methodology was employed to introduce an *Xho*I restriction site at the C-terminus of the *dpgB* gene. The sequence of the forward primer, BFDC_X, is shown in Table 5. The resultant plasmid was digested with *Nde*I and *Xho*I and the 1.6 kb fragment was ligated into *Nde*I- and *Xho*I-digested pET24b, to provide a plasmid, denoted pET24b*Ps*BFDHis. Fidelity of the mutated sequence was confirmed by sequencing at the University of Michigan core facility, Life Science Institute (LSI), University of Michigan (UM), USA.

pET24b*Ps*BFDHis was transformed into *E.coli* strain BL21(DE3)pLysS (Promega) and a single colony was used to inoculate 50 mL of LB broth containing kanamycin (50 μg ml^{-1}) and chloramphenicol (25 μg ml^{-1}). The culture was grown overnight at 37 ^{o}C and used to inoculate 1 l of fresh medium. The fresh culture was grown at 37 ^{o}C until OD_{600} reached 0.8. The culture was cooled to 25 ^{o}C, and the protein expression was induced by the addition of 1 mM IPTG. The culture was grown for an additional 12 h at 25 ^{o}C prior to cell harvesting by centrifugation. The pelleted cells were resuspended in buffer D (50 mM potassium phosphate buffer, pH 8.0, 500 mM NaCl, 0.1 mM ThDP) containing 10 mM imidazole and 0.1 mM PMSF, disrupted by sonication and the cell debris was removed by centrifugation. The CFE was applied to a HIS-select^{TM} Nickel Affinity column (Sigma) previously equilibrated in buffer D. After the column was washed with buffer D containing 20 mM imidazole, the enzyme was eluted with buffer D containing 250 mM imidazole. The fractions with highest purity, as judged by SDS-PAGE, were pooled and the buffer was exchanged for storage buffer (100 mM potassium phosphate buffer, pH 6.0, 1 mM $MgSO_4$, 0.5 mM ThDP, 10% glycerol) using Econo-Pac 10 DG desalting columns (Bio-Rad). The protein was concentrated using Amicon Ultra centrifugal filters (Millipore) before being stored at –20 ^{o}C. Protein concentrations were determined by either the Bradford (47) or UV methods (48).

7.2 Kinetic parameters study

The kinetic parameters K_m and k_{cat} of *Ps*BFDC-his were determined by assaying the enzyme activity using the standard spectrophotometric coupled method described in 9.2 at 30 ^{o}C and 35 ^{o}C. Benzoylformate concentrations were varied appropriately and the reactions were started by the addition of BFDC. Initial velocity data were fitted to the Michaelis-Menten equation using the Enzyme Kinetics module of SigmaPlot® (SPSS Inc.). Kinetic parameters were determined per monomer using molecular mass of 57,367 Da for *Ps*BFDC-his.

8. Study of histidine-tagged benzaldehyde dehydrogenase from *P. stutzeri* ST-201 (*Ps*BADH)

8.1 Cloning and expression of histidine-tagged *Ps*BADH

Based on the sequence of the open reading frame in pBCH2, two primers were designed to amplify the *dpgC* gene which encoded *P. stutzeri* ST-201 benzaldehyde dehydrogenase (*Ps*BADH). The forward (BADH_F) and the reverse (BADH_R) primers (Table 5) consisted of *Nde*I and *Xho*I sites, respectively. Amplification was achieved with *PfuUltra* DNA polymerase (Stratagene), using pBCH2 as the template. The PCR product was purified, digested and ligated into pET19b (Novagen) previously digested with *Nde*I and *Xho*I. This construction added a 10×histidine tag to the N-terminus of the enzyme and generated the expression vector, pET19b*Ps*BADH-His. Fidelity of the amplification was verified by sequencing, then, the plasmid was transformed into *E. coli* strain BL21(DE3)pLysS (Promega) for expression.

Expression and preparation of a cell-free extract of his-tagged *Ps*BADH were carried out similarly as described for *Ps*BFDC-his. The extract was applied to HIS-Select^{TM} Nickel Affinity column previously equilibrated in buffer E (50 mM potassium phosphate buffer, pH 8.0, 300 mM NaCl, 2 mM DTT) containing 10 mM imidazole. After washing with buffer E containing 40 mM imidazole, the enzyme was eluted in buffer E containing 250 mM imidazole. The fractions with highest purity were pooled and the buffer was exchanged for storage buffer (100 mM HEPES buffer, pH 7.5, 100 mM KCl, and 2 mM DTT) using Econo-Pac 10 DG desalting columns (Bio-Rad). The *Ps*BADH-his was then concentrated using Amicon Ultra centrifugal filters (Millipore) before being stored at –20 ^{o}C.

8.2 Kinetic parameters study

Apparent K_m [K_m(app)] values for benzaldehyde were determined by fixing NAD^+ or $NADP^+$ at a concentration of 1 mM and varying the benzaldehyde concentrations as required. For determination of the K_m (app) values for NAD^+ and $NADP^+$, benzaldehyde was maintained at a saturating concentration (1 mM) and the NAD^+ or $NADP^+$ concentrations varied appropriately. Kinetic data were fitted to the Michaelis-Menten equation using the Enzyme Kinetics module of SigmaPlot® (SPSS Inc.). Kinetic parameters were determined per monomer using a molecular mass of 50,278 Da for *Ps*BADH-his.

9. Measurement of enzyme activity

9.1 D-PhgAT

D-PhgAT activity was determined using the spectrophotometric assay in which the rate of benzoylformate formation was measured by monitoring the increase in absorbance at 254 nm (49). The assay was carried out in a buffer (1 ml) containing Tris·HCl buffer (100 mM, pH 9.0), D-phenylglycine (1 mM), α-ketoglutarate (1 mM), pyridoxal-5′-phosphate (25 μM) and EDTA (25 mM). The assay was performed at 25 ^{o}C and the product was measured with a temperature-controlled spectrophotometer (BioSpec 1601, Shimadzu)

9.2 BFDC

BFDC activity was determined using a direct continuous assay based on the decrease in absorbance at 334 nm as benzoylformate was converted to benzaldehyde (4). The reaction mixture (1 ml) contained benzoylformate (8.33 mM) and ThDP (40 μM) in sodium phosphate buffer (66 mM, pH 6.0). The assay was performed at 25 ^{o}C and the product was measured with a temperature-controlled spectrophotometer. In addition to the direct method described above a more sensitive coupled assay (9) was also used for the studies of histidine-tagged *Ps*BFDC. The assay employed decarboxylation of benzoylformate to form benzylaldehyde and followed with the use of horse liver alcohol dehydrogenase (HLADH) to convert benzylaldehyde to benzyl alcohol in the presence of NADH. The assay was performed at an appropriate temperature in 100 mM potassium phosphate buffer, pH 6.0, containing 1.0 mM $MgCl_2$, 0.5 mM ThDP, 0.3 mM NADH and 0.25 U ml^{-1} of HLADH. The decrease in absorbance at 340 nm was measured with a Cary 50 spectrophotometer (Varian) with a temperature-controlled cell holder.

9.3 BADH

Benzaldehyde dehydrogenase activity was monitored spectrophotometrically by observing the increase in A_{340} due to the reduction of NAD^+ (34). Routine activity assays were carried out at 25 ^{o}C in a 1 ml reaction mixture containing 100 mM TAPS buffer, pH 8.5, 100 mM KCl, 1 mM DTT, 1 mM NAD^+ and 1 mM benzaldehyde. The increase in absorbance at 340 nm was measured with a Cary 50 spectrophotometer equipped with a temperature-controlled cell holder.

CHAPTER 4
RESULTS

1. Determining for existence of enzymes involved in mandelate and D-phenylglycine degradation in *P. stutzeri* ST-201

With the exception of *R*-mandelate (10 mM) and *S*-mandelate (10 mM), *P. stutzeri* ST-201 was able to grow on MM agar containing each of the tested carbon sources; D-phenylglycine (10 mM), benzoylformate (10 mM), benzaldehyde (disk containing 10 μL) and benzoate (10 mM).

2. Study on the role of *Ps*BFDC in D-phenylglycine degradation

Neither D-PhgAT activity nor BFDC activity was observed in *P. stutzeri* ST-201 grown in MM containing 10 mM glucose (Figure 15A). However, when the culture medium was changed from LB to MM containing 10 mM D-phenylglycine, D-PhgAT activity was detected after 40 min, and was followed by BFDC activity which appeared after 100 min (Figure 15B). Conversely, in MM with 10 mM benzoylformate as the sole carbon source there was no evidence for D-PhgAT activity but BFDC activity was observed after 60 min (Figure 15C).

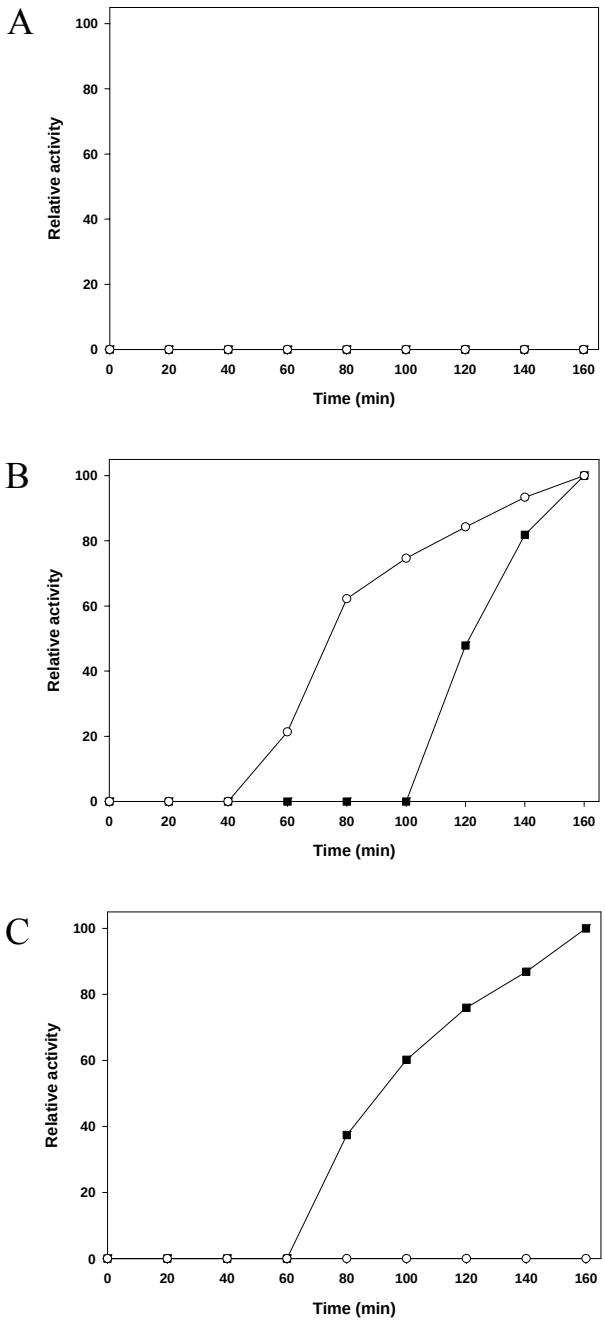

Figure 15. Time course for the appearance of D-phenylglycine aminotransferase (○) and benzoylformate decarboxylase (■) activity. At t=0 the culture medium of *P. stutzeri* ST-201 was changed to a minimal medium containing either (A) glucose, (B) D-phenylglycine or (C) benzoylformate at the concentration of 10 mM. Enzyme activity was measured as described in Materials and Methods and expressed as relative activity to the maximum value at time = 160 min.

3. Study of wt *Ps*BFDC

3.1 Purification of wt *Ps*BFDC

Benzoylformate decarboxylase was found in clarified cell extracts of benzoylformate-induced *P. stutzeri* ST-201 after cell disruption. By ammonium sulfate fractional precipitation, most of *Ps*BFDC precipitated at 45-65% ammonium sulfate saturation and the highest enzyme activity was observed in the fractions between 45-55% saturation (Figure 16). Subsequent hydrophobic interaction chromatography using Phenyl Sepharose FF as a chromatographic media (Figure 17) removed more than 90% of unwanted proteins. Following ultrafiltration and an anion-exchange chromatography step using a Q-Sepharose FF column (Figure 18), the active fraction gave a single band on SDS-PAGE analysis, showing a molecular weight of ~55 kDa. Results from the purification procedures are summarized in Table 6 and Figure 19.

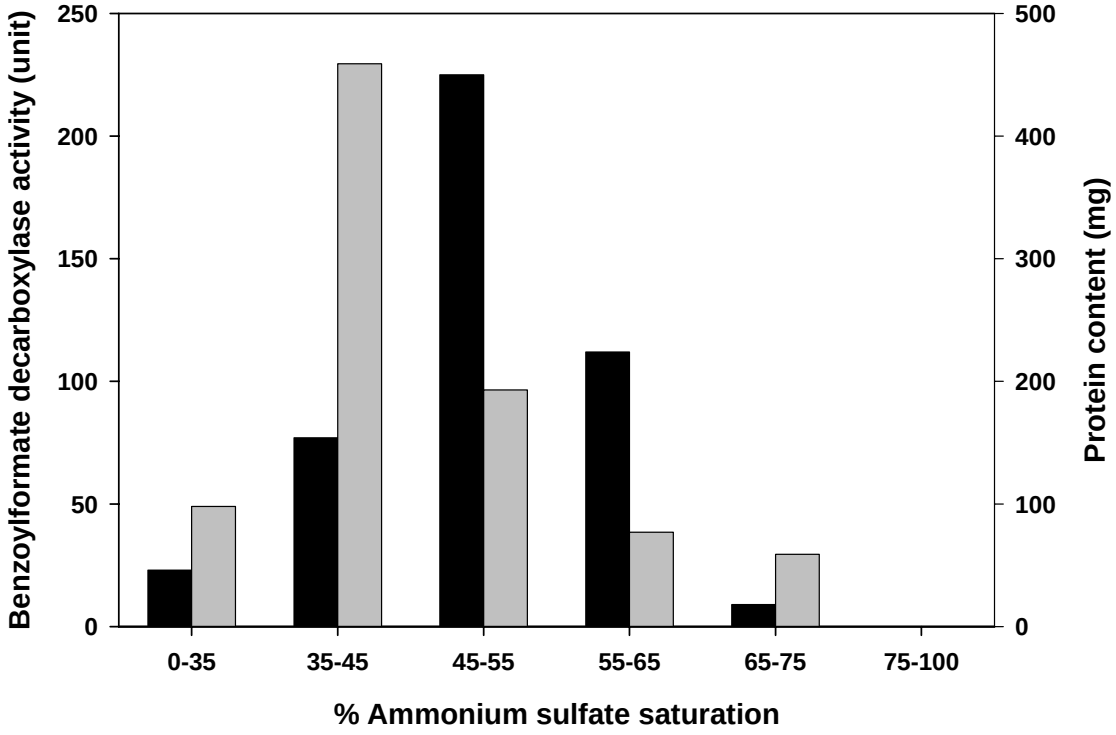

Figure 16. Benzoylformate decarboxylase activity (■) and protein content (□) of ammonium sulfate precipitation fractions of clearified cell extracts. The cell extract was prepared from induced *P. stutzeri* ST-201. The enzyme activity was assayed in 66 mM sodium phosphate buffer, pH 6.0 at 25 ^{o}C.

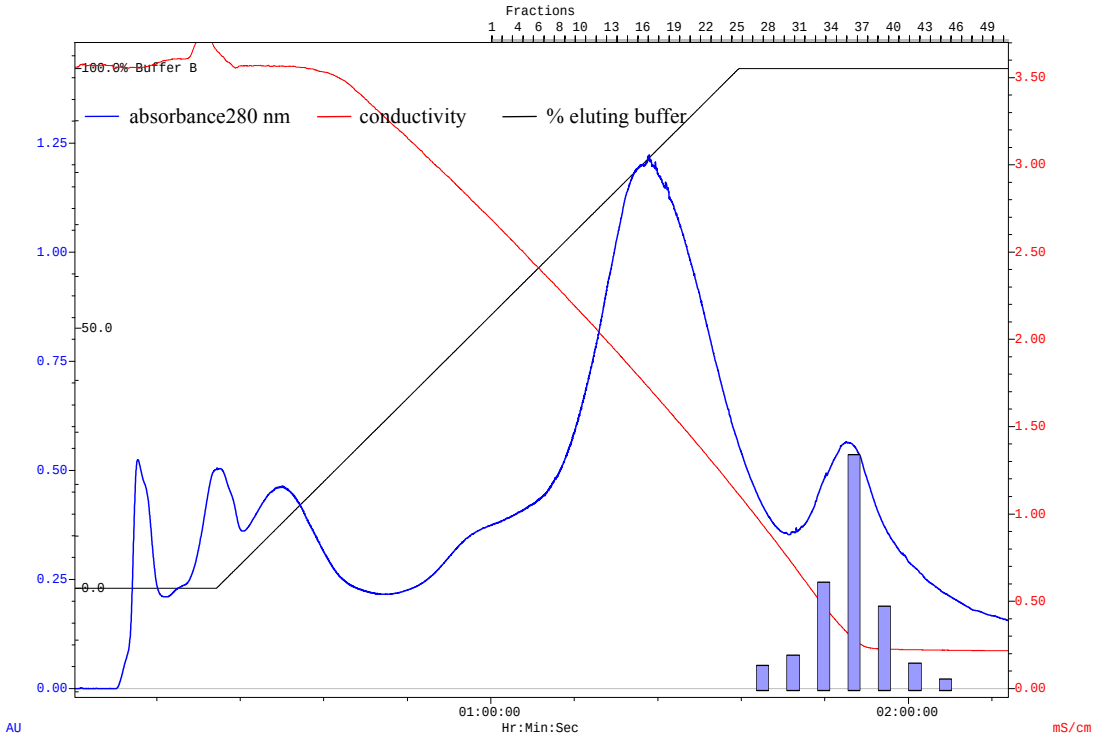

Figure 17. Protein elution pattern of Phenyl Sepharose FF hydrophobic interaction chromatography. Rectangular bars represent activity of benzoylformate decarboxylase found in fractions collected by the FPLC system which were further purified in the subsequent centrifugal ultrafiltration step.

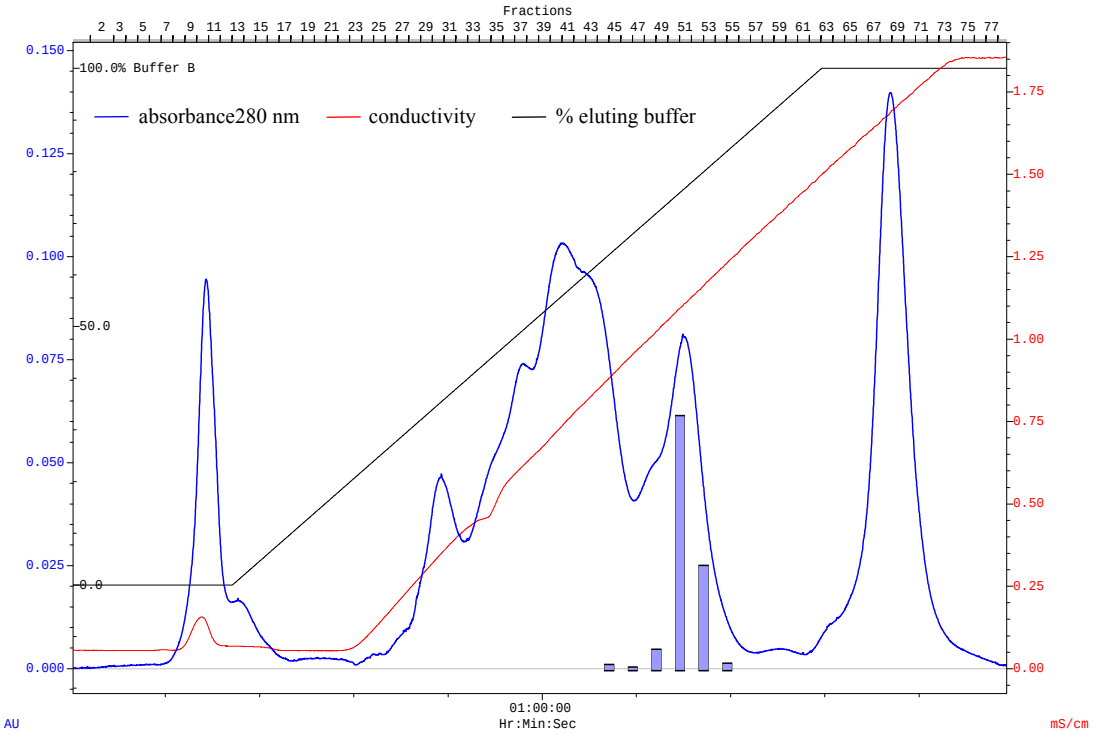

Figure 18. Protein elution pattern of Q-Sepharose FF anion-exchange chromatography. Rectangular bars represent activity of benzoylformate decarboxylase found in each fraction collected by the FPLC system.

Table 6. Summary of purification of wt BFDC from *P. stutzeri* ST-201. The culture volume of *P. stutzeri* ST-201 was 3,200 ml.

Purification step	Total protein (mg)	Total activity (U)	Specific activity (Umg-1)	Purification (fold)	Yield (%)
1. Clarified cell homogenate	1910	691	0.36	1.0	100
2. 45-65% $(NH_4)_2SO_4$ precipitation	270	336	1.2	3.3	49
3. Phenyl Sepharose FF	25	245	9.8	27	35
4. Centrifugal Ultrafiltration	8.5	231	27	75	33
5. Q-Sepharose FF	0.88	156	177	492	23

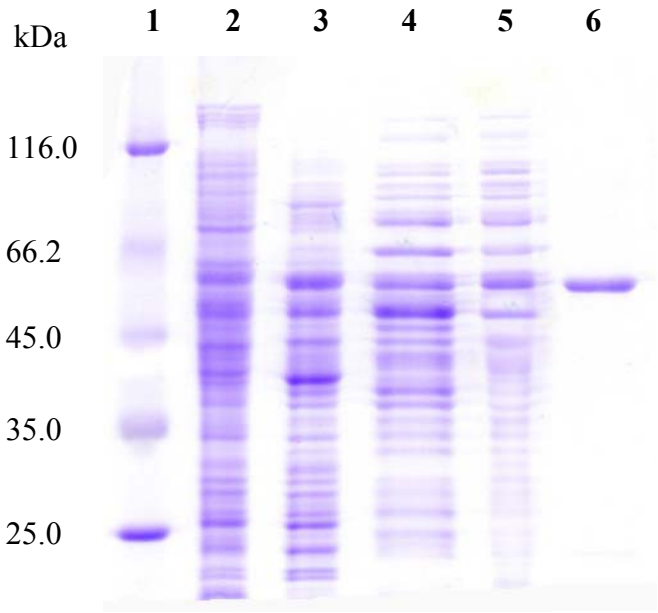

Figure 19. SDS-PAGE analysis of the wt *Ps*BFDC and its purity along the purification process.

Lane 1: Molecular weight markers with their molecular weight indicated

Lane 2: Clarified cell homogenate after cell disruption

Lane 3: Protein from ammonium sulfate precipitation at 45-65% saturation.

Lane 4: Protein resulting from Phenyl Sepharose FF chromatography

Lane 5: Protein after centrifugal ultrafiltration

Lane 6: Protein resulting from Q-Sepharose FF chromatography

3.2 N-Terminal sequencing of wt *Ps*BFDC

Sequencing of the purified enzyme revealed N-terminal sequence (23 amino acids) of **ASVHSITYELLRRQGIDTVFGNP** which was employed to generate degenerate primers used for hybridization experiments. The results were reliable as shown by the well identified signal peaks in HPLC chromatogram of each cycle of Edman degradation.

4. Construction of subgenomic library and cloning of *dpgB* gene

4.1 PCR amplification of part of gene encoding *Ps*BFDC (*dpgB*)

PCR amplification using *P. stutzeri* ST-201 chromosomal DNA template with primers BFDC_F and BFDC_R yielded a PCR product appeared as a single band on agarose gel (Figure 20). The size was estimated about 1,250-1,280 base pairs, which was as expected when compared to that of the deposited BFDC gene (*mdlC*) of *P. putida* ATCC 12633.

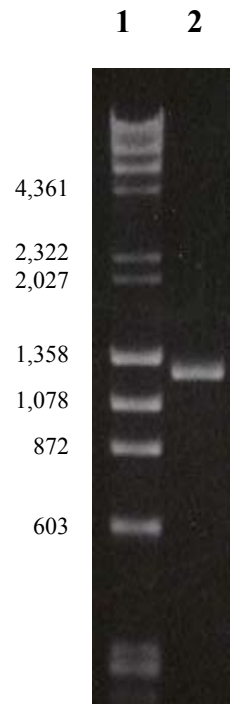

Figure 20. Agarose gel electrophoresis of PCR product for probe preparation.

Lane 1: ϕX174 DNA/*Hae* III and λ DNA/*Hin*d III markers

Lane 2: PCR product amplified from *P. stutzeri* ST-201 genomic DNA with primers BFDC_F and BFDC_R

4.2 DNA sequence of the PCR product

The PCR product was cloned to pGEM-T Easy and submitted for DNA sequence determination at the BSU, NSTDA, Thailand. The result of nucleotide sequencing was shown as a 1,253 base pairs in which the two primers were identified at both ends in Figure 21.

GGCATCGACACGGTGTTCGGCAACCCTGGTTCCAACGAACTGCCGTTTCTGAAGGATTTCCCAGAGGAC
TTTCGCTACATCCTCGCGTTGCAGGAAGCGTGCGTGGTAGGTATTGCTGATGGTTACGCCCAGGCCAGT
CGCAAACCTGCATTCATTAACCTGCATTCTGCAGCGGGCACGGGCAACGCGATGGGCGCGATGAGTAAC
GCCTGGAACTGCCACTCTCCGCTGATCGTGACAGCTGGTCAGCAAAACCGAGCGATGATTGGGGTTGAG
GCACTGTTGACCAACGTCGACGCCGCCAGCCTTCCCCGTCCTCTCGTCAAATGGAGTTACGAGCCGGCG
AGCGCTGCGGAAGTGCCACATGCAATGAGCCGAGCTATTCACATGGCGAGCATGGCACCTCGCGGGCCT
GTGTATCTCTCTGTGCCATACGATGATTGGGACAAGGAAGCGGATCCTCAGTCTCATCACCTGTACGAT
CGGAGTGTCAACTCAGCTGTTCGTCTGAATGACCAAGATCTGGAAGTGCTGGTGGAAGCTCTCAACAGC
GCGTCCAACCCCGCAATTGTGCTCGGCCCAGACGTCGACTCCGCGAATGCAAATGCTGATTGCGTAACA
TTGGCCGAACGACTCAAAGCTCCTGTATGGGTTGCCCCTTCTGCCCCGCGCTGCCCCTTCCCAACCCGA
CACCCCTGTTTCCGAGGGCTTATGCCTGCCGGTATCGCAGCGATCTCTCAACTGCTGGAGGGTCACGAT
GTGGTGTTGGTTATAGGCGCCCCCGTATTCCGCTACCACCAGTACGATCCAGGTCAGTACCTGAAACCA
GGTACCCGCTTGATTTCGATCACCTGTGACCCGCTCGAAGCGGCACGCGCGCCAATGGGCGATGCGATT
GTTGCAGACATCGGTACCATGACCGCTGCGCTCGCCAGCCGCATCGGCGAAAGCGAACGCCAACTTCCA
GCGGTTCTCCCCAGTCCGGAGAGGGTTAACCAGGATGCCGGGCGTCTGCGTCCAGAAACGGTGTTTGAC
ACACTCAACGAGATGGCTCCTGAGGATGCGATTTACCTCAACGAATCCACCTCAACGACCGCCCAAATG
TGGCAGCGTCTGAACATGCGCAACCCGGGCAGCTATTACTTCTGCGCAGCAGGAGGGCTCGGCTTTGCC
CTGCCAGCAGCGATAGGAGTTCAACTGGCGGAACCGGATCGACAAGTCATCGCTGTCATCGG**CGACGGG
TCAGCCAACTA**

Figure 21. Nucleotide sequence of the 1,253-bp PCR product derived from primers BFDC_F and BFDC_R in amplifying genomic DNA from *P. stutzeri* ST-201. The bold letters are primers in both ends.

4.3 Identity of 1,253-bp PCR product

Using the primer sequence as a reference of reading frame, deduced amino acid sequence of 1,253-bp PCR product showed perfect matching with that of the remaining amino acid as shown in Figure 22. The evidence strongly confirmed that correct priming by both N-terminal degenerate primers and internal primers occurred. Thus, the PCR product could then be used as a *Ps*BFDC gene (*dpgB*)-specific probe.

GIDTVFGNPGSNELPFLKDFPEDFRYILALQEACVVGIADGYAQASRKPAFINLHSAAGTGNAMGAMSN
AWNCHSPLIVTAGQQNRAMIGVEALLTNVDAASLPRPLVKWSYEPASAAEVPHAMSRAIHMASMAPRGP
VYLSVPYDDWDKEADPQSHHLYDRSVNSAVRLNDQDLEVLVEALNSASNPAIVLGPDVDSANANADCVT
LAERLKAPVWVAPSAPRCPFPTRHPCFRGLMPAGIAAISQLLEGHDVVLVIGAPVFRYHQYDPGQYLKP
GTRLISITCDPLEAARAPMGDAIVADIGTMTAALASRIGESERQLPAVLPSPERVNQDAGRLRPETVFD
TLNEMAPEDAIYLNESTSTTAQMWQRLNMRNPGSYYFCAAGGLGFALPAAIGVQLAEPDRQVIAVIGDG
SAN

Figure 22. Deduced amino acid sequence translated from the 1,253-bp PCR product. Bold letters show the amino acid sequences that are in agreement with the known amino acid sequence determined by protein sequencing of the N-terminal peptide. Underlined letters are amino acid sequences encoded by primer sequences.

4.4 Similarity search of 1,253-bp PCR product

The deduced amino acid sequence of the 1,253-bp PCR product was analyzed for sequence similarity to the existing protein sequences available in the database at GenBank and SwissProt at the National Center for Biotechnology Information (Bethesda, MD) using the BLAST network server. By performing BLASTp search against non-redundant protein sequences, the results revealed that the score and E-value showed significant similarity to known BFDC from *P. putida* ATCC 12633 (*Pp*BFDC). This information suggested that the 1,253-bp PCR product was potentially a part of the gene encoding for BFDC enzyme. Result of BLASTp search on the database using the translated amino acid sequence of the 1,253-bp PCR product is shown in Figure 23.

RID: K8PW1T6W011

Sequences producing significant alignments:		Score (Bits)	E Value	
pdb|1YNO|A	Chain A, High Resolution Structure Of Benzoylforma...	755	0.0	S
sp|P20906|MDLC_PSEPU	Benzoylformate decarboxylase (BFD) (BFDC...	755	0.0	
pdb|2FWN|A	Chain A, Phosphorylation Of An Active Site Serine ...	755	0.0	S
pdb|2FN3|A	Chain A, High Resolution Structure Of S26a Mutant ...	754	0.0	S
pdb|1PI3|A	Chain A, E28q Mutant Benzoylformate Decarboxylase ...	754	0.0	S
pdb|1PO7|A	Chain A, High Resolution Structure Of E28a Mutant ...	753	0.0	S
ref|YP_001350945.1|	benzoylformate decarboxylase [Pseudomonas...	525	2e-147	G
ref|YP_793369.1|	benzoylformate decarboxylase [Pseudomonas ae...	523	1e-146	G
ref|NP_253588.1|	benzoylformate decarboxylase [Pseudomonas ae...	523	1e-146	G
ref|ZP_01367918.1|	hypothetical protein PaerPA_01005073 [Pseu...	523	1e-146	

> sp|P20906|MDLC_PSEPU Benzoylformate decarboxylase (BFD) (BFDC)
gb|AAC15502.1| benzoylformate decarboxylase [Pseudomonas putida]
Length=528

Score = 755 bits (1950), Expect = 0.0, Method: Composition-based stats.
Identities = 382/417 (91%), Positives = 402/417 (96%), Gaps = 0/417 (0%)

```
Query  1    GIDTVFGNPGSNELPFLKDFPEDFRYILALQEACVVGIADGYAQASRKPAFINLHSAAGT  60
            GIDTVFGNPGSNELPFLKDFPEDFRYILALQEACVVGIADGYAQASRKPAFINLHSAAGT
Sbjct  16   GIDTVFGNPGSNELPFLKDFPEDFRYILALQEACVVGIADGYAQASRKPAFINLHSAAGT  75

Query  61   GNAMGAMSNAWNCHSPLIVTAGQQNRAMIGVEALLTNVDAASLPRPLVKWSYEPASAAEV  120
            GNAMGA+SNAWN HSPLIVTAGQQ RAMIGVEALLTNVDAA+LPRPLVKWSYEPASAAEV
Sbjct  76   GNAMGALSNAWNSHSPLIVTAGQQTRAMIGVEALLTNVDAANLPRPLVKWSYEPASAAEV  135

Query  121  PHAMSRAIHMASMAPRGPVYLSVPYDDWDKEADPQSHHLYDRSVNSAVRLNDQDLEVLVE  180
            PHAMSRAIHMASMAP+GPVYLSVPYDDWDK+ADPQSHHL+DR V+S+VRLNDQDL++LV+
Sbjct  136  PHAMSRAIHMASMAPQGPVYLSVPYDDWDKDADPQSHHLFDRHVSSSVRLNDQDLDILVK  195

Query  181  ALNSASNPAIVLGPDVDSANANADCVTLAERLKAPVWVAPSAPRCPFPTRHPCFRGLMPA  240
            ALNSASNPAIVLGPDVD+ANANADCV LAERLKAPVWVAPSAPRCPFPTRHPCFRGLMPA
Sbjct  196  ALNSASNPAIVLGPDVDAANANADCVMLAERLKAPVWVAPSAPRCPFPTRHPCFRGLMPA  255

Query  241  GIAAISQLLEGHDVVLVIGAPVFRYHQYDPGQYLKPGTRLISITCDPLEAARAPMGDAIV  300
            GIAAISQLLEGHDVVLVIGAPVFRYHQYDPGQYLKPGTRLIS+TCDPLEAARAPMGDAIV
Sbjct  256  GIAAISQLLEGHDVVLVIGAPVFRYHQYDPGQYLKPGTRLISVTCDPLEAARAPMGDAIV  315

Query  301  ADIGTMTAALASRIGESERQLPAVLPSPERVNQDAGRLRPETVFDTLNEMAPEDAIYLNE  360
            ADIG M +ALA+ + ES RQLP   P P +V+QDAGRL PETVFDTLN+MAPE+AIYLNE
Sbjct  316  ADIGAMASALANLVEESSRQLPTAAPEPAKVDQDAGRLHPETVFDTLNDMAPENAIYLNE  375

Query  361  STSTTAQMWQRLNMRNPGSYYFCAAGGLGFALPAAIGVQLAEPDRQVIAVIGDGSAN  417
            STSTTAQMWQRLNMRNPGSYYFCAAGGLGFALPAAIGVQLAEP+RQVIAVIGDGSAN
Sbjct  376  STSTTAQMWQRLNMRNPGSYYFCAAGGLGFALPAAIGVQLAEPERQVIAVIGDGSAN  432
```

Figure 23. BLASTp search result showed the protein sequences producing high scores homology to that of the translated product of 1,253-bp PCR product.

4.5 Subgenomic DNA library construction and isolation of positive clone

4.5.1 Southern hybridization of complete digestion of genomic DNA

Southern hybridization analysis of DNA fragments generated from complete digestion of genomic DNA and detecting with the digoxigenin-labeled 1,253–bp *dpgB*-specific probe showed that *Eco*RI combined with *Hin*dIII or *Sal*I gave positive bands of about 5-7 kb as shown in Figure 24 and *Eco*RV or *Pst*I alone gave positive bands of 4 kb as shown in Figure 25.

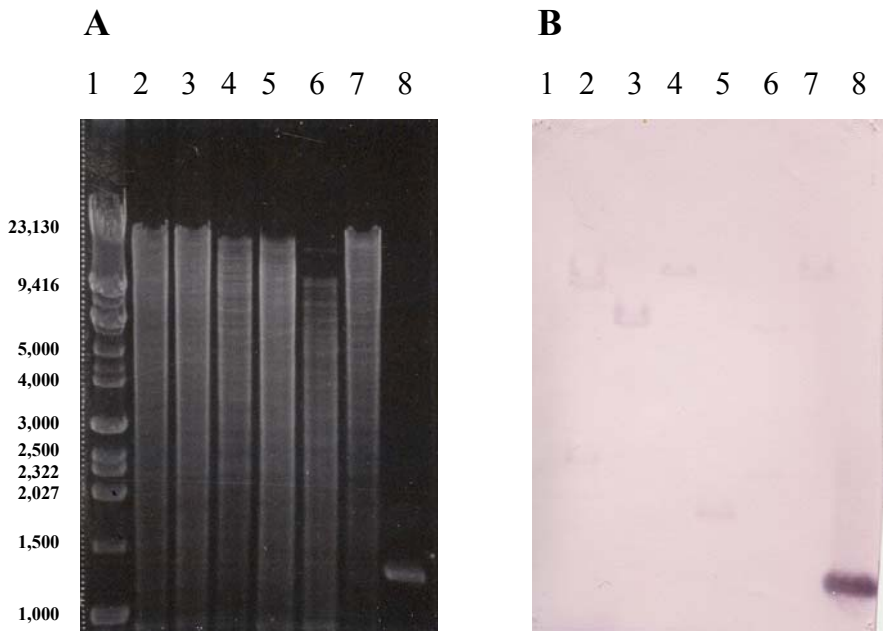

Figure 24. (A) Agarose gel electrophoresis of complete double digestion of *P. stutzeri* ST-201 genomic DNA by two restriction enzymes. (B) Southern hybridization of the corresponding gel with the digoxigenin-labeled 1,253-bp PCR product (*dpgB* gene-specific probe).

Lane 1: λ DNA/*Hin*d III markers and M 11 1Kb DNA Ladder
Lane 2: complete digestion of genomic DNA by *Eco*RI+*Bam*HI
Lane 3: complete digestion of genomic DNA by *Eco*RI+*Hin*dIII
Lane 4: complete digestion of genomic DNA by *Eco*RI+*Not*I
Lane 5: complete digestion of genomic DNA by *Eco*RI+*Sac*I
Lane 6: complete digestion of genomic DNA by *Eco*RI+*Sal*I
Lane 7: complete digestion of genomic DNA by *Eco*RI+*Spe*I
Lane 8: 1,253-bp PCR product

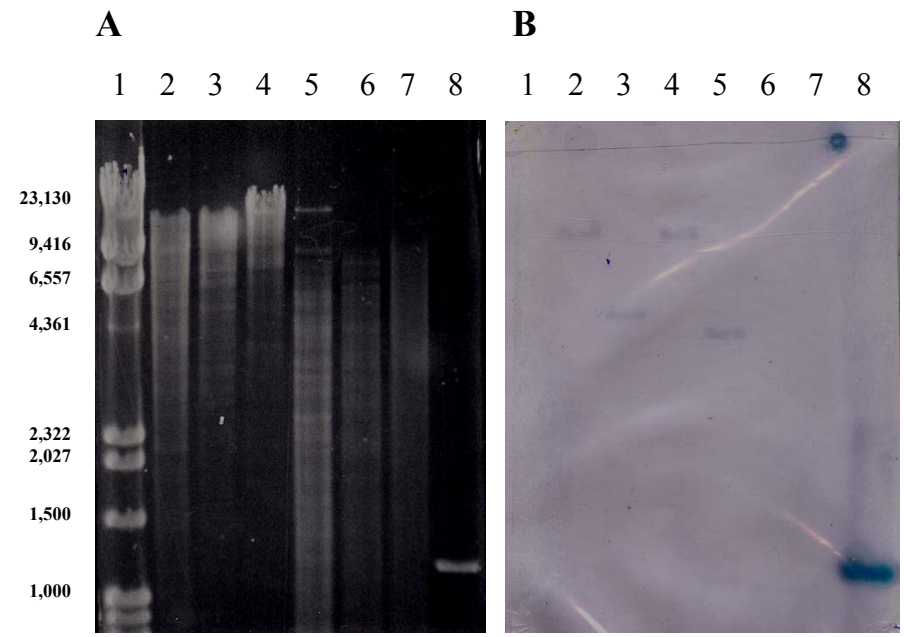

Figure 25. (A) Agarose gel electrophoresis of complete single digestion of *P. stutzeri* ST-201 genomic DNA by one restriction enzyme. (B) Southern hybridization of the corresponding gel with the digoxigenin-labeled 1,253-bp PCR product (*dpgB* gene-specific probe).

Lane 1: λ DNA/*Hin*d III markers and M 13 100 bp + 1.5 Kb DNA Ladder
Lane 2: complete digestion of genomic DNA by *Eco*RI
Lane 3: complete digestion of genomic DNA by *Eco*RV
Lane 4: complete digestion of genomic DNA by *Hin*dIII
Lane 5: complete digestion of genomic DNA by *Pst*I
Lane 6: complete digestion of genomic DNA by *Pvu*II
Lane 7: complete digestion of genomic DNA by *Xho*I
Lane 8: 1,253-bp PCR product

Among the enzymes used, *Eco*RI combined with *Hin*dIII and *Pst*I alone were selected to generate a DNA pool for construction of enriched subgenomic DNA library. This was based on the assumption that the whole *dpgB* gene which encoded for the 55 kDa *Ps*BFDC should be about 1.6 Kb in size and should reside in restriction fragments of 5-7 kb or 4 kb.

4.5.2 Colony hybridization of the subgenomic library

The first subgenomic DNA library was constructed by transforming ligated products of the 5-7 Kb *Eco*RI-*Hin*dIII fragments with *Eco*RI- *Hin*dIII-digested pBluescript II SK into *E. coli* JM 109. The second subgenomic DNA library was constructed by transforming ligated products of the 4 Kb *Pst*I fragments with *Pst*I-digested pBluescript II SK into *E. coli* JM 109. The two libraries were screened by colony hybridization with the digoxigenin-labeled 1,253-bp *dpgB* probe. Of about four hundred colonies screened in each library, one positive colony with strong hybridization signal were found as shown in Figure 26 and 27 which designated as pBCH1 and pBCH2, respectively.

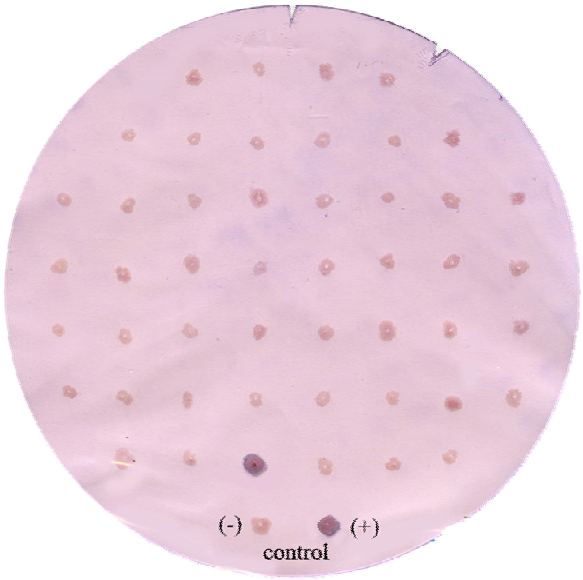

Figure 26. Colony hybridization of the enriched subgenomic DNA library of 5-7 kb *Eco*RI-*Hin*dIII restriction fragments with the digoxigenin-labeled 1,253-bp *dpgB* probe. Result showed one positive colony with a distinctive color as compared to the background. *E. coli* JM 109 harboring pBluescript II SK was used as the negative control (-). *E. coli* JM 109 with pGEM-T Easy containing 1,253-bp PCR product was used as the positive control (+).

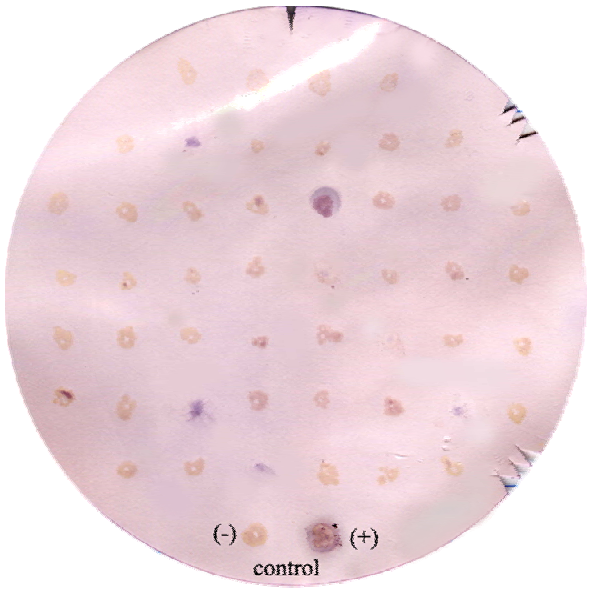

Figure 27. Colony hybridization of the enriched DNA library of 4 kb *Pst*I restriction fragments with the digoxigenin-labeled 1,253-bp *dpgB* probe. Result showed one positive colony with a distinctive color as compared to background. *E. coli* JM 109 harboring pBluescript II SK was used as the negative control (-). *E. coli* JM 109 with pGEM-T Easy containing 1,253-bp PCR product was used as the positive control (+).

4.6 Nucleotide sequence of positive DNA restriction fragment from library screening

4.6.1 Nucleotide sequence of 6.3 kb *Eco*RI- *Hin*dIII insert of pBCH1

The nucleotide sequencing of 6.3 kb *Eco*RI- *Hin*dIII insert DNA in pBCH1 revealed that the insert was 6,273 base pairs long (Figure 28) with an open reading frame (ORF) of 1,581 base pairs which was denoted *dpgB* (Figure 29) and encoded a protein of 526 amino acids with a deduced molecular mass of 56 kDa.

AAGCTTCTGCAACGCACCAACTCATCCCACCGCCACGCCAAAGATGTTCAGTACGAGATCGAGTCCGTCGCCAACAC
AGCCAATAGTTCCATTGCCTCCCTGTTTAGCGATGCGCGTGCGTTCGCGACGTTCATGGTCTGGGTTGCTTTCGGGA
TGTGCATGCTGATTGTCTATGGGTTCAGTCTTCCCTTGGAGCAGAACTTCCTCCTGTTCGGCTTGCCAGGCGTGGTT
GCGGTAATCGCAGAGCTGCTGATTTCACAACGTCATTCAAGCCGGGTGTCTGTGAGCACTCGTCTAAAGCAGAACGC
TTAGTACCTTTCGCTACACCCCGTCCAGGTTCGCAACTCGCCAGCGTACGGGTTTCGGTGCGGCTCTAAAGCTGCGC
CGTTTTTTCAAAAAGTTTCCCCGGACCATTACATGGTTTAGGTAACTGCGTCCAAAAAATACTCGAGCACAAAAGTC
GGAGTGGGGCAGATTAAGCATATTTGTCGTATAGGCTTGGCTGTGATTGGTCGTTGCGTCTTAAGTCATTTAAAGCG
GCGCGTTAAAAGGCTTGATTTCGAAGTTCGTAATACTAAGGTCAAAGCCCGATATGGAGCTGGCTTTGACGAGAATC
GATTGATAACTAGCTATATCTGGAAGTTCTGGTAATCCGCCGAGCGACATGCTTCGAATATCTAAGGAGTGTCGCGC
TGCATAATTGCGAGAGAGGAACTGCTATGGGCATAGAATTGTTGAGCGATCGGAGCAAGGTTTATGACTTCGCAGAT
CCTCATGTGGTGTCCGCGTATGTGAATCAGCATGTAGGCAATCACTCTATAGCGATTTCGGATGGGCGAAGCCAGGC
AATGCTCATCCATCGACAGGTCGCTGATCTGGATTTCTGTCGAATCAGATATGGGAGTGAAACATGTGTTACTTCTA
CAGCGCTTCGCGATAAATATCACATCCAAATTATGCTAGGCGGTAGTTGCTTGCAGCGCATCTCAGGCACGCATCGC
GTTCTCTCGGTAGGTGATCTGGTCGTGATCAATCCAAACGATCCTGTAGATTTGACTTACTCTCATGACTGCGAGAA
ATTTATTCTAAAAGTNCCCTGTCAAACTGGTGGAGGCAGTATGTGATGATCAGCATTGGTGCCGCCCATCAACAGGG
CTCCGTTTTGATGAGAAGGTTTATCAACTTAATGATTTGCAAGGAATGGTTCAGCTGCTCAGTCTTGTTTGTGGTGA
GATTGAAAATGAAAGCATAATTCGAGCAGTTCAAGAGCATTACGTTCAAATAATAATCATCAAAATTTTGACGTCGT
TACTTACAAACCTAGAGTACACGGCGGTGGGCGTTCAGAATCAACTGCTCCGCAAGGTATTGCATCATATTGAAGAT
AATCTGAAGCAGGATATAACCCCTGAAGGACTGGCTAAATATGCCAACGTCAGCCTGCGTAGCCTTTACGTTCTGTT
CGATCAGTATTTAGGTGAACCGCCGCGACGTTACTTTGTCAGAAGGAGGTTGGAACAGGTGCGCGCTGCGCTTCTAG
GTGCTGAGGGGCGCAGGAAGAACGTGACGGAGATTGCGATGGATTACGGCTTCACGCACTTGGGGCGGTTTTCAGCT
GAATACAAAGCTCATTTTGCTGAGCTTCCCTCAGAGACCTTGAAGCATCGTCCCAATAACTGAAAGCACAGGGCCCG
CCTTGGCGGGCCCTGTGCAATGGCTCAGGCCAGGTATTTCTCGATTTCTTTCTCGCGCCAGATGATTCCAACGCCTG
GAAGATCCGGAATAACTGCATTGCCAGCTTCGAAATTCAGCGTGGGCTCCATCACGCTAGCGGCAAGATCCAAACGC
TCCAGCCAGTGGGCAGTTGGAGTAGCAGCCAACACGTGTGCACTGATTTCTTGGAACAGATGGCTGGACATGGGCAC
GCCGAACTGCTGAGCCAGCGCACTGGTCCGGAGCCAACCAGTCACTCCACCAATCTCCATTGCGTCTGGCATTGCCA
GCCGACATGCACCAGCTGTCAGTGCCTTGAACATTTCCTCCGGGCCGAACCAGTTTTCGCCCATCTGCACAGGGATA
TCCAGACTGTTTTGGATGCGCTGGTGGCCTGCATAGTCATGCTGCAAAGTTGGCTCTTCGATCCGGGTGCCGCCCGC
GTCCTGCAGGGCCAAGCCACGCTTGAGGGCAGCTGGCACGTCCAGGCTCTGGTTATAATCGACCAAGATTTCAAAAT
CATCACCGACCGCCTCGCGGATGCTTCCAACTACAGCCAGGTCTTTATCCAGCGTCGGATAACCAATCTTGGTCTTA
ACCGCTCGGAAGCCTGACTTAGCAGCAGTCACTGCGCGTTCAGTCGCGAGCTTTACACCGTCCAGACTGTCGCTGTC
ATAGGCAGGGATCGGGCGAGCCTTGGCGCCGAGCAGATTAACCAGCGGCGTTTCGTGAACCTTAGCCAGAGCATCTC

Figure 28. The 6.3 kb *Eco*RI-*Hin*dIII insert DNA in pBCH1.The *Eco*RI and *Hin*dIII sites are at 3′ and 5′ end of the fragment, respectively. This fragment contains the whole *DpgB* gene encoding for *Ps*BFDC shown in bold letters. The start codon ATG and stop codon TGA of the ORF encoding for *Ps*BFDC are underlined.

AAGCCGCCATGTCGATCCCTGCAGTTGCCATGCGGATAGCCGCGCTGGCGATACTGTGATTCGCACAACGGTAATGG
GCTTCTGCGACAAAAGGTCTCCTCAAATTTGATGATTGCCACCCACTTTTCATGCATAACGGGCCAGCTGCGTCCGG
TTCTGCGCTCCAGCTTGGCCATCGCGTTATTGAGGTGGGTGCGCACTGTCGTGAACCCTATTCCGAGTTGGCGGGCC
ACCTCTTTAACACTGGCACCAGCCGCCACTAGCTTGGCAACTCCGCTTCCCTAAACGACAACAAGTGCTTTCGATCG
GGTGCGGATGCGAAAGCCCTGGCGAAGTATGGTTGAAGCGTCAGCAAGAGCCGCTCTTCGCGCTCGCTGAAAGGCTC
TCGGCCTCTGCCTCTCCATATCCTAAAATCGCCCGTGCTCCATGTCCGCAGGGCGTAGAAAGTCGTTATAGATCTCA
CTGTGAAGCAGGGCAGGGCGCGGCACATGGCAATCGACGCACGCCGGCTTGGCCACTCTGCGCATTACCGGGGTCAC
CATGTCTACCCGATGAAAATGCTGCTGGTACGCCTCCATCTTGTACCCGTCGATGTTGAAGGCACACGGCTGACAGG
GTCGCTGCCCACGCTCATCCCACATAACAGAGGCGATGTGGTCGGCATCGAGAAGGGTCGCCACAGCTTGGAGGGTA
GCTGCGCGAGCATCAGGCTTTCCCTGACACTCAGCCAGAAGCCAGACAAGCTCGGCTATCTGATCCAGGTCGGTTTC
TTGCTGCACTGTCACCATTGACCCCTCCGGAAACTCTGTGGATACGCCCCAAAAACGGAATCAAATTAAATAAGGCG
CATCTATAGATAAATCAAAAATTTATCTATTTGATCTATTTGACCCTCGCTTCTATCGTGGGCTTCGTAATTTGGTA
AGAGATATCCATC**ATG**GCATCGGTACACAGCATCACTTATGAGCTCCTCCGCCGTCAGGGCATCGACACGGTGTTCG
GCAACCCTGGTTCCAACGAACTGCCGTTTCTGAAGGATTTCCCAGAGGACTTTCGCTACATCCTCGCGTTGCAGGAA
GCGTGCGTGGTAGGTATTGCTGATGGTTACGCCCAGGCCAGTCGCAAACCTGCATTCATTAACCTGCATTCTGCAGC
GGGCACGGGCAACGCGATGGGCGCGATGAGTAACGCCTGGAACTGCCACTCTCCGCTGATCGTGACAGCTGGTCAGC
AAAACCGAGCGATGATTGGGGTTGAGGCACTGTTGACCAACGTCGACGCCGCCAGCCTTCCCCGTCCTCTCGTCAAA
TGGAGTTACGAGCCGGCGAGCGCTGCGGAAGTGCCACATGCAATGAGCCGAGCTATTCACATGGCGAGCATGGCACC
TCGCGGGCCTGTGTATCTCTCTGTGCCATACGATGATTGGGACAAGGAAGCGGATCCTCAGTCTCATCACCTGTACG
ATCGGAGTGTCAACTCAGCTGTTCGTCTGAATGACCAAGATCTGGAAGTGCTGGTGGAAGCTCTCAACAGCGCGTCC
AACCCCGCAATTGTGCTCGGCCCAGACGTCGACTCCGCGAATGCAAATGCTGATTGCGTAACATTGGCCGAACGACT
CAAAGCTCCTGTATGGGTTGCCCCTTCTGCCCCGCGCTGCCCCTTCCCAACCCGACACCCCTGTTTCCGAGGGCTTA
TGCCTGCCGGTATCGCAGCGATCTCTCAACTGCTGGAGGGTCACGATGTGGTGTTGGTTATAGGCGCCCCCGTATTC
CGCTACCACCAGTACGATCCAGGTCAGTACCTGAAACCAGGTACCCGCTTGATTTCGATCACCTGTGACCCGCTCGA
AGCGGCACGCGCGCCAATGGGCGATGCGATTGTTGCAGACATCGGTACCATGACCGCTGCGCTCGCCAGCCGCATCG
GCGAAAGCGAACGCCAACTTCCAGCGGTTCTCCCCAGTCCGGAGAGGGTTAACCAGGATGCCGGGCGTCTGCGTCCA
GAAACGGTGTTTGACACACTCAACGAGATGGCTCCTGAGGATGCGATTTACCTCAACGAATCCACCTCAACGACCGC
CCAAATGTGGCAGCGTCTGAACATGCGCAACCCGGGCAGCTATTACTTCTGCGCAGCAGGAGGGCTCGGCTTTGCCC
TGCCAGCAGCGATAGGAGTTCAACTGGCGGAACCGGATCGACAAGTCATCGCTGTCATCGGCGACGGGTCAGCCAAC
TACAGCATTAGTGCCTTGTGGACAGCAGCCCATTACAACATCCCAGCCATCTTCTTGATCATGAACAACGGCACATA
CGGTGCTCTTCGATGGTTTGCTGGTGTGCTGGAAGCCGAGAACGTTCCAGGCTTGGATGTGCCAGGAATCGACTTCT
GCGCGATCGCCAAGGGATATGGTATTCCTGCGCTGAAAGCTGACAATCTTGAGCAGCTCAAAGGCTCCATTCATGAA
GCGCTGTCTGCCAAAGGGCCGGTATTGATCGAGGTCAGCACGGTCAGCCTG**TGA**CGTGAGATTTGACGATGAGTCAG
CAGAATATATTTAGCGTCGAAGACTAGGCATTGAAATCGAAGGTTTGCCTCACAGTGACACGCGGTTGCTAGCAATT
GCTTGCGTCATTGAAGGCATTTTGGGCAGAGGTCCATCTCCTGAGCGAGGAACGTGAAGGCAGCCCAACACTCCATG
TGGCAACTGCTCTGTCTTCTGGAACCAGTCGCTACCCATCGAGCTCGTAACCCGAATAGAGGGATTGTCC***ATGAATT***
ATCTGTCCCCGGCGATGATCGACTCGCTGTTCTCAGCTCAAAAGGCTTTCTTCGCGACCCGCGCAACAGCCGATGTT
GGCTTCAGAAAGCAGGCTTTAAAACGGCTCCGAGACGCGGTGATCAACAACAAGGAGTTCTTCTATTCCGCGTTAGC
AGAAGACTTGGGTAAAACCAGGGAAGTGGTTGACCTAGCGGAAATCGGTGAAGTCCTGCATGAAATCGACTTCGCCC
TGGCGAACCTGGATGAATGGATCGTTCCGGAGTCTGTTCCCACTCCGGAAATTATCGCGCCCTCGGAGTGTTACATC
GTCCAGGAGCCTTACGGTGTCACCTACATCATTGGCCCGTTCAACTACCCGGTAAATCTGACACTGACCCCTCTGAT
CGGCGCCATTATCGGTGGCAACACCTGCATCATCAAACCGTCTGAGACGACTCCCGAGACGTCTCGCGTTATCGAGA
AAATCATCGCGGAAGCATTCTCCCCCGAATACGTCACCGTGATTCAAGGTGGGCTCGCAGAGAACAGCCATCTTTTG
AGCCTGCCTTTCGATTTCATCTTCTTTACTGGCAGCCCCAACGTCGGGAAGGTGGTCATGAAGGCGGCGGCTGAGCA
TCTGACGCCGGTTGTGCTTGAACTTGGGGGAAAATGCCCCCTCATCGTTCTGCCTGACGCTGACCTCGACCAAACTG
TTGATCAATTGATGTTCGGTAAATTCATCAACAGTGGCCAAACCTGTATCGCACCCGATTACCTCTATGCGCATCGC
AGCGTCAAAGATGCTTTGCTGCAACGGGTGGTTGAGCGGGTGAAGAACGACCTGCCTAAGGTTAATTCGACCGGCAA
GATCGTAACCTCACGCCAGGTGGTGCGTTTGGTTTCCTTGCTTGAAGAGACGCGTGGAAAGGTGTTGGTCGGGGCCC
AGGCCGACGTAGACAACAGAGCATTCAGCGCAACGGTAGTGGACAGCGTTCAATGGGACGACCCGCTTATGGCGGAG
GAGCTCTTCGGGCCGATTTTGCCAGTGCTTGAATTC

Figure 28. The 6.3 kb *Eco*RI-*Hin*dIII insert DNA in pBCH1.The *Eco*RI and *Hin*dIII sites are at 3′ and 5′ end of the fragment, respectively. This fragment contains the whole *DpgB* gene encoding for *P*sBFDC shown in bold letters. The start codon ATG and stop codon TGA of the ORF encoding for *P*sBFDC are underlined (continued).

(A)

-35 Putative promoter region -10 +1 Start site Putative RBS

---------**TTGATC**TATTTGACCCTCGCTTC**TATCGT**GGGCT**T**CGTAATTTGGTAA**GAG**ATATCCATC

Start codon

ATGGCATCGGTACACAGCATCACTTATGAGCTCCTCCGCCGTCAGGGCATCGACACGGTGTTCGGCAAC
CCTGGTTCCAACGAACTGCCGTTTCTGAAGGATTTCCCAGAGGACTTTCGCTACATCCTCGCGTTGCAG
GAAGCGTGCGTGGTAGGTATTGCTGATGGTTACGCCCAGGCCAGTCGCAAACCTGCATTCATTAACCTG
CATTCTGCAGCGGGCACGGGCAACGCGATGGGCGCGATGAGTAACGCCTGGAACTGCCACTCTCCGCTG
ATCGTGACAGCTGGTCAGCAAAACCGAGCGATGATTGGGGTTGAGGCACTGTTGACCAACGTCGACGCC
GCCAGCCTTCCCCGTCCTCTCGTCAAATGGAGTTACGAGCCGGCGAGCGCTGCGGAAGTGCCACATGCA
ATGAGCCGAGCTATTCACATGGCGAGCATGGCACCTCGCGGGCCTGTGTATCTCTCTGTGCCATACGAT
GATTGGGACAAGGAAGCGGATCCTCAGTCTCATCACCTGTACGATCGGAGTGTCAACTCAGCTGTTCGT
CTGAATGACCAAGATCTGGAAGTGCTGGTGGAAGCTCTCAACAGCGCGTCCAACCCCGCAATTGTGCTC
GGCCCAGACGTCGACTCCGCGAATGCAAATGCTGATTGCGTAACATTGGCCGAACGACTCAAAGCTCCT
GTATGGGTTGCCCCTTCTGCCCCGCGCTGCCCCTTCCCAACCCGACACCCCTGTTTCCGAGGGCTTATG
CCTGCCGGTATCGCAGCGATCTCTCAACTGCTGGAGGGTCACGATGTGGTGTTGGTTATAGGCGCCCCC
GTATTCCGCTACCACCAGTACGATCCAGGTCAGTACCTGAAACCAGGTACCCGCTTGATTTCGATCACC
TGTGACCCGCTCGAAGCGGCACGCGCGCCAATGGGCGATGCGATTGTTGCAGACATCGGTACCATGACC
GCTGCGCTCGCCAGCCGCATCGGCGAAAGCGAACGCCAACTTCCAGCGGTTCTCCCCAGTCCGGAGAGG
GTTAACCAGGATGCCGGGCGTCTGCGTCCAGAAACGGTGTTTGACACACTCAACGAGATGGCTCCTGAG
GATGCGATTTACCTCAACGAATCCACCTCAACGACCGCCCAAATGTGGCAGCGTCTGAACATGCGCAAC
CCGGGCAGCTATTACTTCTGCGCAGCAGGAGGGCTCGGCTTTGCCCTGCCAGCAGCGATAGGAGTTCAA
CTGGCGGAACCGGATCGACAAGTCATCGCTGTCATCGGCGACGGGTCAGCCAACTACAGCATTAGTGCC
TTGTGGACAGCAGCCCATTACAACATCCCAGCCATCTTCTTGATCATGAACAACGGCACATACGGTGCT
CTTCGATGGTTTGCTGGTGTGCTGGAAGCCGAGAACGTTCCAGGCTTGGATGTGCCAGGAATCGACTTC
TGCGCGATCGCCAAGGGATATGGTATTCCTGCGCTGAAAGCTGACAATCTTGAGCAGCTCAAAGGCTCC
ATTCATGAAGCGCTGTCTGCCAAAGGGCCGGTATTGATCGAGGTCAGCACGGTCAGCCTG

Stop codon **Putative ρ-independent transcriptional terminator**

TGACGTGAGATTTGACGATGAGTCAGCAGAATATATTTAGCGTCGAAGACTAGGCATTGAAATCGAAGG
TTT---------

(B)

MASVHSITYELLRRQGIDTVFGNPGSNELPFLKDFPEDFRYILALQEACVVGIADGYAQASRKPAFINL
HSAAGTGNAMGAMSNAWNCHSPLIVTAGQQNRAMIGVEALLTNVDAASLPRPLVKWSYEPASAAEVPHA
MSRAIHMASMAPRGPVYLSVPYDDWDKEADPQSHHLYDRSVNSAVRLNDQDLEVLVEALNSASNPAIVL
GPDVDSANANADCVTLAERLKAPVWVAPSAPRCPFPTRHPCFRGLMPAGIAAISQLLEGHDVVLVIGAP
VFRYHQYDPGQYLKPGTRLISITCDPLEAARAPMGDAIVADIGTMTAALASRIGESERQLPAVLPSPER
VNQDAGRLRPETVFDTLNEMAPEDAIYLNESTSTTAQMWQRLNMRNPGSYYFCAAGGLGFALPAAIGVQ
LAEPDRQVIAVIGDGSANYSISALWTAAHYNIPAIFLIMNNGTYGALRWFAGVLEAENVPGLDVPGIDF
CAIAKGYGIPALKADNLEQLKGSIHEALSAKGPVLIEVSTVSL

Figure 29. *Ps*BFDC ORF of 1,581 bp which was denoted as *dpgB* (A) and its deduced amino acids of 526 residues (B) are located in the the 6.3 kb *Eco*RI-*Hin*dIII insert DNA in pBCH1. The start codon ATG and stop codon TGA of *dpgB* are in bold letters and highlighted. The putative promoter sequences (-35 and -10), +1 start site, putative ribosome binding site (RBS) and putative ρ-independent transcriptional terminator are in bold letters and underlined.

4.6.2 Nucleotide sequence of 4 kb-*Pst*I insert of pBCH2

The 4 kb *Pst*I insert DNA in pBCH2 was subjected to DNA sequence determination at the BSU, NSTDA, Thailand. The result of nucleotide sequencing was shown as a 4,041 bps long in Figure 30. Sequencing of pBCH2 identified a region which corresponded to part of the *dpgB* gene. However, this insert also carried the full length ORF of 1,311 bp downstream of *dpgB*. The ORF, denoted *dpgC* which was later identified as a gene encoding for benzaldehyde dehydrogenase (*Ps*BADH) as shown in Figure 31, transcribed in the same direction as *dpgB* and encoded a protein of 436 amino acids with a deduced molecular mass of 47.7 kDa.

CTGCAGCGGGCACGGGCAACGCGATGGGCGCGATGAGTAACGCCTGGAACTGCCACTCTCCGCTGATCG
TGACAGCTGGTCAGCAAAACCGAGCGATGATTGGGGTTGAGGCACTGTTGACCAACGTCGACGCCGCCA
GCCTTCCCCGTCCTCTCGTCAAATGGAGTTACGAGCCGGCGAGCGCTGCGGAAGTGCCACATGCAATGA
GCCGAGCTATTCACATGGCGAGCATGGCACCTCGCGGGCCTGTGTATCTCTCTGTGCCATACGATGATT
GGGACAAGGAAGCGGATCCTCAGTCTCATCACCTGTACGATCGGAGTGTCAACTCAGCTGTTCGTCTGA
ATGACCAAGATCTGGAAGTGCTGGTGGAAGCTCTCAACAGCGCGTCCAACCCCGCAATTGTGCTCGGCC
CAGACGTCGACTCCGCGAATGCAAATGCTGATTGCGTAACATTGGCCGAACGACTCAAAGCTCCTGTAT
GGGTTGCCCCTTCTGCCCCGCGCTGCCCCTTCCCAACCCGACACCCCTGTTTCCGAGGGCTTATGCCTG
CCGGTATCGCAGCGATCTCTCAACTGCTGGAGGGTCACGATGTGGTGTTGGTTATAGGCGCCCCCGTAT
TCCGCTACCACCAGTACGATCCAGGTCAGTACCTGAAACCAGGTACCCGCTTGATTTCGATCACCTGTG
ACCCGCTCGAAGCGGCACGCGCGCCAATGGGCGATGCGATTGTTGCAGACATCGGTACCATGACCGCTG
CGCTCGCCAGCCGCATCGGCGAAAGCGAACGCCAACTTCCAGCGGTTCTCCCCAGTCCGGAGAGGGTTA
ACCAGGATGCCGGGCGTCTGCGTCCAGAAACGGTGTTTGACACACTCAACGAGATGGCTCCTGAGGATG
CGATTTACCTCAACGAATCCACCTCAACGACCGCCCAAATGTGGCAGCGTCTGAACATGCGCAACCCGG
GCAGCTATTACTTCTGCGCAGCAGGAGGGCTCGGCTTTGCCCTGCCAGCAGCGATAGGAGTTCAACTGG
CGGAACCGGATCGACAAGTCATCGCTGTCATCGGCGACGGGTCAGCCAACTACAGCATTAGTGCCTTGT
GGACAGCAGCCCATTACAACATCCCAGCCATCTTCTTGATCATGAACAACGGCACATACGGTGCTCTTC
GATGGTTTGCTGGTGTGCTGGAAGCCGAGAACGTTCCAGGCTTGGATGTGCCAGGAATCGACTTCTGCG
CGATCGCCAAGGGATATGGTATTCCTGCGCTGAAAGCTGACAATCTTGAGCAGCTCAAAGGCTCCATTC
ATGAAGCGCTGTCTGCCAAAGGGCCGGTATTGATCGAGGTCAGCACGGTCAGCCTGTGACGTGAGATTT
GACGATGAGTCAGCAGAATATATTTAGCGTCGAAGACTAGGCATTGAAATCGAAGGTTTGCCTCACAGT
GACACGCGGTTGCTAGCAATTGCTTGCGTCATTGAAGGCATTTTGGGCAGAGGTCCATCTCCTGAGCGA
GGAACGTGAAGGCAGCCCAACACTCCATGTGGCAACTGCTCTGTCTTCTGGAACCAGTCGCTACCCATC
GAGCTCGTAACCCGAATAGAGGGATTGTCC***ATGAATTATCTGTCCCCGGCGATGATCGACTCGCTGTTC***
TCAGCTCAAAAGGCTTTCTTCGCGACCCGCGCAACAGCCGATGTTGGCTTCAGAAAGCAGGCTTTAAAA
CGGCTCCGAGACGCGGTGATCAACAACAAGGAGTTCTTCTATTCCGCGTTAGCAGAAGACTTGGGTAAA
ACCAGGGAAGTGGTTGACCTAGCGGAAATCGGTGAAGTCCTGCATGAAATCGACTTCGCCCTGGCGAAC
CTGGATGAATGGATCGTTCCGGAGTCTGTTCCCACTCCGGAAATTATCGCGCCCTCGGAGTGTTACATC
GTCCAGGAGCCTTACGGTGTCACCTACATCATTGGCCCGTTCAACTACCCGGTAAATCTGACACTGACC
CCTCTGATCGGCGCCATTATCGGTGGCAACACCTGCATCATCAAACCGTCTGAGACGACTCCCGAGACG
TCTCGCGTTATCGAGAAAATCATCGCGGAAGCATTCTCCCCCGAATACGTCACCGTGATTCAAGGTGGG
CTCGCAGAGAACAGCCATCTTTTGAGCCTGCCTTTCGATTTCATCTTCTTTACTGGCAGCCCCAACGTC

Figure 30. The 4 kb *Pst*I insert DNA in pBCH2. The *Pst*I sites are at both ends of the fragment. This fragment contains the part of *dpgB* gene encoding for *P*sBFDC shown in bold letters and the whole *dpgC* gene encoding for benzaldehyde dehydrogenase (*P*sBADH) shown in italic letters. The start codon ATG and stop codon TAA of the ORF encoding for *P*sBADH are underlined.

GGGAAGGTGGTCATGAAGGCGGCGGCTGAGCATCTGACGCCGGTTGTGCTTGAACTTGGGGGAAAATGC
CCCCTCATCGTTCTGCCTGACGCTGACCTCGACCAAACTGTTGATCAATTGATGTTCGGTAAATTCATC
AACAGTGGCCAAACCTGTATCGCACCCGATTACCTCTATGCGCATCGCAGCGTCAAAGATGCTTTGCTG
CAACGGGTGGTTGAGCGGGTGAAGAACGACCTGCCTAAGGTTAATTCGACCGGCAAGATCGTAACCTCA
CGCCAGGTGGTGCGTTTGGTTTCCTTGCTTGAAGAGACGCGTGGAAAGGTGTTGGTCGGGGCCCAGGCC
GACGTAGACAACAGAGCATTCAGCGCAACGGTAGTGGACAGCGTTCAATGGGACGACCCGCTTATGGCG
GAGGAGCTCTTCGGGCCGATTTTGCCAGTGCTTGAATTCGATGATGTCCCCACCGCAGTCAATCTGATT
AACAAGCACCACCCCAAGCCCTTGGCCGTTTATGTGTTCGGCAAGGACGTGGATCTCGCAAAAGGCATC
ATCAATCAGATCCAGTCCGGTGACGCGCAGGTCAACGGCGTCATGCTTCATGCCTTCTCTCCATACCTT
CCTTTTGGAGGCATTGGTGCGTCAGGTATGGGCGACTATCACGGGCACTACAGCTACCTCACCTTCACG
CACAAAAAATCCGTCAGGATTGTGCCG<u>TAA</u>CTGAAGACGCGGAGCGCGCTGGGTTGAGTAACTACACTG
GGTGAGCTCGTATGTCTATAAGGGGCATCCAGGCGTTCAGATGAAAGCTCACCACTACTGCTCCATCCT
GAACGAGGATGTCATCCCGTGCGTCATCCTCGATCGCCCCAGGCATCAACAAGAGTGGAGAGCGAGACA
CTGATATTGTCTGTATTTTTGCTGCTGATAGTGCATTGAGAAATTTATCTGTGCGGCTGCGTAATGCAA
ATTATCGAACTTCGGGTCCCGTTCGTGGTATTGATATTACAAGTGTGATTGTTAGCTGTTCTTTTTTGC
TGTTCTAATTGAGGGTGTTCGTTATGGCTTTTCAAAATCTACCGTTCTCAAAATCAAGAGCCTACCAAG
GATTGGTGTTTCTAAGCGGCGAGGTGCCGTTCGATAGTGAGGGAAAAATTCCCGCTGGCGTAGGTGCTC
AGACAGAGCTAACCTTGAGTAACATTAGTGCCACACTTGCCCGAGAAGGGCTCAGCTTGGCCGATGTAA
TCAGTGTTACGGTGTATCTGACTAACCGTGATGATTTTGCAGAGTTCAATCGCGTTTACGCTTCTCACT
TCAGTGCCCCCTTACCGGTGAGAACCACTATTTGCACGCAACTGATGATTGATGCGTGCGTTGAGCTGA
CAGTTATCGCCGCTCGCCACTCTTGAGGTTCGCCTTATGAGGACAGTCATAGTACTCGGCGCTGGTATT
GTTGGCGTCTGCACAGCTTTGCAATTGCGTCGCCGTGGCTGGGATGTAACGCTGGTGGATCGCCGCAGT
CCTGGGCAGGAAACTTCCTACGGCAATGCTGGCATTATTCAGCGTGAAGCGGTAATGCCGTACCCGTTC
CCCAGGGATTTAGCCACTCTGCTAAAAGTTCTGCGCAAAGGTGGGGTTGACGTAAACTACCACGCTAAT
GCGATTCCTGCGTTACTGCCGCGACTTGTGCGTTATTGGCAAGCATCGTCACCTCGGTGTTATGCGCTC
TACGCGCAATCGTTCAGATCATTGATCGAACACTGCATTGAAGAGCATCGCGATCTCATCGAGCACGCC
CAGGCTGGGCACTTGATACATACAGAGGGGTGGCTGCAG

Figure 30. The 4 kb *Pst*I insert DNA in pBCH2. The *Pst*I sites are at both ends of the fragment. This fragment contains the part of *dpgB* gene encoding for *P*sBFDC shown in bold letters and the whole *dpgC* gene encoding for benzaldehyde dehydrogenase (*P*sBADH) shown in italic letters. The start codon ATG and stop codon TAA of the ORF encoding for *P*sBADH are underlined (continued).

(A)

-35 Putative promoter region -10 +1 Start site

-------**TTGACG**ATGAGTCAGCAGAA**TATATT**TAGCG**T**CGAAGACTAGGCATTGAAATCGAAGGTTTG
CCTCACAGTGACACGCGGTTGCTAGCAATTGCTTGCGTCATTGAAGGCATTTTGGGCAGAGGTCCATCT
CCTGAGCGAGGAACGTGAAGGCAGCCCAACACTCCATGTGGCAACTGCTCTGTCTTCTGGAACCAGTCG
CTACCCA TCGAGCTCGTAACCCGAATA**GAG**GGATTGTCC

Putative RBS

Start codon

ATGAATTATCTGTCCCCGGCGATGATCGACTCGCTGTTCTCAGCTCAAAAGGCTTTCTTCGCGACCCGC
GCAACAGCCGATGTTGGCTTCAGAAAGCAGGCTTTAAAACGGCTCCGAGACGCGGTGATCAACAACAAG
GAGTTCTTCTATTCCGCGTTAGCAGAAGACTTGGGTAAAACCAGGGAAGTGGTTGACCTAGCGGAAATC
GGTGAAGTCCTGCATGAAATCGACTTCGCCCTGGCGAACCTGGATGAATGGATCGTTCCGGAGTCTGTT
CCCACTCCGGAAATTATCGCGCCCTCGGAGTGTTACATCGTCCAGGAGCCTTACGGTGTCACCTACATC
ATTGGCCCGTTCAACTACCCGGTAAATCTGACACTGACCCCTCTGATCGGCGCCATTATCGGTGGCAAC
ACCTGCATCATCAAACCGTCTGAGACGACTCCCGAGACGTCTCGCGTTATCGAGAAAATCATCGCGGAA
GCATTCTCCCCCGAATACGTCACCGTGATTCAAGGTGGGCTCGCAGAGAACAGCCATCTTTTGAGCCTG
CCTTTCGATTTCATCTTCTTTACTGGCAGCCCCAACGTCGGGAAGGTGGTCATGAAGGCGGCGGCTGAG
CATCTGACGCCGGTTGTGCTTGAACTTGGGGGAAAATGCCCCCTCATCGTTCTGCCTGACGCTGACCTC
GACCAAACTGTTGATCAATTGATGTTCGGTAAATTCATCAACAGTGGCCAAACCTGTATCGCACCCGAT
TACCTCTATGCGCATCGCAGCGTCAAAGATGCTTTGCTGCAACGGGTGGTTGAGCGGGTGAAGAACGAC
CTGCCTAAGGTTAATTCGACCGGCAAGATCGTAACCTCACGCCAGGTGGTGCGTTTGGTTTCCTTGCTT
GAAGAGACGCGTGGAAAGGTGTTGGTCGGGGCCCAGGCCGACGTAGACAACAGAGCATTCAGCGCAACG
GTAGTGGACAGCGTTCAATGGGACGACCCGCTTATGGCGGAGGAGCTCTTCGGGCCGATTTTGCCAGTG
CTTGAATTCGATGATGTCCCCACCGCAGTCAATCTGATTAACAAGCACCACCCCAAGCCCTTGGCCGTT
TATGTGTTCGGCAAGGACGTGGATCTCGCAAAAGGCATCATCAATCAGATCCAGTCCGGTGACGCGCAG
GTCAACGGCGTCATGCTTCATGCCTTCTCTCCATACCTTCCTTTTGGAGGCATTGGTGCGTCAGGTATG
GGCGACTATCACGGGCACTACAGCTACCTCACCTTCACGCACAAAAAATCCGTCAGGATTGTGCCG**TAA**

Stop codon

CTGAAGACGCGGAGCGCGCTGGGTTGAGTAACTACACTGGGTGAGCTCGTATGTCTATAAGGGGCATCC
A-------- **Putative ρ-independent transcriptional terminator**

(B)

MNYLSPAMIDSLFSAQKAFFATRATADVGFRKQALKRLRDAVINNKEFFYSALAEDLGKTREVVDLAEI
GEVLHEIDFALANLDEWIVPESVPTPEIIAPSECYIVQEPYGVTYIIGPFNYPVNLTLTPLIGAIIGGN
TCIIKPSETTPETSRVIEKIIAEAFSPEYVTVIQGGLAENSHLLSLPFDFIFFTGSPNVGKVVMKAAAE
HLTPVVLELGGKCPLIVLPDADLDQTVDQLMFGKFINSGQTCIAPDYLYAHRSVKDALLQRVVERVKND
LPKVNSTGKIVTSRQVVRLVSLLEETRGKVLVGAQADVDNRAFSATVVDSVQWDDPLMAEELFGPILPV
LEFDDVPTAVNLINKHHPKPLAVYVFGKDVDLAKGIINQIQSGDAQVNGVMLHAFSPYLPFGGIGASGM
GDYHGHYSYLTFTHKKSVRIVP

Figure 31. *Ps*BADH ORF of 1,311 bp which was denoted as *dpgC* (A) and its deduced amino acids of 436 residues (B) are located in the 4 kb-*Pst*I insert DNA in pBCH2. The start codon ATG and stop codon TAA of *dpgC* are in bold letters and highlighted. The putative promoter sequence (-35 and -10), +1 start site, putative ribosome binding site (RBS) and putative ρ-independent transcriptional terminator are in bold letters and underlined.

4.6.3 Nucleotide sequence of 7.65 kb - overlapped fragment of 6.3 kb *Eco*RI- *Hin*dIII insert and 4 kb *Pst*I insert

The 6.3 kb (6,273 base pairs) *Eco*RI- *Hin*dIII insert DNA in pBCH1 and the 4 kb (4,041 base pairs) *Pst*I insert DNA in pBCH2 were overlapped and combined to be 7.65 kb (7,653 base pairs) genomic DNA fragment which was shown in Figure 32. Consequently, the 7.65 Kb fragment contained both *dpgB* gene and *dpgC* gene. The sequence of the combined fragment has been deposited under GenBank accession no. EF419244.

AAGCTTCTGCAACGCACCAACTCATCCCACCGCCACGCCAAAGATGTTCAGTACGAGATCGAGTCCGTC
GCCAACACAGCCAATAGTTCCATTGCCTCCCTGTTTAGCGATGCGCGTGCGTTCGCGACGTTCATGGTC
TGGGTTGCTTTCGGGATGTGCATGCTGATTGTCTATGGGTTCAGTCTTCCCTTGGAGCAGAACTTCCTC
CTGTTCGGCTTGCCAGGCGTGGTTGCGGTAATCGCAGAGCTGCTGATTTCACAACGTCATTCAAGCCGG
GTGTCTGTGAGCACTCGTCTAAAGCAGAACGCTTAGTACCTTTCGCTACACCCCGTCCAGGTTCGCAAC
TCGCCAGCGTACGGGTTTCGGTGCGGCTCTAAAGCTGCGCCGTTTTTTCAAAAAGTTTCCCCGGACCAT
TACATGGTTTAGGTAACTGCGTCCAAAAAATACTCGAGCACAAAAGTCGGAGTGGGGCAGATTAAGCAT
ATTTGTCGTATAGGCTTGGCTGTGATTGGTCGTTGCGTCTTAAGTCATTTAAAGCGGCGCGTTAAAAGG
CTTGATTTCGAAGTTCGTAATACTAAGGTCAAAGCCCGATATGGAGCTGGCTTTGACGAGAATCGATTG
ATAACTAGCTATATCTGGAAGTTCTGGTAATCCGCCGAGCGACATGCTTCGAATATCTAAGGAGTGTCG
CGCTGCATAATTGCGAGAGAGGAACTGCTATGGGCATAGAATTGTTGAGCGATCGGAGCAAGGTTTATG
ACTTCGCAGATCCTCATGTGGTGTCCGCGTATGTGAATCAGCATGTAGGCAATCACTCTATAGCGATTT
CGGATGGGCGAAGCCAGGCAATGCTCATCCATCGACAGGTCGCTGATCTGGATTTCTGTCGAATCAGAT
ATGGGAGTGAAACATGTGTTACTTCTACAGCGCTTCGCGATAAATATCACATCCAAATTATGCTAGGCG
GTAGTTGCTTGCAGCGCATCTCAGGCACGCATCGCGTTCTCTCGGTAGGTGATCTGGTCGTGATCAATC
CAAACGATCCTGTAGATTTGACTTACTCTCATGACTGCGAGAAATTTATTCTAAAAGTNCCCTGTCAAA
CTGGTGGAGGCAGTATGTGATGATCAGCATTGGTGCCGCCCATCAACAGGGCTCCGTTTTGATGAGAAG
GTTTATCAACTTAATGATTTGCAAGGAATGGTTCAGCTGCTCAGTCTTGTTTGTGGTGAGATTGAAAAT
GAAAGCATAATTCGAGCAGTTCAAGAGCATTACGTTCAAATAATAATCATCAAAATTTTGACGTCGTTA
CTTACAAACCTAGAGTACACGGCGGTGGGCGTTCAGAATCAACTGCTCCGCAAGGTATTGCATCATATT
GAAGATAATCTGAAGCAGGATATAACCCCTGAAGGACTGGCTAAATATGCCAACGTCAGCCTGCGTAGC
CTTTACGTTCTGTTCGATCAGTATTTAGGTGAACCGCCGCGACGTTACTTTGTCAGAAGGAGGTTGGAA
CAGGTGCGCGCTGCGCTTCTAGGTGCTGAGGGGCGCAGGAAGAACGTGACGGAGATTGCGATGGATTAC
GGCTTCACGCACTTGGGGCGGTTTTCAGCTGAATACAAAGCTCATTTTGCTGAGCTTCCCTCAGAGACC
TTGAAGCATCGTCCCAATAACTGAAAGCACAGGGCCCGCCTTGGCGGGCCCTGTGCAATGGCTCAGGCC
AGGTATTTCTCGATTTCTTTCTCGCGCCAGATGATTCCAACGCCTGGAAGATCCGGAATAACTGCATTG
CCAGCTTCGAAATTCAGCGTGGGCTCCATCACGCTAGCGGCAAGATCCAAACGCTCCAGCCAGTGGGCA
GTTGGAGTAGCAGCCAACACGTGTGCACTGATTTCTTGGAACAGATGGCTGGACATGGGCACGCCGAAC
TGCTGAGCCAGCGCACTGGTCCGGAGCCAACCAGTCACTCCACCAATCTCCATTGCGTCTGGCATTGCC
AGCCGACATGCACCAGCTGTCAGTGCCTTGAACATTTCCTCCGGGCCGAACCAGTTTTCGCCCATCTGC
ACAGGGATATCCAGACTGTTTTGGATGCGCTGGTGGCCTGCATAGTCATGCTGCAAAGTTGGCTCTTCG
ATCCGGGTGCCGCCCGCGTCCTGCAGGGCCAAGCCACGCTTGAGGGCAGCTGGCACGTCCAGGCTCTGG
TTATAATCGACCAAGATTTCAAAATCATCACCGACCGCCTCGCGGATGCTTCCAACTACAGCCAGGTCT
TTATCCAGCGTCGGATAACCAATCTTGGTCTTAACCGCTCGGAAGCCTGACTTAGCAGCAGTCACTGCG
CGTTCAGTCGCGAGCTTTACACCGTCCAGACTGTCGCTGTCATAGGCAGGGATCGGGCGAGCCTTGGCG

Figure 32. Nucleotide sequence of the 7.65 kb combined fragment. The *Hin*dIII and *Pst*I sites are underlined at 5′ and 3′ end of the fragment, respectively. This fragment contains the whole *dpgB* gene encoding for *Ps*BFDC in bold letters and the whole *dpgC* gene encoding for *Ps*BADH in bold and italic letters.

CCGAGCAGATTAACCAGCGGCGTTTCGTGAACCTTAGCCAGAGCATCTCAAGCCGCCATGTCGATCCCT
GCAGTTGCCATGCGGATAGCCGCGCTGGCGATACTGTGATTCGCACAACGGTAATGGGCTTCTGCGACA
AAAGGTCTCCTCAAATTTGATGATTGCCACCCACTTTTCATGCATAACGGGCCAGCTGCGTCCGGTTCT
GCGCTCCAGCTTGGCCATCGCGTTATTGAGGTGGGTGCGCACTGTCGTGAACCCTATTCCGAGTTGGCG
GGCCACCTCTTTAACACTGGCACCAGCCGCCACTAGCTTGGCAACTCCGCTTCCCTAAACGACAACAAG
TGCTTTCGATCGGGTGCGGATGCGAAAGCCCTGGCGAAGTATGGTTGAAGCGTCAGCAAGAGCCGCTCT
TCGCGCTCGCTGAAAGGCTCTCGGCCTCTGCCTCTCCATATCCTAAAATCGCCCGTGCTCCATGTCCGC
AGGGCGTAGAAAGTCGTTATAGATCTCACTGTGAAGCAGGGCAGGGCGCGGCACATGGCAATCGACGCA
CGCCGGCTTGGCCACTCTGCGCATTACCGGGGTCACCATGTCTACCCGATGAAAATGCTGCTGGTACGC
CTCCATCTTGTACCCGTCGATGTTGAAGGCACACGGCTGACAGGGTCGCTGCCCACGCTCATCCCACAT
AACAGAGGCGATGTGGTCGGCATCGAGAAGGGTCGCCACAGCTTGGAGGGTAGCTGCGCGAGCATCAGG
CTTTCCCTGACACTCAGCCAGAAGCCAGACAAGCTCGGCTATCTGATCCAGGTCGGTTTCTTGCTGCAC
TGTCACCATTGACCCCTCCGGAAACTCTGTGGATACGCCCCAAAAACGGAATCAAATTAAATAAGGCGC
ATCTATAGATAAATCAAAAATTTATCTATTTGATCTATTTGACCCTCGCTTCTATCGTGGGCTTCGTAA
TTTGGTAAGAGATATCCATC**ATGGCATCGGTACACAGCATCACTTATGAGCTCCTCCGCCGTCAGGGCA**
TCGACACGGTGTTCGGCAACCCTGGTTCCAACGAACTGCCGTTTCTGAAGGATTTCCCAGAGGACTTTC
GCTACATCCTCGCGTTGCAGGAAGCGTGCGTGGTAGGTATTGCTGATGGTTACGCCCAGGCCAGTCGCA
AACCTGCATTCATTAACCTGCATTCTGCAGCGGGCACGGGCAACGCGATGGGCGCGATGAGTAACGCCT
GGAACTGCCACTCTCCGCTGATCGTGACAGCTGGTCAGCAAAACCGAGCGATGATTGGGGTTGAGGCAC
TGTTGACCAACGTCGACGCCGCCAGCCTTCCCCGTCCTCTCGTCAAATGGAGTTACGAGCCGGCGAGCG
CTGCGGAAGTGCCACATGCAATGAGCCGAGCTATTCACATGGCGAGCATGGCACCTCGCGGGCCTGTGT
ATCTCTCTGTGCCATACGATGATTGGGACAAGGAAGCGGATCCTCAGTCTCATCACCTGTACGATCGGA
GTGTCAACTCAGCTGTTCGTCTGAATGACCAAGATCTGGAAGTGCTGGTGGAAGCTCTCAACAGCGCGT
CCAACCCCGCAATTGTGCTCGGCCCAGACGTCGACTCCGCGAATGCAAATGCTGATTGCGTAACATTGG
CCGAACGACTCAAAGCTCCTGTATGGGTTGCCCCTTCTGCCCCGCGCTGCCCCTTCCCAACCCGACACC
CCTGTTTCCGAGGGCTTATGCCTGCCGGTATCGCAGCGATCTCTCAACTGCTGGAGGGTCACGATGTGG
TGTTGGTTATAGGCGCCCCCGTATTCCGCTACCACCAGTACGATCCAGGTCAGTACCTGAAACCAGGTA
CCCGCTTGATTTCGATCACCTGTGACCCGCTCGAAGCGGCACGCGCGCCAATGGGCGATGCGATTGTTG
CAGACATCGGTACCATGACCGCTGCGCTCGCCAGCCGCATCGGCGAAAGCGAACGCCAACTTCCAGCGG
TTCTCCCCAGTCCGGAGAGGGTTAACCAGGATGCCGGGCGTCTGCGTCCAGAAACGGTGTTTGACACAC
TCAACGAGATGGCTCCTGAGGATGCGATTTACCTCAACGAATCCACCTCAACGACCGCCCAAATGTGGC
AGCGTCTGAACATGCGCAACCCGGGCAGCTATTACTTCTGCGCAGCAGGAGGGCTCGGCTTTGCCCTGC
CAGCAGCGATAGGAGTTCAACTGGCGGAACCGGATCGACAAGTCATCGCTGTCATCGGCGACGGGTCAG
CCAACTACAGCATTAGTGCCTTGTGGACAGCAGCCCATTACAACATCCCAGCCATCTTCTTGATCATGA
ACAACGGCACATACGGTGCTCTTCGATGGTTTGCTGGTGTGCTGGAAGCCGAGAACGTTCCAGGCTTGG
ATGTGCCAGGAATCGACTTCTGCGCGATCGCCAAGGGATATGGTATTCCTGCGCTGAAAGCTGACAATC
TTGAGCAGCTCAAAGGCTCCATTCATGAAGCGCTGTCTGCCAAAGGGCCGGTATTGATCGAGGTCAGCA
CGGTCAGCCTGTGACGTGAGATTTGACGATGAGTCAGCAGAATATATTTAGCGTCGAAGACTAGGCATT
GAAATCGAAGGTTTGCCTCACAGTGACACGCGGTTGCTAGCAATTGCTTGCGTCATTGAAGGCATTTTG
GGCAGAGGTCCATCTCCTGAGCGAGGAACGTGAAGGCAGCCCAACACTCCATGTGGCAACTGCTCTGTC

Figure 32. Nucleotide sequence of the 7.65 kb combined fragment. The *Hin*dIII and *Pst*I sites are underlined at 5′ and 3′ end of the fragment, respectively. This fragment contains the whole *dpgB* gene encoding for *Ps*BFDC in bold letters and the whole *dpgC* gene encoding for *Ps*BADH in bold and italic letters (continued).

TTCTGGAACCAGTCGCTACCCATCGAGCTCGTAACCCGAATAGAGGGATTGTCC***ATGAATTATCTGTCC***
CCGGCGATGATCGACTCGCTGTTCTCAGCTCAAAAGGCTTTCTTCGCGACCCGCGCAACAGCCGATGTT
GGCTTCAGAAAGCAGGCTTTAAAACGGCTCCGAGACGCGGTGATCAACAACAAGGAGTTCTTCTATTCC
GCGTTAGCAGAAGACTTGGGTAAAACCAGGGAAGTGGTTGACCTAGCGGAAATCGGTGAAGTCCTGCAT
GAAATCGACTTCGCCCTGGCGAACCTGGATGAATGGATCGTTCCGGAGTCTGTTCCCACTCCGGAAATT
ATCGCGCCCTCGGAGTGTTACATCGTCCAGGAGCCTTACGGTGTCACCTACATCATTGGCCCGTTCAAC
TACCCGGTAAATCTGACACTGACCCCTCTGATCGGCGCCATTATCGGTGGCAACACCTGCATCATCAAA
CCGTCTGAGACGACTCCCGAGACGTCTCGCGTTATCGAGAAAATCATCGCGGAAGCATTCTCCCCCGAA
TACGTCACCGTGATTCAAGGTGGGCTCGCAGAGAACAGCCATCTTTTGAGCCTGCCTTTCGATTTCATC
TTCTTTACTGGCAGCCCCAACGTCGGGAAGGTGGTCATGAAGGCGGCGGCTGAGCATCTGACGCCGGTT
GTGCTTGAACTTGGGGGAAAATGCCCCCTCATCGTTCTGCCTGACGCTGACCTCGACCAAACTGTTGAT
CAATTGATGTTCGGTAAATTCATCAACAGTGGCCAAACCTGTATCGCACCCGATTACCTCTATGCGCAT
CGCAGCGTCAAAGATGCTTTGCTGCAACGGGTGGTTGAGCGGGTGAAGAACGACCTGCCTAAGGTTAAT
TCGACCGGCAAGATCGTAACCTCACGCCAGGTGGTGCGTTTGGTTTCCTTGCTTGAAGAGACGCGTGGA
AAGGTGTTGGTCGGGGCCCAGGCCGACGTAGACAACAGAGCATTCAGCGCAACGGTAGTGGACAGCGTT
CAATGGGACGACCCGCTTATGGCGGAGGAGCTCTTCGGGCCGATTTTGCCAGTGCTTGAATTCGATGAT
GTCCCCACCGCAGTCAATCTGATTAACAAGCACCACCCCAAGCCCTTGGCCGTTTATGTGTTCGGCAAG
GACGTGGATCTCGCAAAAGGCATCATCAATCAGATCCAGTCCGGTGACGCGCAGGTCAACGGCGTCATG
CTTCATGCCTTCTCTCCATACCTTCCTTTTGGAGGCATTGGTGCGTCAGGTATGGGCGACTATCACGGG
CACTACAGCTACCTCACCTTCACGCACAAAAAATCCGTCAGGATTGTGCCGTAACTGAAGACGCGGAGC
GCGCTGGGTTGAGTAACTACACTGGGTGAGCTCGTATGTCTATAAGGGGCATCCAGGCGTTCAGATGAA
AGCTCACCACTACTGCTCCATCCTGAACGAGGATGTCATCCCGTGCGTCATCCTCGATCGCCCCAGGCA
TCAACAAGAGTGGAGAGCGAGACACTGATATTGTCTGTATTTTTGCTGCTGATAGTGCATTGAGAAATT
TATCTGTGCGGCTGCGTAATGCAAATTATCGAACTTCGGGTCCCGTTCGTGGTATTGATATTACAAGTG
TGATTGTTAGCTGTTCTTTTTTGCTGTTCTAATTGAGGGTGTTCGTTATGGCTTTTCAAAATCTACCGT
TCTCAAAATCAAGAGCCTACCAAGGATTGGTGTTTCTAAGCGGCGAGGTGCCGTTCGATAGTGAGGGAA
AAATTCCCGCTGGCGTAGGTGCTCAGACAGAGCTAACCTTGAGTAACATTAGTGCCACACTTGCCCGAG
AAGGGCTCAGCTTGGCCGATGTAATCAGTGTTACGGTGTATCTGACTAACCGTGATGATTTTGCAGAGT
TCAATCGCGTTTACGCTTCTCACTTCAGTGCCCCCTTACCGGTGAGAACCACTATTTGCACGCAACTGA
TGATTGATGCGTGCGTTGAGCTGACAGTTATCGCCGCTCGCCACTCTTGAGGTTCGCCTTATGAGGACA
GTCATAGTACTCGGCGCTGGTATTGTTGGCGTCTGCACAGCTTTGCAATTGCGTCGCCGTGGCTGGGAT
GTAACGCTGGTGGATCGCCGCAGTCCTGGGCAGGAAACTTCCTACGGCAATGCTGGCATTATTCAGCGT
GAAGCGGTAATGCCGTACCCGTTCCCCAGGGATTTAGCCACTCTGCTAAAAGTTCTGCGCAAAGGTGGG
GTTGACGTAAACTACCACGCTAATGCGATTCCTGCGTTACTGCCGCGACTTGTGCGTTATTGGCAAGCA
TCGTCACCTCGGTGTTATGCGCTCTACGCGCAATCGTTCAGATCATTGATCGAACACTGCATTGAAGAG
CATCGCGATCTCATCGAGCACGCCCAGGCTGGGCACTTGATACATACAGAGGGGTGGCTGCAG

Figure 32. Nucleotide sequence of the 7.65 kb combined fragment. The *Hin*dIII and *Pst*I sites are underlined at 5′ and 3′ end of the fragment, respectively. This fragment contains the whole *dpgB* gene encoding for *Ps*BFDC in bold letters and the whole *dpgC* gene encoding for *Ps*BADH in bold and italic letters (continued).

4.7 Sequence homology between BFDC from *P. stutzeri* ST-201 (*Ps*BFDC) and BFDC from other *Pseudomonas* species

Multiple sequence alignment of BFDC from *P. stutzeri* ST-201 (*Ps*BFDC) to that of BFDC from other *Pseudomonas* species using the Clustal W algorithm of multiple alignments is shown in Figure 33. The results show the identity between *Ps*BFDC and BFDC from *P. putida* ATCC 12633 (*Pp*BFDC) is 91%, and the identity between *Ps*BFDC compared with BFDC from *P. aeruginosa* PAO1 (*Pa*BFDC) is 63%.

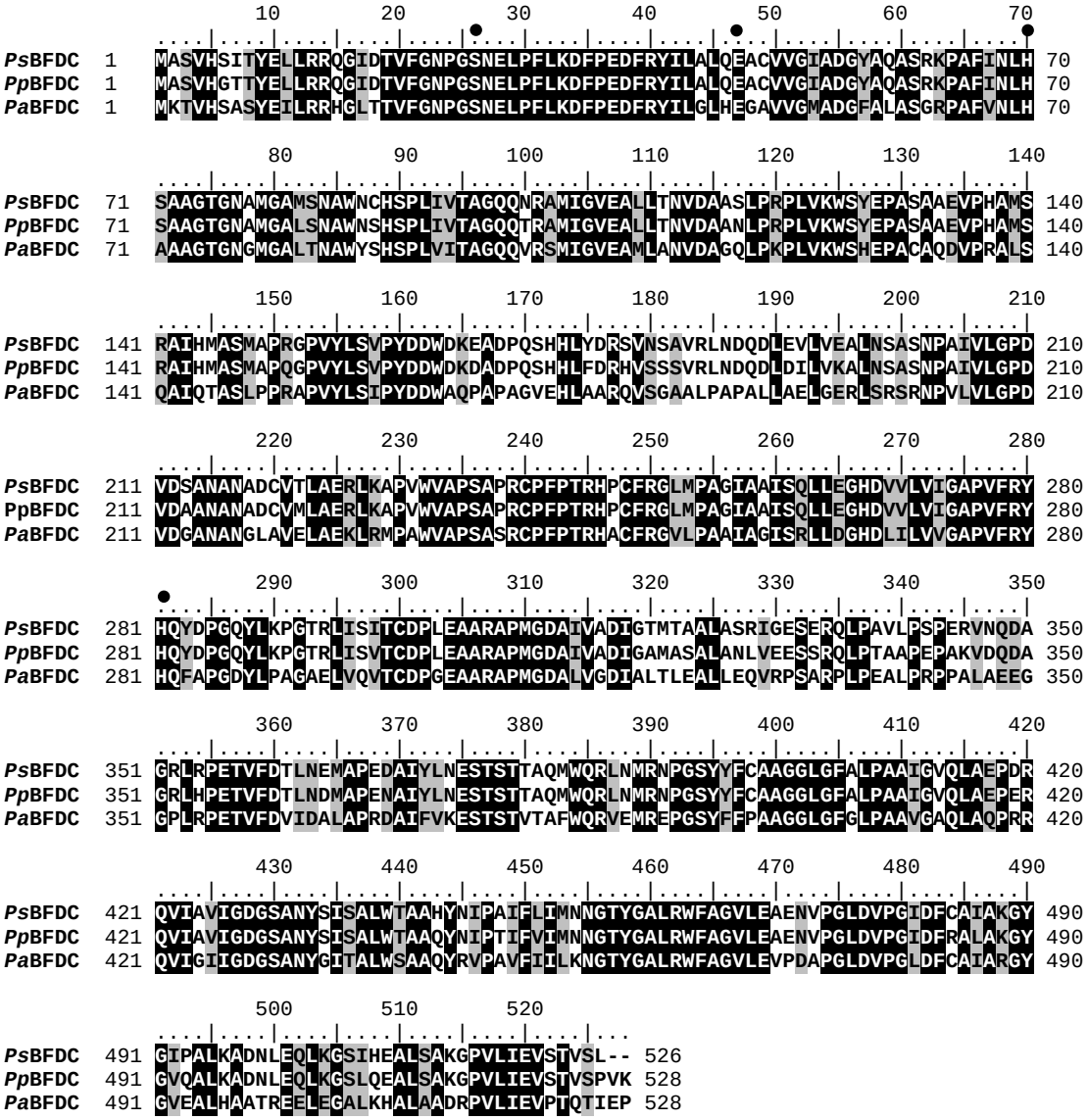

Figure 33. Multiple amino acid sequence alignment of BFDC from *P. stutzeri* ST-201 (*Ps*BFDC) with BFDC from *P. putida* ATCC 12633 (*Pp*BFDC) and BFDC from *P. aeruginosa* PAO1 (*Pa*BFDC). Dark and light shadings show identical and similar residues among sequences. Amino acids tagged with a dot are residues implicated in the catalytic mechanism of BFDC.

4.8 Homology between BADH from *P. stutzeri* ST-201(*Ps*BADH) and BADH from *P. putida* ATCC 12633 (*Pp*BADH)

Multiple sequence alignment of BADH from *P. stutzeri* ST-201 (*Ps*BADH) to that of BADH from *P. putida* ATCC 12633 (*Pp*BADH) using the Clustal W algorithm of multiple alignment is shown in Figure 34. The results show identity between *Ps*BADH and *Pp*BADH is 86%.

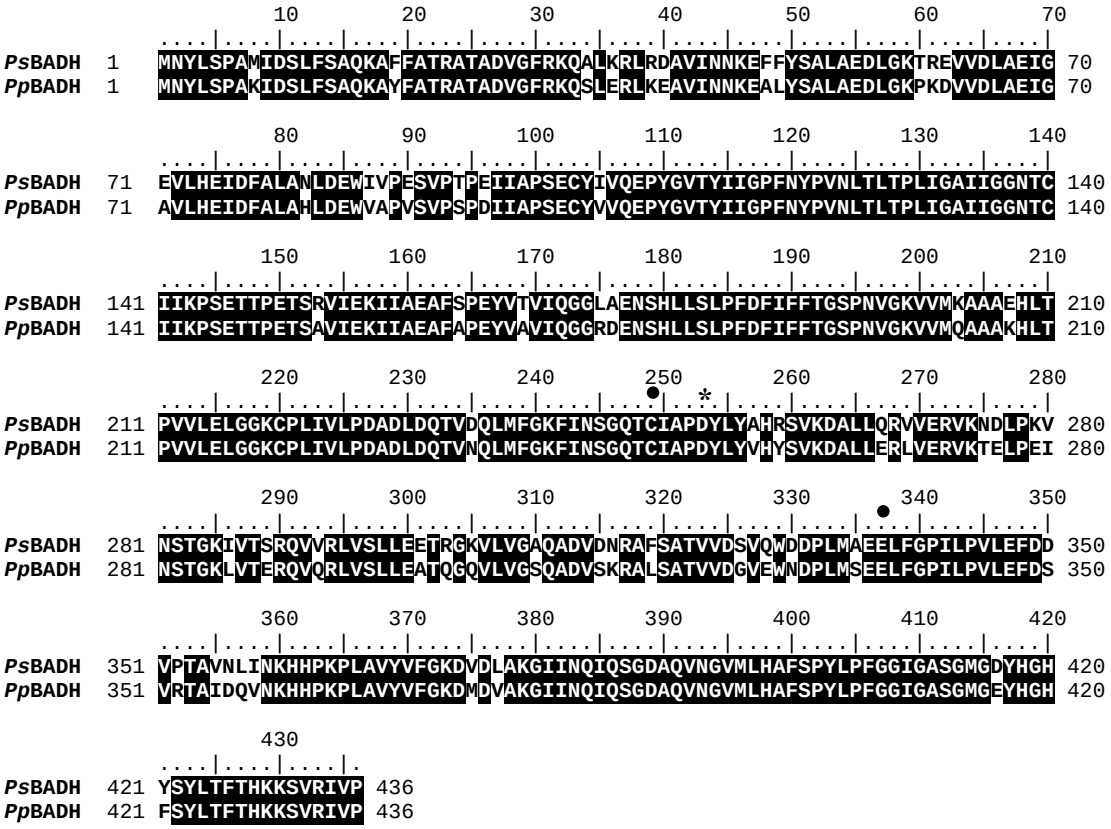

Figure 34. Multiple amino acid sequence alignment of BADH from *P. stutzeri* ST-201 (*Ps*BADH) to that of BADH from *P. putida* ATCC 12633 (*Pp*BADH). Dark and light shadings show identical and similar residues among sequences. Amino acids involved in catalytic mechanism are indicated by dot. A residue tagged with an asterisk is involved in linking conserved domains in class 3 aldehyde dehydrogenase.

5. Expression of *P. stutzeri* ST-201 *dpgB* gene in *E.coli* and purification of recombinant *Ps*BFDC

BFDC activity was found in the CFE from IPTG-induced *E. coli* BL21 (DE3) harboring the plasmid pET17b*Ps*BFDC. The majority of the BFDC activity precipitated at 45–65% ammonium sulfate saturation (Figure 35). Following hydrophobic interaction chromatography using Phenyl Sepharose FF as a chromatographic media (Figure 36), centrifugal ultrafiltration and ion-exchange chromatography using a Q-Sepharose FF column (Figure 37), the enzyme ran as a single band by SDS-PAGE analysis. The purified enzyme, which showed a single band on SDS-PAGE was stored at 4 °C in a storage buffer containing 50 mM sodium phosphate buffer, pH 6.0, 0.2 mM ThDP and 0.1 mM $MgCl_2$ and used for further characterization. Results from the purification procedure are summarized in Table 7 and Figure 38.

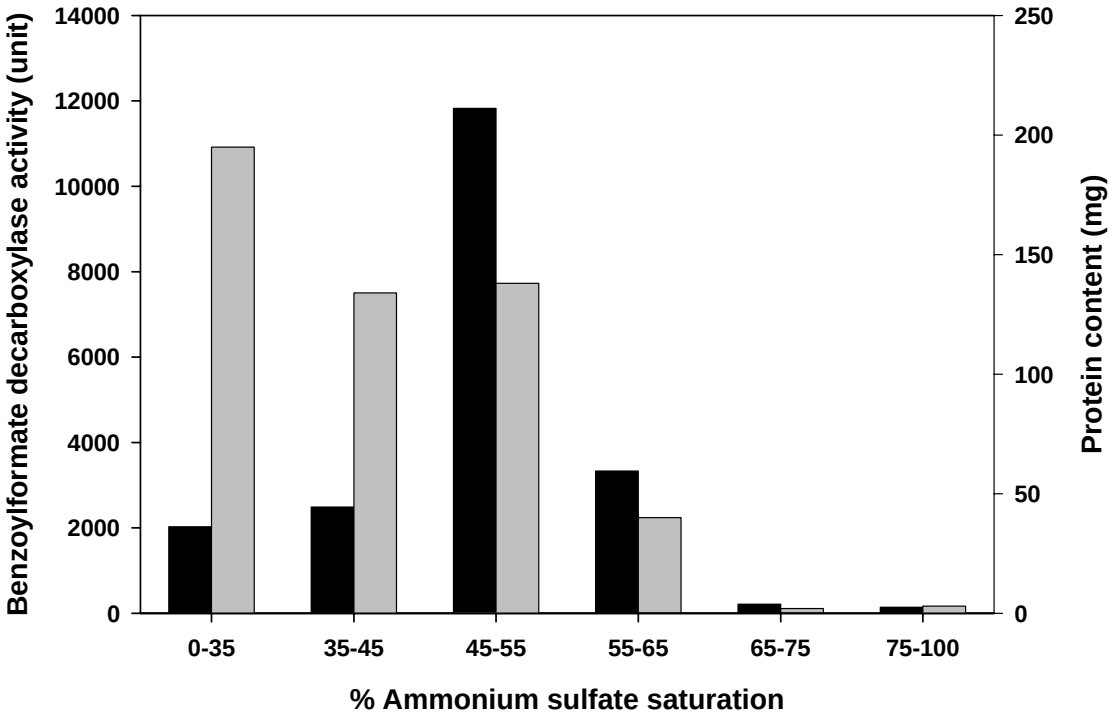

Figure 35. Benzoylformate decarboxylase (BFDC) activity (■) and protein content (□) ammonium sulphate precipitation fractions of cell-free extracts. The cell extracts were prepared from IPTG-induced *E. coli* BL21 (DE3) harboring the plasmid pET17b*Ps*BFDC.The enzyme activity was assayed in 66 mM sodium phosphate buffer, pH 6.0 at 25 ^{o}C.

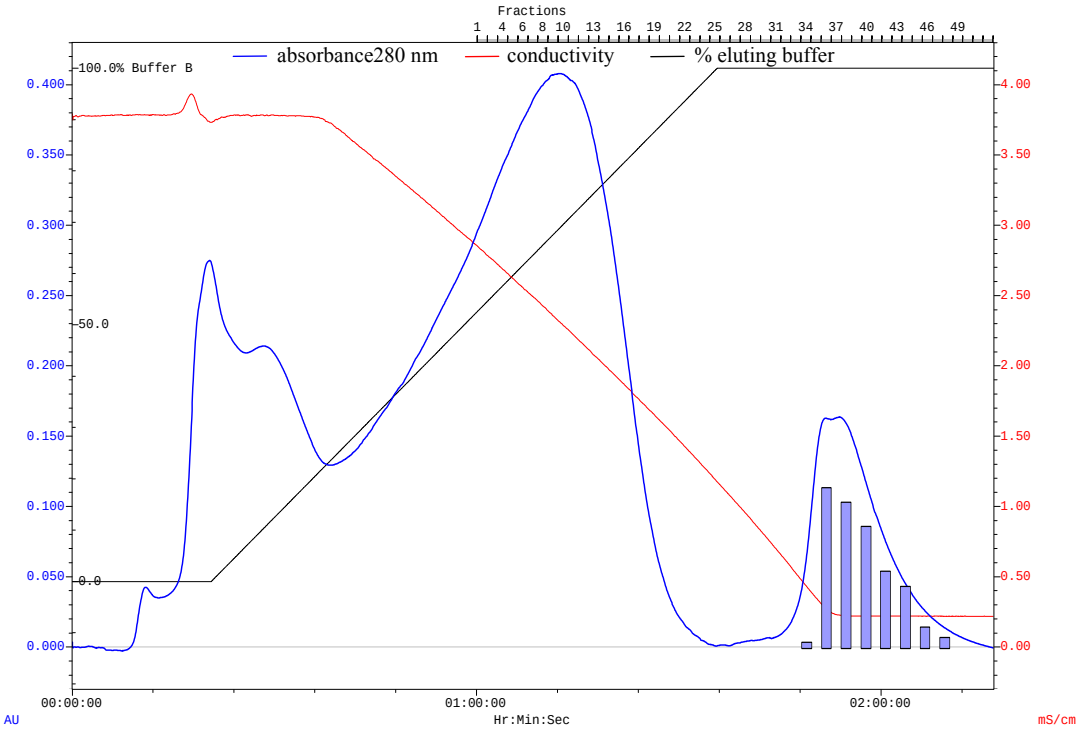

Figure 36. Protein elution pattern of Phenyl Sepharose FF hydrophobic interaction chromatography. Rectangular bars represent activity of benzoylformate decarboxylase found in each fraction collected by the FPLC system for concentration and purification by using centrifugal ultrafiltration.

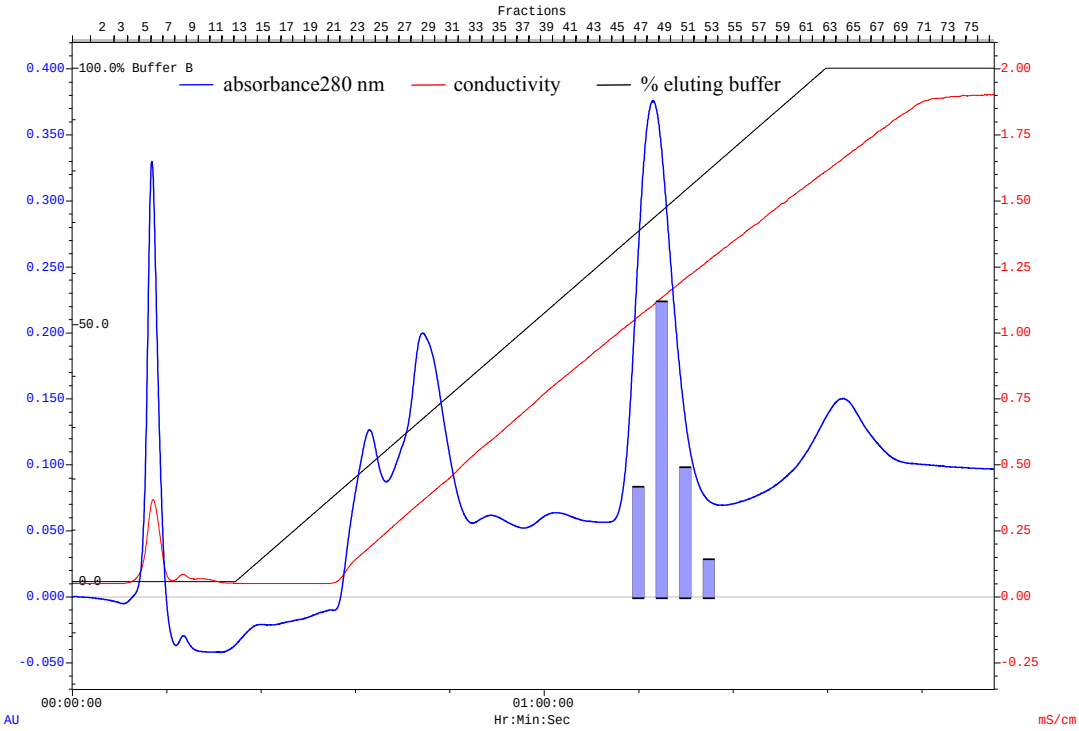

Figure 37. Protein elution pattern of Q-Sepharose FF anion-exchange chromatography. Rectangular bars represent activity of benzoylformate decarboxylase found in each fraction collected by the FPLC system.

Table 7. Summary of purification of recombinant BFDC from *P. stutzeri* ST-201. The culture volume of *E.coli* strain BL21 (DE3) was 1,200 ml.

Purification step	Total protein (mg)	Total activity (U)	Specific activity (Umg-1)	Purification (fold)	Yield (%)
1. Clarified cell homogenate	260	24180	93	1.0	100
2. 45-65% $(NH_4)_2SO_4$ precipitation	139	15151	109	1.2	63
3. Phenyl Sepharose FF	45.7	7982	175	1.9	33
4. Centrifugal Ultrafiltration	30.5	5753	189	2.0	24
5. Q-Sepharose FF	13.3	3228	243	2.6	13

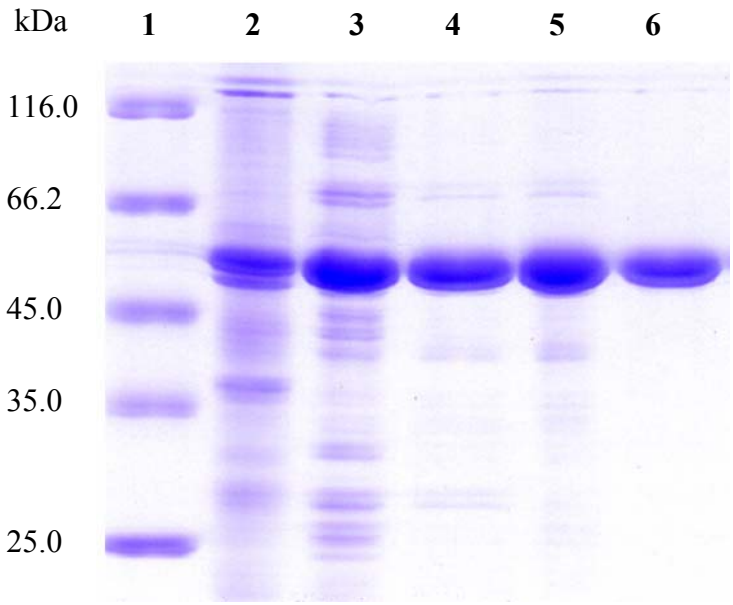

Figure 38. SDS-PAGE analysis of the recombinant *Ps*BFDC and its purity along the purification process.

Lane 1: Molecular weight markers with their molecular weight indicated

Lane 2: Crude cell lysate after cell disruption

Lane 3: Protein from ammonium sulfate precipitation at 45-65% saturation

Lane 4: Protein resulting from Phenyl Sepharose FF chromatography

Lane 5: Protein after centrifugal ultrafiltration

Lane 6: Protein resulting from Q-Sepharose FF chromatography

6. Characteristics of recombinant *Ps*BFDC

6.1 Molecular weight

6.1.1 Native molecular weight

The molecular weight of native recombinant *Ps*BFDC was estimated after gel filtration chromatography with the Superdex 200 HR 10/30 column running with the FPLC system as shown in Figure 39. A standard calibration curve between log molecular weights of protein markers and the partition coefficient values, K_{av} was constructed. The results are shown in Figure 40 and that the molecular weight of the native recombinant *Ps*BFDC was estimated to be 224 kDa.

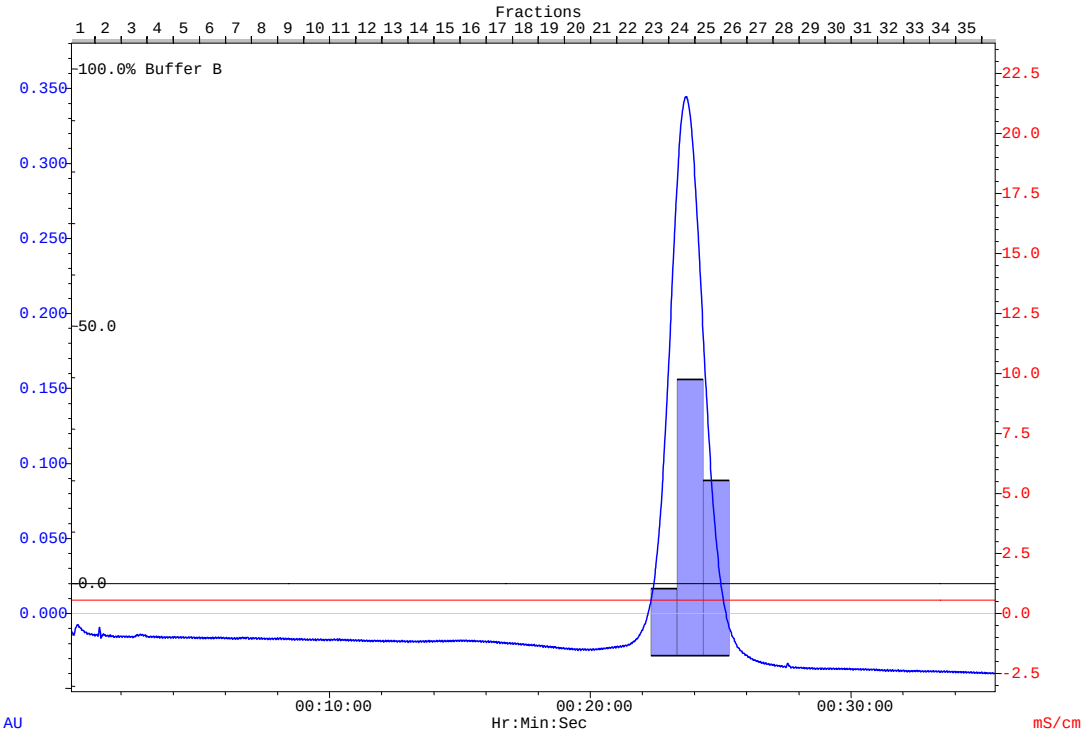

Figure 39. Protein elution pattern of Superdex 200 HR 10/30 gel filtration chromatography. Rectangular bars represent activity of benzoylformate decarboxylase found in each fraction collected by the FPLC system.

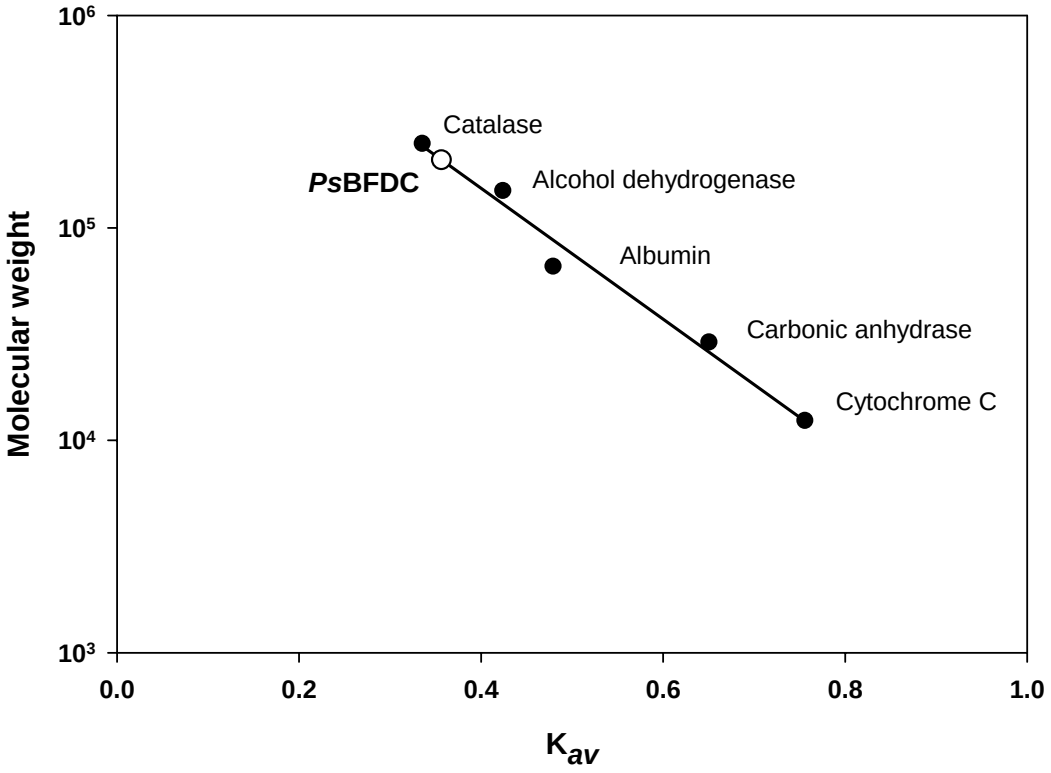

Figure 40. A standard calibration curve for native molecular weight determination of recombinant *Ps*BFDC by a Superdex 200 HR 10/30 column. The protein molecular weight markers were: cytochrome C (12.4 kDa), carbonic anhydrase (29 kDa), albumin (66 kDa), alcohol dehydrogenase (150 kDa) and catalase (250 kDa). The partition coefficient values, K_{av} as plotted against log molecular weights of each protein. The molecular weight of native recombinant *Ps*BFDC was estimated to be 224,000 Da.

6.1.2 Molecular weight of enzyme subunit

The molecular weight of recombinant *Ps*BFDC subunit was estimated after SDS-PAGE analysis. The enzyme was electrophoresed along with the standard. A standard calibration curve between log molecular weights of protein markers and the relative mobility, R_f was constructed. The results are shown in Figure 41 and that the molecular weight of native recombinant *Ps*BFDC was estimated to be 56 kDa.

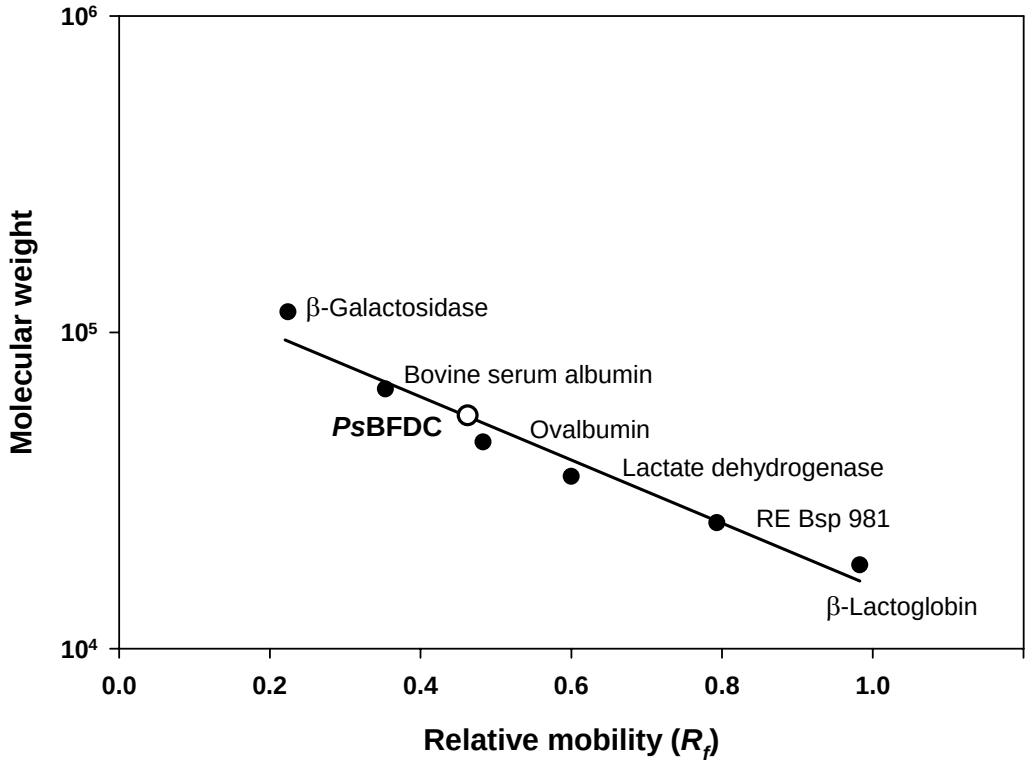

Figure 41. A standard calibration curve for determining molecular weight of enzyme subunit of recombinant *Ps*BFDC by SDS-PAGE analysis. The protein molecular weight markers were: β-lactoglobin (18.4 kDa) RE Bsp981 (25.0 kDa), lactate dehydrogenase (35.0 kDa), ovalbumin (45.0 kDa), bovine serum albumin (66.2 kDa) and β-galactosidase (116 kDa). The relative mobility, R_f was plotted against log molecular weight of each protein. The molecular weight of recombinant *Ps*BFDC subunit was estimated to be 56,000 Da.

6.2 Effect of temperature and pH

6.2.1 Effect of temperature on enzyme activity

Effect of temperature on the recombinant *Ps*BFDC activity was determined under the standard direct continuous assay condition at temperatures ranging from 10 to 80 ^{o}C. The temperature-activity profile of *Ps*BFDC is shown in Figure 42. *Ps*BFDC activity increased with increasing temperature up to 45 ^{o}C. It then sharply declined when the temperature was above 55 ^{o}C and the enzyme was inactivated at 70 ^{o}C. In the temperature range of 35-50 ^{o}C, the enzyme was found to be most active.

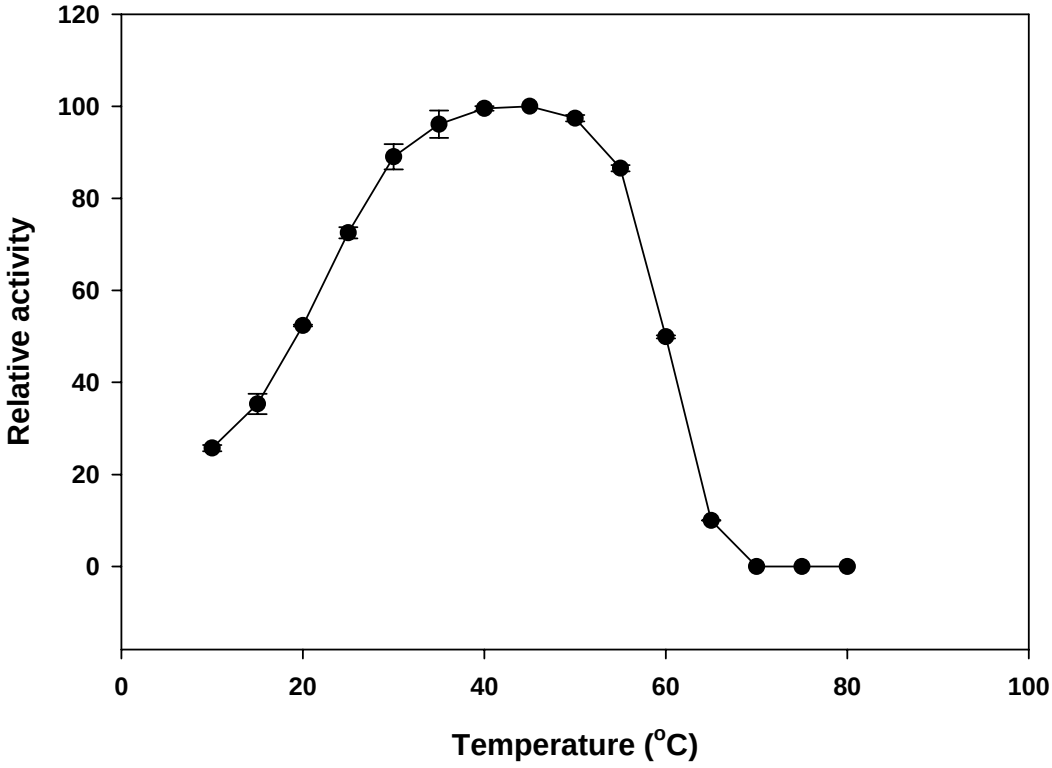

Figure 42. Effect of temperature on the recombinant *Ps*BFDC activity. *Ps*BFDC activity was determined under the standard direct continuous assay condition at temperatures ranging from 10 to 80 ^{o}C. *Ps*BFDC activity values were expressed as relative activity to the maximum value. Data plotted were averages of triplicate experiments.

6.2.2 Effect of temperature on enzyme stability

Effect of temperature on the recombinant *Ps*BFDC stability was studied by pre-incubating the enzyme at various temperatures from 15 to 80 ^{o}C for 20 min, after which the remaining activity was determined under the standard direct continuous assay condition at 35 ^{o}C. The thermal stability profile of *Ps*BFDC is shown in Figure 43. *Ps*BFDC was found to be stable up to 50 ^{o}C. It was, then, deteriorated when the temperature was higher and the enzyme was completely inactivated at 70 ^{o}C

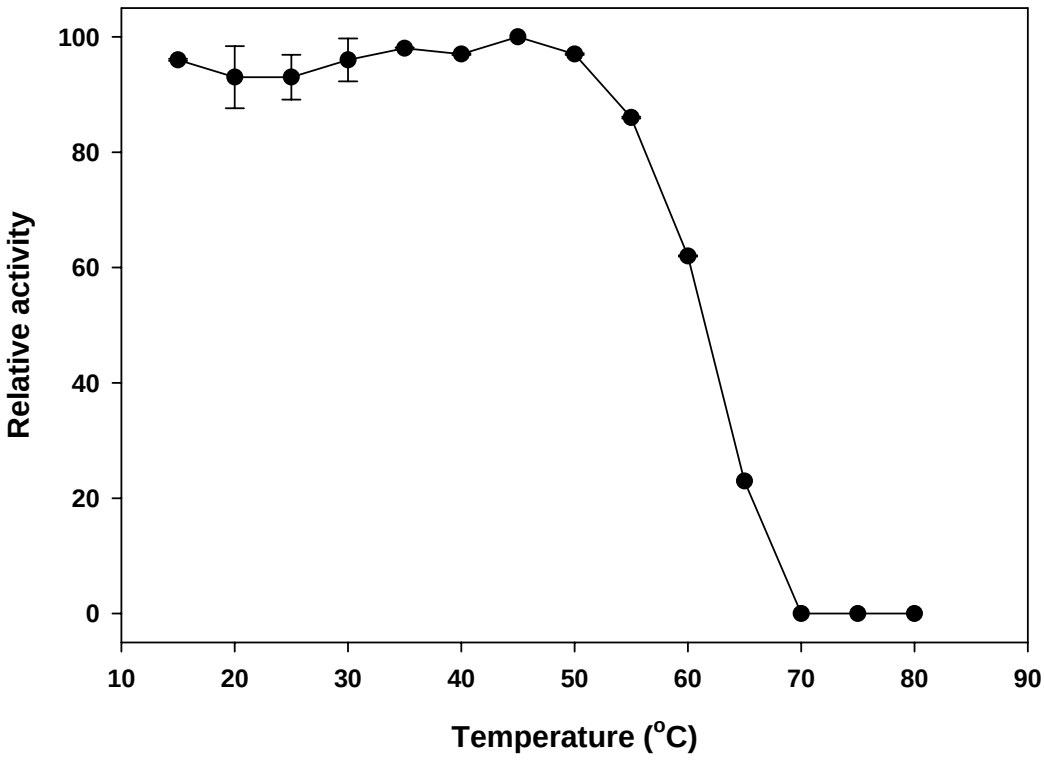

Figure 43. Effect of temperature on the recombinant *Ps*BFDC stability. In this experiment, the enzyme was pre-incubated at the temperatures between 15 and 80 ^{o}C for 20 min, after which the remaining activity was determined under the standard direct continuous assay condition at 35 ^{o}C. *Ps*BFDC activity values were expressed as relative activity to the maximum value. Data plotted were averages of triplicate experiments.

6.2.3 Effect of pH on enzyme activity

Effect of pH on the recombinant *Ps*BFDC activity was investigated in sodium citrate buffer (pH 3-6), sodium phosphate buffer (pH 6-8), Tris-HCl buffer (pH 8-9), glycine-NaOH buffer (pH 9-10) and 3-[cyclohexylamino]-1-propanesulfonic acid (CAPS) buffer (pH 10-12), each at 66 mM in standard direct continuous assay condition at 35 ^{o}C . The relationship between pH and *Ps*BFDC activity is shown in Figure 44. The optimal pH of *Ps*BFDC was found to be at 6.0 and reduction in activity was found at pH values below pH 5.5 and over 7.5.

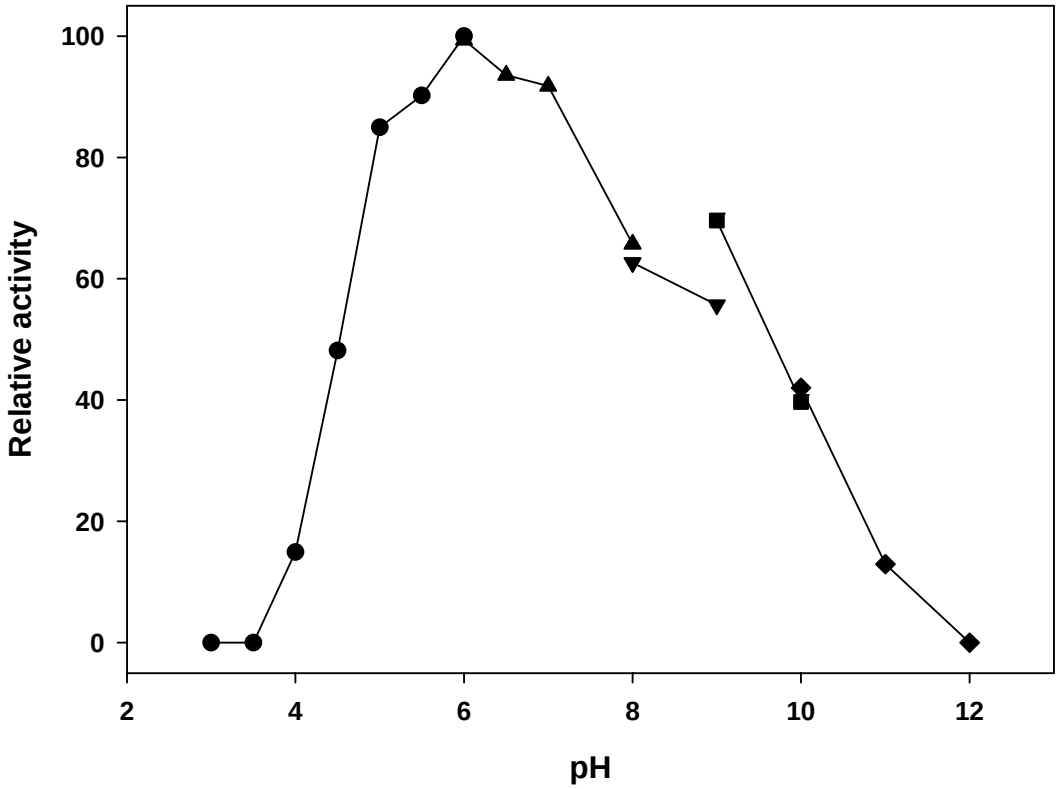

Figure 44. Effect of pH on the activity of recombinant *Ps*BFDC. Different buffers were used in the study; sodium citrate buffer (●), sodium phosphate buffer (▲), Tris-HCl buffer (▼), Glycine-NaOH buffer (■) and CAPS buffer (♦). Relative activities were expressed in the study. Data plotted were averages of triplicate experiments.

6.2.4 Effect of pH on enzyme stability

Effect of pH on the recombinant *Ps*BFDC stability was studied by pre-incubating the enzyme in different buffers with different pH from 3 to 12 for 20 min, after which the remaining activity was determined under the standard direct continuous assay condition at 35 ^{o}C. The pH stability profile of *Ps*BFDC is shown in Figure 45. *Ps*BFDC was found to be most stable at pH 6.0 in sodium phosphate buffer. The enzyme stability declined when pH was lower 5.0 and higher than 7.0.

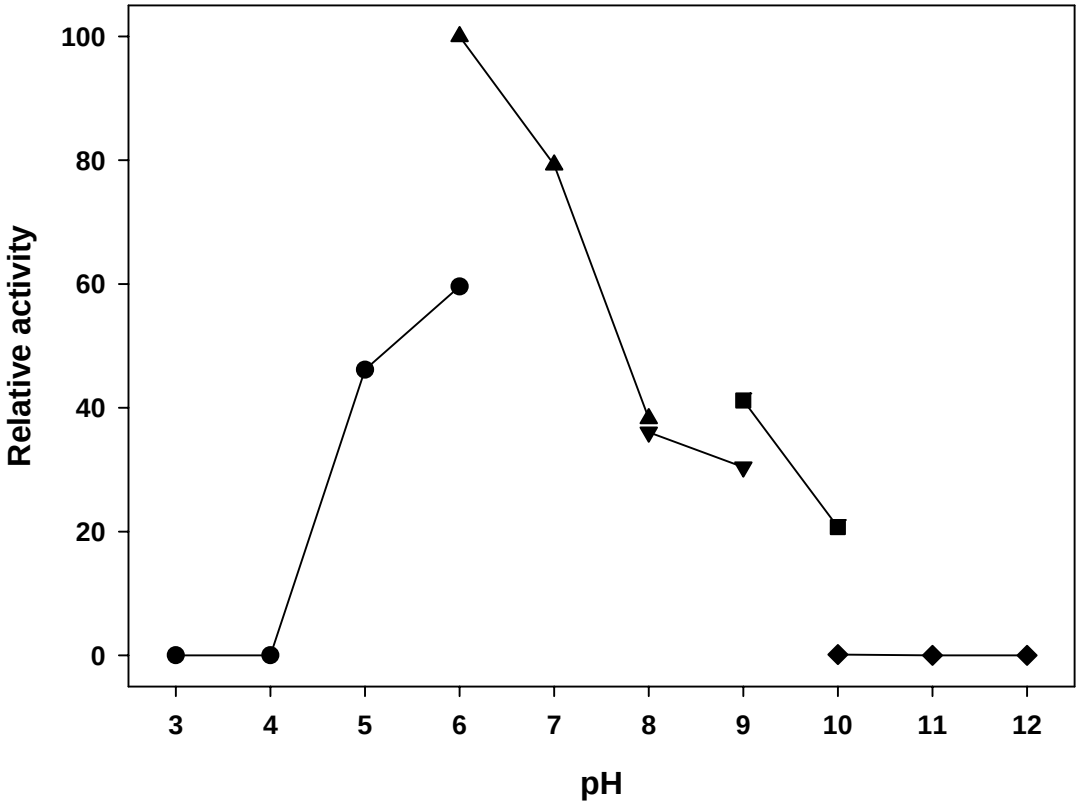

Figure 45. Effect of pH on stability of recombinant *Ps*BFDC. Different buffers were used in the study; sodium citrate buffer (●), sodium phosphate buffer (▲), Tris-HCl buffer (▼), Glycine-NaOH buffer (■) and CAPS buffer (♦). Relative activities were expressed in the study. Data plotted were averages of triplicate experiments.

6.3 Isoelectric point (p*I*) estimation

p*I* of the recombinant *Ps*BFDC was determined by isoelectric focusing in an automated run, IPGphor Isoelectric Focusing system of the two-dimensional polyacrylamide gel electrophoresis from Immobiline Dry strip kit. By using a highly guaranteed reproducible standard calibration curve between pH versus % gel length provided by the kit's supplier (Amersham Biosciences), p*I* of the native recombinant *Ps*BFDC was estimated to be 5.2.

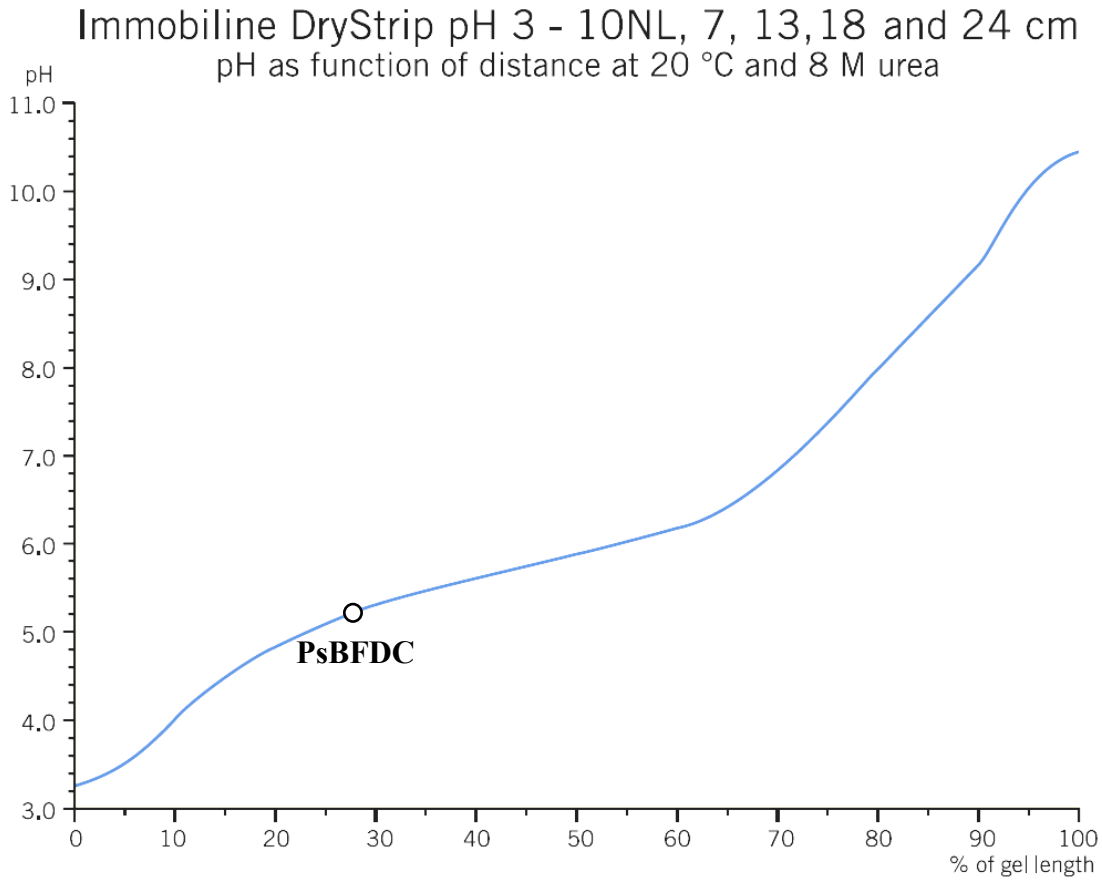

Figure 46. A standard calibration curve for p*I* estimation and a plot representing the p*I* of native recombinant *Ps*BFDC (p*I* = 5.2).

6.4 Kinetic parameters

Table 8 shows Michaelis-Menten parameters of *Ps*BFDC as well as *Ps*BFDC-his and *Pp*BFDC-his. The experiments were performed at the temperature 30 or 35 °C and at pH 6.0. The data are the averages of at least 3 separate experiments and are reported as ± SD.

Table 8. Kinetic parameters for *Ps*BFDC.

Enzyme	Temperature (°C)	K_m (mM)	k_{cat} (s^{-1})	k_{cat} / K_m (s^{-1} M^{-1})
wt *Ps*BFDC	35	0.69 ± 0.10	222 ± 3	3.2×10^5
*Ps*BFDC-his	35	0.44 ± 0.07	284 ± 12	6.4×10^5
*Ps*BFDC-his	30	0.43 ± 0.05	213 ± 7	5.0×10^5
*Pp*BFDC-his[a]	30	0.54 ± 0.05	342 ± 13	6.3×10^5

[a] Data from Lingen et al. (17)

7. Expression and purification of histidine-tagged *Ps*BFDC

ThDP-dependent enzymes are often purified as his_6-tagged variants to avoid loss of activity during multi-step purifications (14, 50). So, to facilitate a more rapid purification, *Ps*BFDC in this study was also prepared and expressed with a C-terminal histidine tag, and a homogenous preparation was obtained in a single step purification as shown by SDS-PAGE (Figure 47).

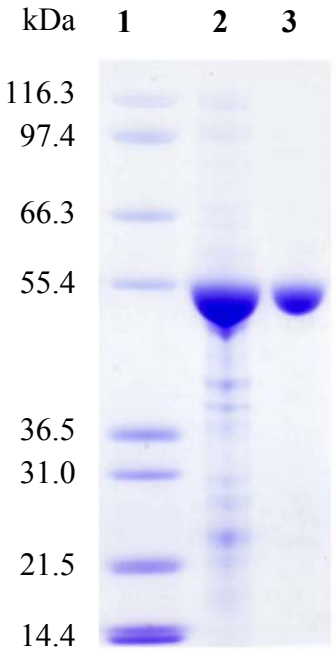

Figure 47. The purity of *Ps*BFDC-his obtained from single step purification after His-Select nickel affinity chromatography.

Lane 1: Molecular mass standards (kDa)

Lane 2: Crude cell lysate

Lane 3: After His-Select nickel affinity chromatography

8. Study on benzaldehyde dehydrogenase from *P. stutzeri* ST-201 (*Ps*BADH)l

8.1 Preparation and purification of histidine-tagged *Ps*BADH

The *dpgC* gene which encoded *Ps*BADH was amplified from pBCH2 and placed in the expression vector pET19b which adds an N-terminal His_{10}-tag. The enzyme was purified in a single step using a nickel affinity column. The purified protein showed a single band on SDS-PAGE with an estimated molecular mass consistent with that calculated from the gene sequence (Figure 48).

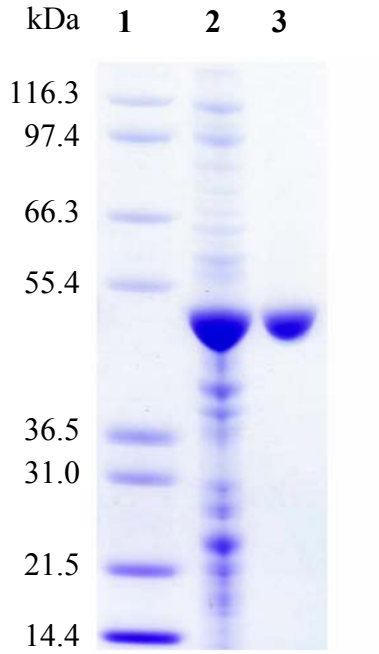

Figure 48. The purity of *Ps*BADH-his obtained from single step purification after His-Select nickel affinity chromatography.

Lane 1: Molecular mass standards (kDa)

Lane 2: Crude cell lysate

Lane 3: After His-Select nickel affinity chromatography

8.2 Kinetic parameters

Table 9 shows Michaelis-Menten parameters of *Ps*BADH studied at 25 °C and pH 8.5. The data are the means of at least 3 separate experiments and are reported as $\pm$ SD. Concentration of the fixed substrate was maintained at 1 mM.

Table 9. Kinetic parameters for *Ps*BADH.

Variable substrate	Fixed substrate	K_m(app) (μM)	k_{cat} (s^{-1})	k_{cat} / K_m (s^{-1} M^{-1})
Benzaldehyde	NAD^+	7.1 ± 0.6	57 ± 8	8.0×10^6
Benzaldehyde	$NADP^+$	6.9 ± 0.4	6.4 ± 0.4	9.3×10^5
NAD^+	Benzaldehyde	997 ± 111	176 ± 9	1.8×10^5
$NADP^+$	Benzaldehyde	6140 ± 375	40 ± 3	6.5×10^3

CHAPTER 5
DISCUSSION

1. Enzymes involved in mandelate and D-phenylglycine degradation in *P. stutzeri* ST-201

With the exception of *R*- and *S*-mandelate, *P. stutzeri* ST-201 was able to grow on MM agar containing each of the tested carbon sources. The results demonstrated that the organism could produce enzymes capable of catabolizing D-phenylglycine, benzoylformate, benzaldehyde and benzoate but not *R*- and *S*-mandelate. Therefore, the results suggested that *P. stutzeri* ST-201 lacked *S*-mandelate dehydrogenase and/or mandelate racemase which both were found in the mandelate pathway of *P. putida* ATCC 12633 (Figure 2) (3).

2. Induction of *Ps*BFDC in D-phenylglycine degradation pathway

As previously reported, benzoylformate was found in cultures of *P. stutzeri* ST-201 grown on D-phenylglycine (21). Therefore, the most likely reaction involved was the transamination of D-phenylglycine in the initial step of D-phenylglycine degradation as proposed in Figure 2. Furthermore, *P. stutzeri* ST-201 could grow on the substrates shown as intermediates in the proposed pathway suggesting that the catabolizing enzymes including benzoylformate decarboxylase and benzaldehyde dehydrogenase might exist. Whether or not these enzymes including D-PhgAT are coordinately regulated need to be proven. In *P. putida* ATCC 12633 some of the enzymes of the mandelate pathway are coordinately regulated. BFDC activity, for example, can be induced by the addition of either *R*- or *S*-mandelate or benzoylformate (but not benzoate) to the culture medium (3). In *P. stutzeri* ST-201 neither D-PhgAT activity nor BFDC activity was observed in MM containing glucose (Figure 15A). However, when the culture medium was changed from LB to MM containing D-phenylglycine, D-PhgAT activity was detected after 40 minutes, and was

followed by BFDC activity which appeared after 100 min (Figure 15B). Conversely, in MM with benzoylformate as the sole carbon source there was no D-PhgAT activity detected but BFDC activity was observed after 60 min (Figure 15C). Evidently, benzoylformate induces only the expression of the BFDC whereas D-phenylglycine brings about an increase in the levels of both enzymes. What is not clear is whether this is because D-phenylglycine actually induces the genes for both enzymes or whether the gene for D-PhgAT is induced and the benzoylformate subsequently produced induces the BFDC gene. Based on the times at which the two enzyme activities are observed the latter is the most likely explanation. Regardless, the sequential expression of the enzymes substantiates the involvement of BFDC in the pathway in a step following D-phenylglycine degradation.

3. Purification of wt *Ps*BFDC

When cell-free extract from the benzoylformate-induced *P. stutzeri* ST-201 culture was assayed for BFDC activity, there was a decrease with time in the absorbance of benzoylformate due to substrate depletion, as well as the occurrence of the characteristic odor of benzaldehyde product. These results also imply that *P. stutzeri* ST-201 probably produced BFDC. Nevertheless, the presence of a *Ps*BFDC could only be confirmed by purification of the enzyme to homogeneity. This was achieved in a series of four steps including ammonium sulfate fractionation, followed by hydrophobic interaction chromatography, centrifugal utrafiltration and ion-exchange chromatography. At the end of these steps, the SDS-PAGE analysis showed a single protein band with a molecular weight of ~55 kDa**.**

In ammonium sulfate precipitation step, most of the enzyme was precipitated at 45-65% saturation which indicated that enzyme is rather hydrophobic in nature. Hydrophobic interaction chromatography was chosen as the next purification step because the proteins were in a high salt medium, so no desalting step was required prior to column loading. In the following step, the enzyme was purified and concentrated in one step by utrafiltration in which molecules smaller than 100 kDa were removed. Finally, Q-Sepharose FF ion-exchange chromatography effectively purified the enzyme to yield *Ps*BFDC with 492 fold purification and with 23% yield. The purified wt *Ps*BFDC had a specific activity of 177 U mg^{-1}. In the previous report

by Hegeman working with *P. putida*, specific activity of the purified wt *Pp*BFDC was 193 U mg^{-1} (4).

4. N-terminal amino acid sequence of wt *Ps*BFDC

Sequencing of the purified enzyme informed an N-terminal sequence of ASVHSITYELLRRQGIDTVFGNP, which was useful for two purposes. First, it was compared with the amino acid sequences deposited in available databases. The BlastP search with 23 amino acids sequence from 55 kDa wt *Ps*BFDC protein indicated a 91% identity with N-terminal amino acids sequence lacking methionine of *Pp*BFDC. Therefore, 55 kDa wt *Ps*BFDC protein was likely confirmed to be ThDP-dependent BFDC. The other purpose was to use this sequence for the design of degenerate primer employed in the gene cloning.

5. Physical structure, orientation and classification of *dpgB* gene and its product

Two clones containing *dpgB* gene designated as pBCH1 and pBCH2 were obtained after detecting with the *dpgB* gene-specific probe (1,253-bp). The probe was constructed by PCR labeling with forward degenerate primer from N-terminal amino acids sequence of wt *Ps*BFDC and reverse primer from consensus cofactor-binding region of orthologous genes of *Pp*BFDC and *Pa*BFDC. The probe was used in southern hybridization as well as colony hybridization with subgenomic DNA libraries.

Sequencing of pBCH1 revealed an open reading frame (ORF) of 1,581 base pairs denoted *dpgB*. It encoded a protein of 526 amino acids with a deduced molecular mass of 56 kDa. This was in good agreement with the size observed on SDS-PAGE (55 kDa) for the BFDC purified from induced *P. stutzeri* ST-201 cells. In addition, the deduced amino acid sequence of the N-terminal 23 amino acids of *dpgB* was identical to that of the native *Ps*BFDC lacking the N-terminal methionine.

BLASTp analysis of the deduced amino acid sequence of *dpgB* revealed significant homology to other bacterial benzoylformate decarboxylases, with the highest sequence identity being 91% to *Pp*BFDC (gi:3915757) and 63% to *Pa*BFDC (gi:15600094) (Figure 33). Those residues implicated in the catalytic mechanism of *Pp*BFDC, including Ser26, Glu47, His70 and His281 (11), all were also conserved in

*Ps*BFDC. Analysis of the DNA sequence upstream of *dpgB* gene identified a putative ribosome binding site and -10 and -35 putative promoter regions. No ORF was identified in the 300 bp sequence upstream from *dpgB* while downstream of the *dpgB* ORF a putative *ρ*-independent transcriptional terminator with ΔG = -9.7 kcal $mol^{-1}$was identified. In addition a partial ORF of *dpgC* was found about 250 bp downstream of *dpgB* (Figure 49A). Overall these results suggested that *dpgB* was transcribed monocistronically, unlike the gene encoding *Pp*BFDC which was arranged and transcribed in the *mdlCBA* operon (Figure 49B) (8).

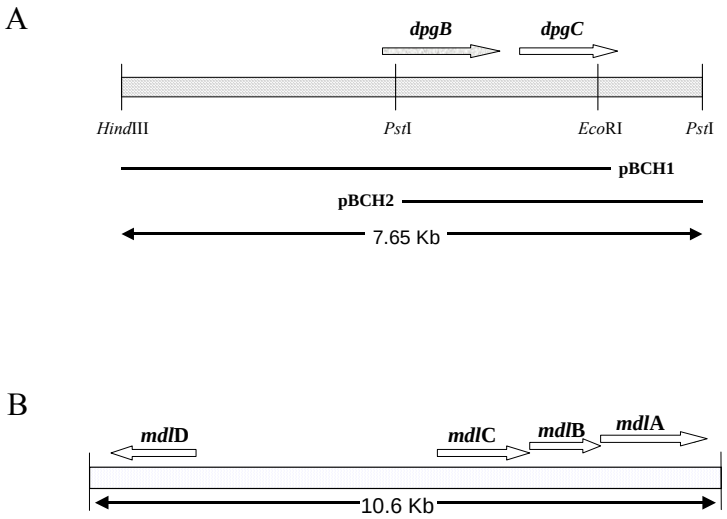

Figure 49. (A) Restriction fragment of the genomic DNA from *P. stutzeri* ST-201 carrying the genes for benzoylformate decarboxylase (*dpgB*) and benzaldehyde dehydrogenase (*dpgC*). The fragment (7.65 kb) shown is the combination of two overlapping genomic DNA fragments contained in pBCH1 and pBCH2. The arrows show the position and orientation of the genes, and relevant restriction sites are indicated. The sequence of the combined fragment has been deposited under GenBank accession no. EF419244. (B) Organization of the mandelate pathway genes based on GenBank accession no. AY143338. Benzoylformate decarboxylase (*mdlC*), *S*-mandelate dehydrogenase (*mdlB*) and mandelate racemase (*mdlA*) make up the *mdlCBA* operon while benzaldehyde dehydrogenase (*mdlD*) is transcribed independently.

The evidence for BFDC activity coupled with the observations that *P. stutzeri* ST-201 was able to grow on benzaldehyde and that benzoate could be found in the culture medium, suggested the likely presence of a BADH. Consequently, it was not surprising when a BLAST search of the full length amino acid sequence indicated that the *dpgC* gene product was likely to be an aldehyde dehydrogenase, probably of the class 3 type. Dehydrogenases of this class are characterized by the ability to utilize both NAD^+ and $NADP^+$ (51). The *dpgC* gene sequence was 86% identical to that of the BADH from *P. putida* ATCC 12633 *Pp*BADH (34) (Figure 34). The catalytic residues, including the catalytic thiol (Cys249) and the general base (Glu337) were conserved as was the aspartic acid residue (Asp253) that links conserved domains in class 3 aldehyde dehydrogenases (52). *Ps*BADH also shared 30-40% sequence identity with other aldehyde dehydrogenases from pseudomonads, including the *p*-hydroxy-benzaldehyde dehydrogenase from *P. putida* NCIMB 9866 (53). However, although they are closely related phylogenetically, the other pseudomonad aldehyde dehydrogenases are not class 3 enzymes (51).

6. Expression of *P. stutzeri* ST-201 *dpgB* gene in *E. coli* and characterization of recombinant *Ps*BFDC

Pure recombinant *Ps*BFDC was successfully achieved using the same protocol as that with wt *Ps*BFDC, i.e., using a series of four steps including ammonium sulfate fractionation, followed by hydrophobic interaction chromatography, centrifugal utrafiltration and ion-exchange chromatography. The enzyme was finally purified 2.6 fold with 13% yield. The purified recombinant *Ps*BFDC had a specific activity of 243 U mg^{-1}.

The subunit molecular mass of the recombinant enzyme by SDS-PAGE, ~56 kDa, was in good agreement with the molecular mass calculated from the *dpgB* gene sequence, 56 kDa. Superdex 200 HR 10/30, gel-filtration experiments provided a native molecular mass of ~224 kDa. This indicated that BFDC from *P. stutzeri* ST-201 associates as a homotetramer, a characteristic common in bacterial BFDCs (5, 13). Crystal structure of *Pp*BFDC has demonstrated that the active tetramer are assembled by binding the cofactors ThDP, $Mg^{2+}$and Ca^{2+} (13), whereas monomers and dimers of indolepyruvate decarboxylase are inactive (54).

The enzyme was active over a broad range of temperature with maximum activity at 35-50 ^{o}C which was similar to that of the BFDC from *Neurospora crassa* (40 ^{o}C) (7). The effect of temperature on enzyme stability showed that the enzyme was stable up to 50 ^{o}C. Higher temperature gradually inactivated the enzyme and complete inactivation was registered after heating at 70 ^{o}C.

The enzyme showed optimal pH at 6.0 which was similar to that of the BFDC from *P. putida* (pH 6.2) (4) and reduced activity was observed at pH values over 7.5 and below pH 5.5. Loss of activity at both basic and acidic pH valued could be related to pH dependent subunit association equilibrium of the enzyme as it was described for the *E. cloacae* indolepyruvate decarboxylase tetramer structure, which was stabilized in the range of pH 5.6-7.5 (55). The *Ps*BFDC enzyme showed most stability at pH 6.0 which was in the range to that of pH 5.5-7.5 of *Pp*BFDC (12).

The p*I* of the *Ps*BFDC was estimated by denaturing IEF to be 5.2, which was in a good agreement with p*I* calculated from the deduced amino acid sequence. In the previous report, the p*I* of *Pp*BFDC was estimated by native IEF to be 6.5 (12)**.**

Michaelis-Menten parameters were determined for *Ps*BFDC by direct continuous assay under optimal conditions with temperature at 35 °C and pH 6.0. The K_m value for benzoylformate of 0.69 mM was similar to that for *Pp*BFDC. This was not surprising given that there is 91% sequence identity between the two enzymes, and those changes in sequence are located at some distance from the active site. However, at 222 s^{-1} the k_{cat} value for *Ps*BFDC was 35% lower than that of *Pp*BFDC even though the latter was determined by the coupled assay at a lower temperature (30 °C). Since both *Ps*BFDC and *Pp*BFDC showed high sequence identity , therefore, the differences in k_{cat} value could be due to the differences in purity of the enzyme used. ThDP-dependent enzymes are often purified as his_6-tagged variants to avoid loss of activity during multi-step purifications (14, 50). So, to facilitate a more rapid purification, *Ps*BFDC was also prepared with a C-terminal histidine tag, and a homogenous preparation was successfully obtained in a single step. This preparation showed an increase in k_{cat} to 284 s^{-1} and a decrease in K_m value to 0.43 mM. At 30 °C *Ps*BFDC had both K_m and k_{cat} values lower than those of its *P. putida* counterpart although the k_{cat}/K_m values were virtually identical. Predictably, as suggested by the high sequence

identity, preliminary experiments indicate that the substrate range for *Ps*BFDC is unlikely to be different from that of *Pp*BFDC (data not shown).

7. Preparation and purification of histidine-tagged *Ps*BADH

The X-ray structure of the class 3 aldehyde dehydrogenase from rat liver (38) shows that the C-terminal residues interact with other regions of the protein whereas the N-terminal residues are fully accessible. Based on this data an N-terminal histidine tag has been successfully employed to purify *Pp*BADH-his. The kinetic constants for this variant were essentially identical to those of the wt enzyme (C. Yeung and M. McLeish, unpublished results). Given the 86% sequence identity between *Pp*BADH and the putative *Ps*BADH it seemed reasonable to use an N-terminal histidine tag to facilitate the purification of the *dpg*C gene product. Accordingly the *dpg*C gene was amplified from pBCH2 and placed in the expression vector pET19b which adds an N-terminal His_{10}-tag. The enzyme was purified in a single step using a nickel affinity column. The purified protein showed a single band on SDS-PAGE with an estimated molecular mass consistent with that calculated from the gene sequence.

As predicted, the enzyme was able to oxidize benzaldehyde using either NAD^+ or $NADP^+$ as the cofactor. *Ps*BADH prefers NAD^+ over $NADP^+$ which is similar to both the rat aldehyde dehydrogenase (56) and *Pp*BADH (34). The K_m(app) values for NAD^+ and $NADP^+$ were obtained at saturating benzaldehyde concentration and, therefore, are indicative of the true K_m values. However, for comparison with data for *Pp*BADH (34), K_m(app) values for benzaldehyde were obtained at 1 mM $NAD(P)^+$ which is less than saturating. As with *Pp*BADH, it was likely that benzaldehyde was the natural substrate for *Ps*BADH as its apparent K_m values were in the low micromolar range. Overall, in keeping with their relative sequence identities, the kinetic properties of *Ps*BADH and *Pp*BADH are very similar.

CHAPTER 6
CONCLUSION

Firstly, this thesis showed that growth of *Pseudomonas stutzeri* ST-201 on minimal medium (MM) containing D-phenylglycine resulted initially in the induction of D-phenylglycine aminotransferase (D-PhgAT) activity and subsequently in the induction of benzoylformate decarboxylase (BFDC) activity. Conversely, growth of *P. stutzeri* ST-201 on MM containing benzoylformate only induced BFDC activity. The sequential expression of the two enzymes substantiated the role of BFDC from *P. stutzeri* ST-201(*Ps*BFDC) in D-phenylglycine degradation in a step following D-PhgAT. Secondly, this thesis described a strategy used for cloning *dpgB* gene of *Ps*BFDC. Not only, the *dpgB* was successfully cloned in one genomic restriction fragment but also the *dpgC* gene of benzaldehyde dehydrogenase (*Ps*BADH) was cloned in another overlapped genomic restriction fragment which contained partial *dpgB* gene. Thirdly, this thesis demonstrated the expression of *dpgB* gene in *E. coli*, purification and characterization of the recombinant *Ps*BFDC. Finally, this thesis also explained the expression of *dpgC* gene in *E. coli*, purification and characterization of recombinant BADH from *P. stutzeri* ST-201 (*Ps*BADH).

The two enzymes share a high degree of sequence identity with the homologous enzymes in the mandelate pathway of *P. putida*. Moreover, their kinetic parameters are similar, suggestive of comparable metabolic roles. It is possible that *Ps*BFDC and *Ps*BADH are components of the mandelate pathway yet *P. stutzeri* ST-201 is unable to utilize mandelate as a carbon source. Furthermore, the genes are organized quite differently. In *P. putida* ATCC 12633, the gene encoding BFDC (*mdlC*) forms part of an operon with those encoding mandelate racemase (*mdlA*) and *S*-mandelate dehydrogenase (*mdlB*), while the BADH gene (*mdlD*) is located upstream of the *mdlCBA* operon and is transcribed in the opposite direction. In *P. stutzeri* ST-201, the BFDC gene (*dpgB*) is independently transcribed, and the BADH gene

(*dpgC*) is located downstream of, and transcribed in the same direction as, *dpgB*. Taken together the data suggest that, in combination with D-phenylglycine aminotransferase, the two enzymes form a pathway for the degradation of D-phenylglycine with the product, benzoate, presumably entering the β-ketoadipate pathway (6). Whether benzoate is initially converted to 4-hydroxybenzoate or to catechol, and whether subsequent cleavage occurs by the ortho or meta pathway (6, 57), is the subject of future experiments.

REFERENCES

1. Sprenger GA, Pohl M. Synthetic potential of thiamin diphosphate-dependent enzymes. J Mol Catal B: Enzym 1999; 6: 145-159.
2. Hoey ME, Fewson CA. Is there a mandelate enzyme complex in *Acinitobacter calcoaceticus* or *Pseudomonas putida*?. J Gen Microbiol 1990; 136: 219-226.
3. Hegeman GD. Synthesis of the enzymes of the mandelate pathway by *Pseudomonas putida*: I. Synthesis of enzymes by the wild type. J Bacteriol 1966; 91: 1140-1154.
4. Hegeman GD. Benzoylformate decarboxylase (*Pseudomonas putida*). Methods Enzymol 1970; 17A: 674-678.
5. Barrowman MM, Fewson CA. Phenylglyoxylate decarboxylase and phenylpyruvate decarboxylase from *Acinetobacter calcoaceticus*. Curr Microbiol 1985; 12: 235-240.
6. Fewson CA. Microbial metabolism of mandelate: a microcosm of diversity. FEMS Microbiol Rev 1988; 4: 85-110.
7. Ramakrishna Rao DN, Vaidyanathan CS. Metabolism of mandelic acid by *Neurospora crassa*. Can J Microbiol 1997; 23: 1496-1499.
8. Tsou AY, Ransom SC, Gerlt JA, Buechter DD, Babbitt PC, Kenyon GL. Mandelate pathway of *Pseudomonas putida*: sequence relationships involving mandelate racemase, (*S*)-mandelate dehydrogenase, and benzoylformate decarboxylase and expression of benzoylformate decarboxylase in *Escherichia coli*. Biochemistry 1990; 29: 9856-9862.
9. Weiss PM, Garcia GA, Kenyon GL, Cleland WW, Cook PF. Kinetics and mechanism of benzoylformate decarboxylase using ^{13}C and solvent deuterium isotope effects on benzoylformate and benzoylformate analogues. Biochemistry 1988; 27: 2197-2205.

10. Sergienko EA, Wang J, Polovnikova L, Hasson MS, McLeish MJ, Kenyon GL, Jordan F. Spectroscopic detection of transient thiamin diphosphate-bound intermediates on benzoylformate decarboxylase. Biochemistry 2000; 39: 13862-13869.
11. Polovnikova ES, McLeish MJ, Sergienko EA, Burgner JT, Anderson NL, Bera AK, Jordan F, Kenyon GL, Hasson MS. Structural and kinetic analysis of catalysis by a thiamin diphosphate-dependent enzyme, benzoylformate decarboxylase. Biochemistry 2003; 42: 1820-1830.
12. Hasson MS, Muscate A, Henehan GT, Guidinger PF, Petsko GA, Ringe D, Kenyon GL. Purification and crystallization of benzoylformate decarboxylase. Protein Sci 1995; 4: 955-9.
13. Hasson MS, Muscate A, McLeish MJ, Polovnikova LS, Gerlt JA, Kenyon GL, Petsko GA, Ringe D. The crystal structure of benzoylformate decarboxylase at 1.6 Å resolution: diversity of catalytic residues in thiamin diphosphate-dependent enzymes. Biochemistry 1998; 37: 9918-9930.
14. Iding H, Dünnwald T, Greiner L, Liese A, Müller M, Siegert P, Grötzinger J, Demir AS, Pohl M. Benzoylformate decarboxylase from *Pseudomonas putida* as stable catalyst for the synthesis of chiral 2-hydroxy ketones. Chem Eur J 2000; 6:1483-1495.
15. Dünnwald T, Demir AS, Siegert P, Pohl M, Müller M. Enantioselective synthesis of *(S)*-2-hydroxypropanone derivatives by benzoylformate decarboxylase catalyzed C-C bond formation. Eur J Org Chem 2000; 2161-2170.
16. Dünkelmann P, Kolter-Jung D, Nitsche A, Demir AS, Siegert P, Lingen B, Baumann M, Pohl M, Müller M. Development of a donor-acceptor concept for enzymatic cross-coupling reactions of aldehydes: the first asymmetric cross- benzoin condensation. J Am Chem Soc 2002; 124: 12084-5.
17. Lingen B, Grotzinger J, Kolter D, Kula MR, Pohl M. Improving the carboligase activity of benzoylformate decarboxylase from *Pseudomonas putida* by a combination of directed evolution and site-directed mutagenesis. Protein Eng 2002; 15: 585-93.

18. B Lingen, Kolter-Jung D, Dunkelmann P, Feldmann R, Grotzinger J, Pohl M, Muller M. Alteration of the substrate specificity of benzoylformate decarboxylase from *Pseudomonas putida* by directed evolution. Chembiochem 2003;4: 721-6.
19. Siegert P, McLeish MJ, Baumann M, Kneen MM, Kenyon GL, Pohl M. Exchanging the substrate specificities of pyruvate decarboxylase from *Zymomonas mobilis* and benzoylformate decarboxylase from *Pseudomonas putida*. Prot Eng Des Sel 2005; 18: 345-357.
20. Henning H, Leggewie C, Pohl M, Muller M, Eggert T, Jaeger KE. Identification of novel benzoylformate decarboxylases by growth selection. Appl Environ Microbiol 2006; 72: 7510-7.
21. Wiyakrutta S, Meevootisom V. A stereo-inverting D-phenylglycine aminotransferase from *Pseudomonas stutzeri* ST-201: purification, characterization and application for D-phenylglycine synthesis. J Biotechnol 1997;55(3): 193-203.
22. Drrauz K, Waldmann H (Eds.). Enzyme Catalysis in Organic Synthesis. VCH, Weinheim ; 1996.
23. Kluger R. Mechanisms of enzymic carbon-carbon bond formation and cleavage In: Sigman D.S. (Hrsg.). The enzymes. 10th edition. New York: Academic Press; 1992. p. 271-315.
24. Csuk R, Glanzer BI. Baker's Yeast Mediated Transformations in Organic Chemistry. Chem Rev 1991; 91: 49-91.
25. Idling H, Siegert P, Mesch K , Pohl M. Application of α-keto acid decarboxylases in biotransformations. Biochim Biophys Acta 1998; 1385: 307-32.
26. Kern D, Kern G, Neef H, Tittmann K, Killenberg-Jabs M, Wikner C, Schneider G, Hubner G. How thiamin diphosphate is activated in enzymes. Science 1997; 275: 67-70.
27. Reynolds LJ, Garcia GA, Kozarich JW, Kenyon GL. Differential reactivity in the processing of [*p*-(halomethyl)benzoyl] formates by benzoylformate decarboxylase , a thiamin pyrophosphate dependent enzyme. Biochemistry 1988; 27: 5530-5538.

28. Dirmaier LJ, Garcia GA, Kozarich JW, Kenyon GL. Inhibition of benzoylformate decarboxylase by [p-(bromomethyl)benzoyl]formate. Enzyme-catalyzed modification of thiamine pyrophosphate by halide elimination and tautomerization. J Am Chem Soc 1986; 108 : 3149-3150.
29. Barrowman MM, Harnett W, Scott AJ, Fewson CA, Kusel JR. Immunological comparison of microbial TPP-dependent non-oxidative alpha-keto acid decarboxylase . FEMS Microbiol Lett 1986; 34: 57-60.
30. Tsou AY, Ransom SC, Gerlt JA, Powers VM, Kenyon GL. Selection and characterization of a mutant of the cloned gene for mandelate racemase that confers resistance to an affinity label by greatly enhanced production of enzyme. Biochemistry 1989; 28: 969–975.
31. Wheelis ML, Stanier RY. The genetic control of dissimilartory pathways in *Pseudomonas putida*. Genetics 1970; 66: 245–266.
32. Ransom SC, Gerlt JA, Powers VM, Kenyon GL. Cloning, DNA sequence analysis, and expression in *Escherichia coli* of the gene for mandelate racemase from *Pseudomonas putida*. Biochemistry 1988; 27: 540–545.
33. Tsou AY. A study of the genes encoding the enzymes in the mandelate pathway in *Pseudomonas putida.* Ph.D. Thesis. University of Maryland, College Park 1990.
34. McLeish MJ, Kneen MM, Gopalakrishna KN, Koo CW, Babbitt PC, Gerlt JA, Kenyon GL. Identification and characterization of a mandelamide hydrolase and an $NAD(P)^+$-dependent benzaldehyde dehydrogenase from *Pseudomonas putida* ATCC 12633. J Bacteriol 2003; 185: 2451-2456.
35. Wilcocks R, Ward OP, Collins S, Dewdney NJ, Hong Y, Prosen E. acyloin formation by benzoylformate decarboxylase from *Pseudomonas putida*: a novel biotransformation. Appl Environ Microbiol 1992; 58: 1699-1704.
36. Wilcocks R, Ward OP. Factors affecting 2-hydroxypropiophenone formation by benzoylformate decarboxylases from *Pseudomonas putida*. Biotechnol Bioeng 1992; 39: 1058-1063
37. Melandrinos G, Louloudi M, Hadjiliadis N. Thiamine models and perspectives on the mechanism of action of thiamine-dependent enzymes. Chem Soc Rev 2006; 35: 684-692.

38. Liu ZJ, Sun YJ, Rose J, Chung YJ, Hsiao CD, Chang WR, Kuo I, Perozich J, Lindahl R, Hempel J, Wang BC. The first structure of an aldehyde dehydrogenase reveals novel interactions between NAD and the Rossmann fold. Nat Struct Biol 1997; 4: 317-26.
39. Lalucat J, Bennasar A, Bosch R, Garcia-Valdes E, Palleroni NJ. Biology of *Pseudomonas stutzeri*. Microbiol Mol Biol Rev 2006; 70: 510-547.
40. Wiyakrutta S. Purification and characterization of a stereospecific transaminase for D-phenylglycine synthesis: Ph.D. Thesis, Mahidol University 1996.
41. Laowanapiban P. D-Phenylglycine aminotransferase from *Pseudomonas stutzeri* ST-201: gene cloning, sequence analysis, comparative structural modeling and over-expression in *Escherichia coli*: Ph.D. Thesis, Mahidol University 2001.
42. Kongsaeree P, Samanchart C, Laowanapiban P, Wiyakrutta S, Meevootisom V. Crystallization and preliminary x-ray crystallographic analysis of D-phenylglycine aminotransferase from *Pseudomonas stutzeri* ST-201. Acta Cryst 2003; D59: 953-54.
43. Beggs JD, Fewson CA. Regulation of synthesis of benzyl alcohol dehydrogenase in *Acinetobacter calcoaceticus* NCIB8250. J Gen Microbiol 1997; 103: 127-140.
44. Sambrook J, Fritsch EF, Maniatis T. Molecular cloning: a laboratory manual. 2nd edition. Cold Spring Harbor, New York: Cold Spring Harbor Laboratory Press; 1989.
45. Southern E.M. Detection of specific sequences among DNA fragments separated by gel electrophoresis. J Mol Biol 1975; 98: 503-517.
46. Grunstein M, Hogness DS. Colony hybridization: a method for the isolation of cloned DNAs that contain specific gene. Biotechnology 1992; 24: 117-21.
47. Bradford MM. A rapid and sensitive method for the quantitation of microgram quantities of protein utilizing the principle of protein-dye binding. Anal Biochem. 1976; 72: 248-54.
48. Pace CN, Vajdos F, Fee L, Grimsley G, Gray T. How to measure and predict the molar absorption coefficient of a protein. Protein Sci 1995; 4: 2411-23.

49. Rojanarata T. Genetic engineering of D-phenylglycine aminotransferase to facilitate immobilization and maximize catalytic performance: Ph.D. Thesis, Mahidol University 2004.
50. Pohl M, Siegert P, Mesch K , Bruhn H , Grotzinger J. Active site mutants of pyruvate decarboxylase from *Zymomonas mobilis*-a site-directed mutagenesis study of L112, I472, I476, E473, and N482. Eur J Biochem 1998; 257: 538-546.
51. Perozich J, Nicholas H, Wang BC, Lindahl R, Hempel J. Relationships within the aldehyde dehydrogenase extended family. Protein Sci 1999; 8: 137-146.
52. Hempel J, Kuo I, Perozich J, Wang BC, Lindahl R, Nicholas H. Aldehyde dehydrogenase. Maintaining critical active site geometry at motif 8 in the class 3 enzyme. Eur J Biochem 2001; 268: 722-6.
53. Cronin CN, Kim J, Fuller JH, Zhang X, McIntire WS. Organization and sequences of *p*-hydroxybenzaldehyde dehydrogenase and other plasmid-encoded genes for early enzymes of the p-cresol degradative pathway in *Pseudomonas putida* NCIMB 9866 and 9869. DNA Seq 1999; 10: 7-17.
54. Koga J, Adachi T, Hidaka T. Purification and characterization of indolepyruvate decarboxylase-a novel enzyme for indole-3-acetic-acid biosynthesis in *Enterobacter cloacae*. J Biol Chem 1992; 267: 15823-15828.
55. Schutz A, Golbik R, Tittmann K, Svergun DI, Koch MHJ, Hubner G, Konig S. Studies on structure function relationships of indolepyruvate decarboxylase from *Enterobacter cloacae*, a key enzyme of the indole acetic acid pathway. Eur J Biochem 2003; 270: 2322-2331.
56. Perozich J, Kuo I, Wang BC, Boesch JS, Lindahl R, Hempel J. Shifting the NAD/NADP preference in class 3 aldehyde dehydrogenase. Eur J Biochem 2000; 267: 6197-6203.
57. Cowles CE, Nichols NN, Harwood CS. BenR, a XylS homologue, regulates three different pathways of aromatic acid degradation in *Pseudomonas putida*. J Bacteriol 2000; 182: 6339-6346.

APPENDIX

APPENDIX

1. Properties of benzoylformic acid

Chemical Names

Benzoylformic acid

Phenylglyoxylic acid

CAS-No. 611-73-4

Chemical Formulae $C_8H_6O_3$

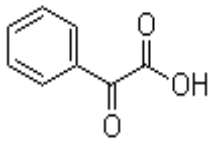

Molecular Weight 150.13

Melting Point 60-69°C

2. GenBank Accesssion No. EF419244 (*Pseudomonas stutzeri* isolate ST-201 benzoylformate decarboxylase (*dpgB*) and benzaldehyde dehydrogenase (*dpgC*) genes, complete cds)

EF419244. Reports ___ Pseudomonas stutzeri [gi:126202186]

```
LOCUS       EF419244              7653 bp    DNA     linear   BCT 09-OCT-2007
DEFINITION  Pseudomonas stutzeri isolate ST-201 benzoylformate decarboxylase
            (dpgB) and benzaldehyde dehydrogenase (dpgC) genes, complete cds.
ACCESSION   EF419244
VERSION     EF419244.1  GI:126202186
KEYWORDS    .
SOURCE      Pseudomonas stutzeri
  ORGANISM  Pseudomonas stutzeri
            Bacteria; Proteobacteria; Gammaproteobacteria; Pseudomonadales;
            Pseudomonadaceae; Pseudomonas.
REFERENCE   1(bases 1 to 7653)
  AUTHORS   Saehuan,C., Rojanarata,T., Wiyakrutta,S., McLeish,M.J. and
            Meevootisom,V.
  TITLE     Isolation and characterization of a benzoylformate decarboxylase
            and a NAD(+)/NADP(+)-dependent benzaldehyde dehydrogenase
            involved in D-phenylglycine metabolism in Pseudomonas stutzeri
            ST-201
  JOURNAL   Biochim. Biophys. Acta 1770 (11), 1585-1592 (2007)
  PUBMED    17916405
```

```
REFERENCE   2 (bases 1 to 7653)
  AUTHORS   Saehuan,C., Rojanarata,T., Wiyakrutta,S. and Meevootisom,V.
  TITLE     Direct Submission
  JOURNAL   Submitted (02-FEB-2007) Microbiology, Faculty of Science, Mahidol
            University, Rama 6 Road, Bangkok 10400, Thailand
FEATURES             Location/Qualifiers
     source          1..7653
                     /organism="Pseudomonas stutzeri"
                     /mol_type="genomic DNA"
                     /isolate="ST-201"
                     /db_xref="taxon:316"
     gene            3402..4982
                     /gene="dpgB"
     CDS             3402..4982
                     /gene="dpgB"
                     /note="ThDP-dependent decarboxylase"
                     /codon_start=1
                     /transl_table=11
                     /product="benzoylformate decarboxylase"
                     /protein_id="ABN80423.1"
                     /db_xref="GI:126202187"

/translation="MASVHSITYELLRRQGIDTVFGNPGSNELPFLKDFPEDFRYILA
LQEACVVGIADGYAQASRKPAFINLHSAAGTGNAMGAMSNAWNCHSPLIVTAGQQNRA
MIGVEALLTNVDAASLPRPLVKWSYEPASAAEVPHAMSRAIHMASMAPRGPVYLSVPY
DDWDKEADPQSHHLYDRSVNSAVRLNDQDLEVLVEALNSASNPAIVLGPDVDSANANA
DCVTLAERLKAPVWVAPSAPRCPFPTRHPCFRGLMPAGIAAISQLLEGHDVVLVIGAP
VFRYHQYDPGQYLKPGTRLISITCDPLEAARAPMGDAIVADIGTMTAALASRIGESER
QLPAVLPSPERVNQDAGRLRPETVFDTLNEMAPEDAIYLNESTSTTAQMWQRLNMRNP
GSYYFCAAGGLGFALPAAIGVQLAEPDRQVIAVIGDGSANYSISALWTAAHYNIPAIF
LIMNNGTYGALRWFAGVLEAENVPGLDVPGIDFCAIAKGYGIPALKADNLEQLKGSIH
EALSAKGPVLIEVSTVSL"

     gene            5230..6540
                     /gene="dpgC"
     CDS             5230..6540
                     /gene="dpgC"
                     /note="NAD(P)-dependent aldehyde dehydrogenase"
                     /codon_start=1
                     /transl_table=11
                     /product="benzaldehyde dehydrogenase"
                     /protein_id="ABN80424.1"
                     /db_xref="GI:126202188"

/translation="MNYLSPAMIDSLFSAQKAFFATRATADVGFRKQALKRLRDAVIN
NKEFFYSALAEDLGKTREVVDLAEIGEVLHEIDFALANLDEWIVPESVPTPEIIAPSE
CYIVQEPYGVTYIIGPFNYPVNLTLTPLIGAIIGGNTCIIKPSETTPETSRVIEKIIA
EAFSPEYVTVIQGGLAENSHLLSLPFDFIFFTGSPNVGKVVMKAAAEHLTPVVLELGG
KCPLIVLPDADLDQTVDQLMFGKFINSGQTCIAPDYLYAHRSVKDALLQRVVERVKND
LPKVNSTGKIVTSRQVVRLVSLLEETRGKVLVGAQADVDNRAFSATVVDSVQWDDPLM
AEELFGPILPVLEFDDVPTAVNLINKHHPKPLAVYVFGKDVDLAKGIINQIQSGDAQV
```

```
ORIGIN
        1 aagcttctgc aacgcaccaa ctcatcccac cgccacgcca aagatgttca gtacgagatc
       61 gagtccgtcg ccaacacagc caatagttcc attgcctccc tgtttagcga tgcgcgtgcg
      121 ttcgcgacgt tcatggtctg ggttgctttc gggatgtgca tgctgattgt ctatgggttc
      181 agtcttccct tggagcagaa cttcctcctg ttcggcttgc caggcgtggt tgcggtaatc
      241 gcagagctgc tgatttcaca acgtcattca agccgggtgt ctgtgagcac tcgtctaaag
      301 cagaacgctt agtacctttc gctacacccc gtccaggttc gcaactcgcc agcgtacggg
      361 tttcggtgcg gctctaaagc tgcgccgttt tttcaaaaag tttccccgga ccattacatg
      421 gtttaggtaa ctgcgtccaa aaaatactcg agcacaaaag tcggagtggg gcagattaag
      481 catatttgtc gtataggctt ggctgtgatt ggtcgttgcg tcttaagtca tttaaagcgg
      541 cgcgttaaaa ggcttgattt cgaagttcgt aatactaagg tcaaagcccg atatggagct
      601 ggctttgacg agaatcgatt gataactagc tatatctgga agttctggta atccgccgag
      661 cgacatgctt cgaatatcta aggagtgtcg cgctgcataa ttgcgagaga ggaactgcta
      721 tgggcataga attgttgagc gatcggagca aggtttatga cttcgcagat cctcatgtgg
      781 tgtccgcgta tgtgaatcag catgtaggca atcactctat agcgatttcg gatgggcgaa
      841 gccaggcaat gctcatccat cgacaggtcg ctgatctgga tttctgtcga atcagatatg
      901 ggagtgaaac atgtgttact tctacagcgc ttcgcgataa atatcacatc caaattatgc
      961 taggcggtag ttgcttgcag cgcatctcag gcacgcatcg cgttctctcg gtaggtgatc
     1021 tggtcgtgat caatccaaac gatcctgtag atttgactta ctctcatgac tgcgagaaat
     1081 ttattctaaa agtnccctgt caaactggtg gaggcagtat gtgatgatca gcattggtgc
     1141 cgcccatcaa cagggctccg ttttgatgag aaggtttatc aacttaatga tttgcaagga
     1201 atggttcagc tgctcagtct tgtttgtggt gagattgaaa atgaaagcat aattcgagca
     1261 gttcaagagc attacgttca aataataatc atcaaaattt tgacgtcgtt acttacaaac
     1321 ctagagtaca cggcggtggg cgttcagaat caactgctcc gcaaggtatt gcatcatatt
     1381 gaagataatc tgaagcagga tataacccct gaaggactgg ctaaatatgc caacgtcagc
     1441 ctgcgtagcc tttacgttct gttcgatcag tatttaggtg aaccgccgcg acgttacttt
     1501 gtcagaagga ggttggaaca ggtgcgcgct gcgcttctag gtgctgaggg gcgcaggaag
     1561 aacgtgacgg agattgcgat ggattacggc ttcacgcact tggggcggtt ttcagctgaa
     1621 tacaaagctc attttgctga gcttccctca gagaccttga agcatcgtcc caataactga
     1681 aagcacaggg cccgccttgg cgggccctgt gcaatggctc aggccaggta tttctcgatt
     1741 tctttctcgc gccagatgat tccaacgcct ggaagatccg gaataactgc attgccagct
     1801 tcgaaattca gcgtgggctc catcacgcta gcggcaagat ccaaacgctc cagccagtgg
     1861 gcagttggag tagcagccaa cacgtgtgca ctgatttctt ggaacagatg gctggacatg
     1921 ggcacgccga actgctgagc cagcgcactg gtccggagcc aaccagtcac tccaccaatc
     1981 tccattgcgt ctggcattgc cagccgacat gcaccagctg tcagtgcctt gaacatttcc
     2041 tccgggccga accagttttc gcccatctgc acagggatat ccagactgtt ttggatgcgc
     2101 tggtggcctg catagtcatg ctgcaaagtt ggctcttcga tccgggtgcc gcccgcgtcc
     2161 tgcagggcca agccacgctt gagggcagct ggcacgtcca ggctctggtt ataatcgacc
     2221 aagatttcaa aatcatcacc gaccgcctcg cggatgcttc caactacagc caggtcttta
     2281 tccagcgtcg gataaccaat cttggtctta accgctcgga agcctgactt agcagcagtc
     2341 actgcgcgtt cagtcgcgag ctttacaccg tccagactgt cgctgtcata ggcagggatc
     2401 gggcgagcct tggcgccgag cagattaacc agcggcgttt cgtgaacctt agccagagca
     2461 tctcaagccg ccatgtcgat ccctgcagtt gccatgcgga tagccgcgct ggcgatactg
     2521 tgattcgcac aacggtaatg ggcttctgcg acaaaaggtc tcctcaaatt tgatgattgc
     2581 cacccacttt tcatgcataa cgggccagct gcgtccggtt ctgcgctcca gcttggccat
     2641 cgcgttattg aggtgggtgc gcactgtcgt gaaccctatt ccgagttggc gggccacctc
     2701 tttaacactg gcaccagccg ccactagctt ggcaactccg cttccctaaa cgacaacaag
     2761 tgctttcgat cgggtgcgga tgcgaaagcc ctggcgaagt atggttgaag cgtcagcaag
     2821 agccgctctt cgcgctcgct gaaaggctct cggcctctgc ctctccatat cctaaaatcg
     2881 cccgtgctcc atgtccgcag ggcgtagaaa gtcgttatag atctcactgt gaagcagggc
     2941 agggcgcggc acatggcaat cgacgcacgc cggcttggcc actctgcgca ttaccggggt
     3001 caccatgtct acccgatgaa aatgctgctg gtacgcctcc atcttgtacc cgtcgatgtt
     3061 gaaggcacac ggctgacagg gtcgctgccc acgctcatcc cacataacag aggcgatgtg
     3121 gtcggcatcg agaagggtcg ccacagcttg gagggtagct gcgcgagcat caggctttcc
     3181 ctgacactca gccagaagcc agacaagctc ggctatctga tccaggtcgg tttcttgctg
     3241 cactgtcacc attgacccct ccggaaactc tgtggatacg ccccaaaaac ggaatcaaat
     3301 taaataaggc gcatctatag ataaatcaaa aatttatcta tttgatctat ttgaccctcg
     3361 cttctatcgt gggcttcgta atttggtaag agatatccat catggcatcg gtacacagca
     3421 tcacttatga gctcctccgc cgtcagggca tcgacacggt gttcggcaac cctggttcca
     3481 acgaactgcc gtttctgaag gatttcccag aggactttcg ctacatcctc gcgttgcagg
     3541 aagcgtgcgt ggtaggtatt gctgatggtt acgcccaggc cagtcgcaaa cctgcattca
     3601 ttaacctgca ttctgcagcg ggcacgggca acgcgatggg cgcgatgagt aacgcctgga
     3661 actgccactc tccgctgatc gtgacagctg gtcagcaaaa ccgagcgatg attggggttg
     3721 aggcactgtt gaccaacgtc gacgccgcca gccttccccg tcctctcgtc aaatggagtt
```

```
3781 acgagccggc gagcgctgcg gaagtgccac atgcaatgag ccgagctatt cacatggcga
3841 gcatggcacc tcgcgggcct gtgtatctct ctgtgccata cgatgattgg gacaaggaag
3901 cggatcctca gtctcatcac ctgtacgatc ggagtgtcaa ctcagctgtt cgtctgaatg
3961 accaagatct ggaagtgctg gtggaagctc tcaacagcgc gtccaacccc gcaattgtgc
4021 tcggcccaga cgtcgactcc gcgaatgcaa atgctgattg cgtaacattg gccgaacgac
4081 tcaaagctcc tgtatgggtt gccccttctg ccccgcgctg ccccttccca acccgacacc
4141 cctgtttccg agggcttatg cctgccggta tcgcagcgat ctctcaactg ctggagggtc
4201 acgatgtggt gttggttata ggcgcccccg tattccgcta ccaccagtac gatccaggtc
4261 agtacctgaa accaggtacc cgcttgattt cgatcacctg tgacccgctc gaagcggcac
4321 gcgcgccaat gggcgatgcg attgttgcag acatcggtac catgaccgct gcgctcgcca
4381 gccgcatcgg cgaaagcgaa cgccaacttc cagcggttct ccccagtccg gagagggtta
4441 accaggatgc cgggcgtctg cgtccagaaa cggtgtttga cacactcaac gagatggctc
4501 ctgaggatgc gatttacctc aacgaatcca cctcaacgac cgcccaaatg tggcagcgtc
4561 tgaacatgcg caacccgggc agctattact tctgcgcagc aggagggctc ggctttgccc
4621 tgccagcagc gataggagtt caactggcgg aaccggatcg acaagtcatc gctgtcatcg
4681 gcgacgggtc agccaactac agcattagtg ccttgtggac agcagcccat tacaacatcc
4741 cagccatctt cttgatcatg aacaacggca catacggtgc tcttcgatgg tttgctggtg
4801 tgctggaagc cgagaacgtt ccaggcttgg atgtgccagg aatcgacttc tgcgcgatcg
4861 ccaagggata tggtattcct gcgctgaaag ctgacaatct tgagcagctc aaaggctcca
4921 ttcatgaagc gctgtctgcc aaagggccgg tattgatcga ggtcagcacg gtcagcctgt
4981 gacgtgagat ttgacgatga gtcagcagaa tatatttagc gtcgaagact aggcattgaa
5041 atcgaaggtt tgcctcacag tgacacgcgg ttgctagcaa ttgcttgcgt cattgaaggc
5101 attttgggca gaggtccatc tcctgagcga ggaacgtgaa ggcagcccaa cactccatgt
5161 ggcaactgct ctgtcttctg gaaccagtcg ctacccatcg agctcgtaac ccgaatagag
5221 ggattgtcca tgaattatct gtccccggcg atgatcgact cgctgttctc agctcaaaag
5281 gctttcttcg cgacccgcgc aacagccgat gttggcttca gaaagcaggc tttaaaacgg
5341 ctccgagacg cggtgatcaa caacaaggag ttcttctatt ccgcgttagc agaagacttg
5401 ggtaaaacca gggaagtggt tgacctagcg gaaatcggtg aagtcctgca tgaaatcgac
5461 ttcgccctgg cgaacctgga tgaatggatc gttccggagt ctgttcccac tccggaaatt
5521 atcgcgccct cggagtgtta catcgtccag gagccttacg gtgtcaccta catcattggc
5581 ccgttcaact acccggtaaa tctgacactg acccctctga tcggcgccat tatcggtggc
5641 aacacctgca tcatcaaacc gtctgagacg actcccgaga cgtctcgcgt tatcgagaaa
5701 atcatcgcgg aagcattctc ccccgaatac gtcaccgtga ttcaaggtgg gctcgcagag
5761 aacagccatc ttttgagcct gcctttcgat ttcatcttct ttactggcag ccccaacgtc
5821 gggaaggtgg tcatgaaggc ggcggctgag catctgacgc cggttgtgct tgaacttggg
5881 ggaaaatgcc ccctcatcgt tctgcctgac gctgacctcg accaaactgt tgatcaattg
5941 atgttcggta aattcatcaa cagtggccaa acctgtatcg cacccgatta cctctatgcg
6001 catcgcagcg tcaaagatgc tttgctgcaa cgggtggttg agcgggtgaa gaacgacctg
6061 cctaaggtta attcgaccgg caagatcgta acctcacgcc aggtggtgcg tttggtttcc
6121 ttgcttgaag agacgcgtgg aaaggtgttg gtcggggccc aggccgacgt agacaacaga
6181 gcattcagcg caacggtagt ggacagcgtt caatgggacg acccgcttat ggcggaggag
6241 ctcttcgggc cgattttgcc agtgcttgaa ttcgatgatg tccccaccgc agtcaatctg
6301 attaacaagc accaccccaa gcccttggcc gtttatgtgt tcggcaagga cgtggatctc
6361 gcaaaaggca tcatcaatca gatccagtcc ggtgacgcgc aggtcaacgg cgtcatgctt
6421 catgccttct ctccatacct tccttttgga ggcattggtg cgtcaggtat gggcgactat
6481 cacgggcact acagctacct caccttcacg cacaaaaaat ccgtcaggat tgtgccgtaa
6541 ctgaagacgc ggagcgcgct gggttgagta actacactgg gtgagctcgt atgtctataa
6601 ggggcatcca ggcgttcaga tgaaagctca ccactactgc tccatcctga acgaggatgt
6661 catcccgtgc gtcatcctcg atcgccccag gcatcaacaa gagtggagag cgagacactg
6721 atattgtctg tatttttgct gctgatagtg cattgagaaa tttatctgtg cggctgcgta
6781 atgcaaatta tcgaacttcg ggtcccgttc gtggtattga tattacaagt gtgattgtta
6841 gctgttcttt tttgctgttc taattgaggg tgttcgttat ggcttttcaa aatctaccgt
6901 tctcaaaatc aagagcctac caaggattgg tgtttctaag cggcgaggtg ccgttcgata
6961 gtgagggaaa aattcccgct ggcgtaggtg ctcagacaga gctaaccttg agtaacatta
7021 gtgccacact tgcccgagaa gggctcagct tggccgatgt aatcagtgtt acggtgtatc
7081 tgactaaccg tgatgatttt gcagagttca atcgcgttta cgcttctcac ttcagtgccc
7141 ccttaccggt gagaaccact atttgcacgc aactgatgat tgatgcgtgc gttgagctga
7201 cagttatcgc cgctcgccac tcttgaggtt cgccttatga ggacagtcat agtactcggc
7261 gctggtattg ttggcgtctg cacagctttg caattgcgtc gccgtggctg ggatgtaacg
7321 ctggtggatc gccgcagtcc tgggcaggaa acttcctacg gcaatgctgg cattattcag
7381 cgtgaagcgg taatgccgta cccgttcccc agggatttag ccactctgct aaaagttctg
7441 cgcaaaggtg gggttgacgt aaactaccac gctaatgcga ttcctgcgtt actgccgcga
7501 cttgtgcgtt attggcaagc atcgtcacct cggtgttatg cgctctacgc gcaatcgttc
7561 agatcattga tcgaacactg cattgaagag catcgcgatc tcatcgagca cgcccaggct
7621 gggcacttga tacatacaga ggggtggctg cag
```

3. GenBank Accesssion No. ABN80423 (benzoylformate decarboxylase [*Pseudomonas stutzeri*])

```
ABN80423. Reports     benzoylformate decarboxylase [gi:126202187]

LOCUS       ABN80423   526 aa    linear   BCT 09-OCT-2007
DEFINITION  benzoylformate decarboxylase [Pseudomonas stutzeri].
ACCESSION   ABN80423
VERSION     ABN80423.1  GI:126202187
DBSOURCE    accession EF419244.1
KEYWORDS    .
SOURCE      Pseudomonas stutzeri
  ORGANISM  Pseudomonas stutzeri
            Bacteria; Proteobacteria; Gammaproteobacteria; Pseudomonadales;
            Pseudomonadaceae; Pseudomonas.
REFERENCE   1  (residues 1 to 526)
  AUTHORS   Saehuan,C., Rojanarata,T., Wiyakrutta,S., McLeish,M.J. and
            Meevootisom,V.
  TITLE     Isolation and characterization of a benzoylformate decarboxylase
            and a NAD(+)/NADP(+)-dependent benzaldehyde dehydrogenase
            involved in D-phenylglycine metabolism in Pseudomonas stutzeri
            ST-201
  JOURNAL   Biochim. Biophys. Acta 1770 (11), 1585-1592 (2007)
   PUBMED   17916405
REFERENCE   2  (residues 1 to 526)
  AUTHORS   Saehuan,C., Rojanarata,T., Wiyakrutta,S. and Meevootisom,V.
  TITLE     Direct Submission
  JOURNAL   Submitted (02-FEB-2007) Microbiology, Faculty of Science, Mahidol
            University, Rama 6 Road, Bangkok 10400, Thailand
COMMENT     Method: conceptual translation supplied by author.
FEATURES             Location/Qualifiers
     source          1..526
                     /organism="Pseudomonas stutzeri"
                     /isolate="ST-201"
                     /db_xref="taxon:316"
     Protein         1..526
                     /product="benzoylformate decarboxylase"
                     /name="ThDP-dependent decarboxylase"
     Region          1..523
                     /region_name="PRK07092"
                     /note="benzoylformate decarboxylase; PRK07092"
                     /db_xref="CDD:75925"
     Region          2..171
                     /region_name="TPP_enzyme_N"
                     /note="Thiamine pyrophosphate enzyme, N-terminal TPP
                     binding domain; pfam02776"
                     /db_xref="CDD:66460"
     Region          190..325
                     /region_name="TPP_enzyme_M"
                     /note="Thiamine pyrophosphate enzyme, central domain.
                     Thecentral domain of TPP enzymes contains a 2-fold
                     Rossman
                     fold; pfam00205"
                     /db_xref="CDD:79513"
     Region          353..523
                     /region_name="TPP_BFDC"
                     /note="Thiamine pyrophosphate (TPP) family, BFDC
                     subfamily, TPP-binding module; composed of proteins
                     similar to Pseudomonas putida benzoylformate
                     decarboxylase
                     (BFDC). P; cd02002"
```

```
                     /db_xref="CDD:48165"
     Site            order(377..378,401,403,427..430,433,455,457,459..460)
                     /site_type="other"
                     /note="TPP-binding site"
                     /db_xref="CDD:48165"
     Site            order(399,432..433,439,443,458,474..475,479,481..482,
                     489..490)
                     /site_type="other"
                     /note="dimer interface"
                     /db_xref="CDD:48165"
     CDS             1..526
                     /gene="dpgB"
                     /coded_by="EF419244.1:3402..4982"
                     /transl_table=11
ORIGIN
        1 masvhsitye llrrqgidtv fgnpgsnelp flkdfpedfr yilalqeacv vgiadgyaqa
       61 srkpafinlh saagtgnamg amsnawnchs plivtagqqn ramigveall tnvdaaslpr
      121 plvkwsyepa saaevphams raihmasmap rgpvylsvpy ddwdkeadpq shhlydrsvn
      181 savrlndqdl evlvealnsa snpaivlgpd vdsananadc vtlaerlkap vwvapsaprc
      241 pfptrhpcfr glmpagiaai sqlleghdvv lvigapvfry hqydpgqylk pgtrlisitc
      301 dpleaarapm gdaivadigt mtaalasrig eserqlpavl pspervnqda grlrpetvfd
      361 tlnemapeda iylneststt aqmwqrlnmr npgsyyfcaa gglgfalpaa igvqlaepdr
      421 qviavigdgs anysisalwt aahynipaif limnngtyga lrwfagvlea envpgldvpg
      481 idfcaiakgy gipalkadnl eqlkgsihea lsakgpvlie vstvsl
```

4. GenBank Accesssion No.ABN80424 (benzaldehyde dehydrogenase [*Pseudomonas stutzeri*])

```
ABN80424. Reports ___ benzaldehyde dehydrogenase   [gi:126202188]

LOCUS       ABN80424           436 aa     linear   BCT 09-OCT-2007
DEFINITION  benzaldehyde dehydrogenase [Pseudomonas stutzeri].
ACCESSION   ABN80424
VERSION     ABN80424.1  GI:126202188
DBSOURCE    accession EF419244.1
KEYWORDS    .
SOURCE      Pseudomonas stutzeri
  ORGANISM  Pseudomonas stutzeri
            Bacteria; Proteobacteria; Gammaproteobacteria; Pseudomonadales;
            Pseudomonadaceae; Pseudomonas.
REFERENCE   1  (residues 1 to 436)
  AUTHORS   Saehuan,C., Rojanarata,T., Wiyakrutta,S., McLeish,M.J. and
            Meevootisom,V.
  TITLE     Isolation and characterization of a benzoylformate decarboxylase
            and a NAD(+)/NADP(+)-dependent benzaldehyde dehydrogenase
            involved in D-phenylglycine metabolism in Pseudomonas stutzeri
            ST-201
  JOURNAL   Biochim. Biophys. Acta 1770 (11), 1585-1592 (2007)
   PUBMED   17916405
REFERENCE   2  (residues 1 to 436)
  AUTHORS   Saehuan,C., Rojanarata,T., Wiyakrutta,S. and Meevootisom,V.
  TITLE     Direct Submission
  JOURNAL   Submitted (02-FEB-2007) Microbiology, Faculty of Science, Mahidol
            University, Rama 6 Road, Bangkok 10400, Thailand
COMMENT     Method: conceptual translation supplied by author.
FEATURES             Location/Qualifiers
     source          1..436
                     /organism="Pseudomonas stutzeri"
                     /isolate="ST-201"
```

```
                     /db_xref="taxon:316"

     Protein         1..436
                     /product="benzaldehyde dehydrogenase"
                     /name="NAD(P)-dependent aldehyde dehydrogenase"
     Region          4..434
                     /region_name="PutA"
                     /note="NAD-dependent aldehyde dehydrogenases [Energy
                     production and conversion]; COG1012"
                     /db_xref="CDD:31216"
     Region          5..432
                     /region_name="Aldedh"
                     /note="Aldehyde dehydrogenase family. This family of
                     dehydrogenases act on aldehyde substrates. Members use
                     NADP as a cofactor. The family includes the following
                     members: The prototypical members are the aldehyde
                     dehydrogenases EC:1.2.1.3; pfam00171"
                     /db_xref="CDD:64056"
     CDS             1..436
                     /gene="dpgC"
                     /coded_by="EF419244.1:5230..6540"
                     /transl_table=11
ORIGIN
        1 mnylspamid slfsaqkaff atratadvgf rkqalkrlrd avinnkeffy salaedlgkt
       61 revvdlaeig evlheidfal anldewivpe svptpeiiap secyivqepy gvtyiigpfn
      121 ypvnltltpl igaiiggntc iikpsettpe tsrviekiia eafspeyvtv iqgglaensh
      181 llslpfdfif ftgspnvgkv vmkaaaehlt pvvlelggkc plivlpdadl dqtvdqlmfg
      241 kfinsgqtci apdylyahrs vkdallqrvv ervkndlpkv nstgkivtsr qvvrlvslle
      301 etrgkvlvga qadvdnrafs atvvdsvqwd dplmaeelfg pilpvlefdd vptavnlink
      361 hhpkplavyv fgkdvdlakg iinqiqsgda qvngvmlhaf spylpfggig asgmgdyhgh
      421 ysyltfthkk svrivp
```

Available online at www.sciencedirect.com
ScienceDirect
Biochimica et Biophysica Acta 1770 (2007) 1585–1592
Biochimica et Biophysica Acta BBA
www.elsevier.com/locate/bbagen

Isolation and characterization of a benzoylformate decarboxylase and a NAD^+/$NADP^+$-dependent benzaldehyde dehydrogenase involved in D-phenylglycine metabolism in *Pseudomonas stutzeri* ST-201

Choedchai Saehuan [a,b], Theerasak Rojanarata [c], Suthep Wiyakrutta [a], Michael J. McLeish [b,*], Vithaya Meevootisom [a]

[a] *Department of Microbiology, Faculty of Science, Mahidol University, Thailand*
[b] *Department of Medicinal Chemistry, College of Pharmacy, University of Michigan, 428 Church St., Ann Arbor, MI 48109, USA*
[c] *Department of Pharmaceutical Chemistry, Faculty of Pharmacy, Silpakorn University, Thailand*

Received 6 July 2007; received in revised form 7 August 2007; accepted 8 August 2007
Available online 25 August 2007

Abstract

Following induction with D-phenylglycine both D-phenylglycine aminotransferase activity and benzoylformate decarboxylase activity were observed in cultures of *Pseudomonas stutzeri* ST-201. Induction with benzoylformate, on the other hand, induced only benzoylformate decarboxylase activity. Purification of the benzoylformate decarboxylase, followed by N-terminal sequencing, enabled the design of probes for hybridization with *P. stutzeri* ST-201 genomic DNA libraries. Sequencing of two overlapping genomic DNA restriction fragments revealed two open reading frames which were denoted *dpgB* and *dpgC*. Sequence alignments suggested that the genes encoded a thiamin-diphosphate-dependent decarboxylase and an aldehyde dehydrogenase, respectively. Both genes were isolated and expressed in *Escherichia coli*. The *dpgB* gene product was confirmed as a benzoylformate decarboxylase while the *dpgC* gene product was characterized as a NAD^+/$NADP^+$-dependent benzaldehyde dehydrogenase. In keeping with their high sequence identities (both greater than 85%) the kinetic properties of the two enzymes were similar to those of the homologous enzymes in the mandelate pathway of *Pseudomonas putida* ATCC 12633. However, *Pseudomonas stutzeri* ST-201 was unable to grow on either isomer of mandelate, and sequencing indicated that the *dpgB* gene did not form part of an operon. Thus it appears that the two enzymes form part of a D-phenylglycine, rather than mandelate, degrading pathway.

Keywords: Gene cloning; Southern hybridization; Histidine tag; Mandelate pathway; Enzyme; D-phenylglycine pathway

1. Introduction

Benzoylformate decarboxylase (BFDC; EC 4.1.1.7) is a thiamin diphosphate (ThDP)-dependent enzyme that catalyzes the decarboxylation of benzoylformate forming benzaldehyde and carbon dioxide [1]. BFDC was initially identified as a member of the mandelate pathway, which enables bacteria to utilize mandelate as a sole carbon source. In this pathway, benzoylformate is formed via the oxidation of *S*-mandelate (Fig. 1) [2–4]. To date, the enzyme has been found in *Pseudomonas* and *Acinetobacter* species [5,6], as well as *Neurospora crassa* [7], with the most detailed studies being carried out on the BFDC from *Pseudomonas putida* ATCC 12633 (*Pp*BFDC). These include enzyme purification and characterization [3,4], gene cloning [8], kinetic and mechanistic studies [9–11], and X-ray crystallography [12,13]. Over the past few years *Pp*BFDC has become increasingly useful for the synthesis of enantiomerically pure pharmaceutical and chemical compounds [14–16]. Consequently, there is commercial interest in identifying BFDCs with an expanded substrate range whether by protein engineering [17–19] or from alternative sources [20].

Recently, benzoylformate was reported as the product of the reaction catalyzed by a D-phenylglycine aminotransferase

* Corresponding author. Tel.: +1 734 615 1787; fax: +1 734 615 3079.
E-mail address: mcleish@umich.edu (M.J. McLeish).

0304-4165/$ - see front matter © 2007 Elsevier B.V. All rights reserved.
doi:10.1016/j.bbagen.2007.08.007

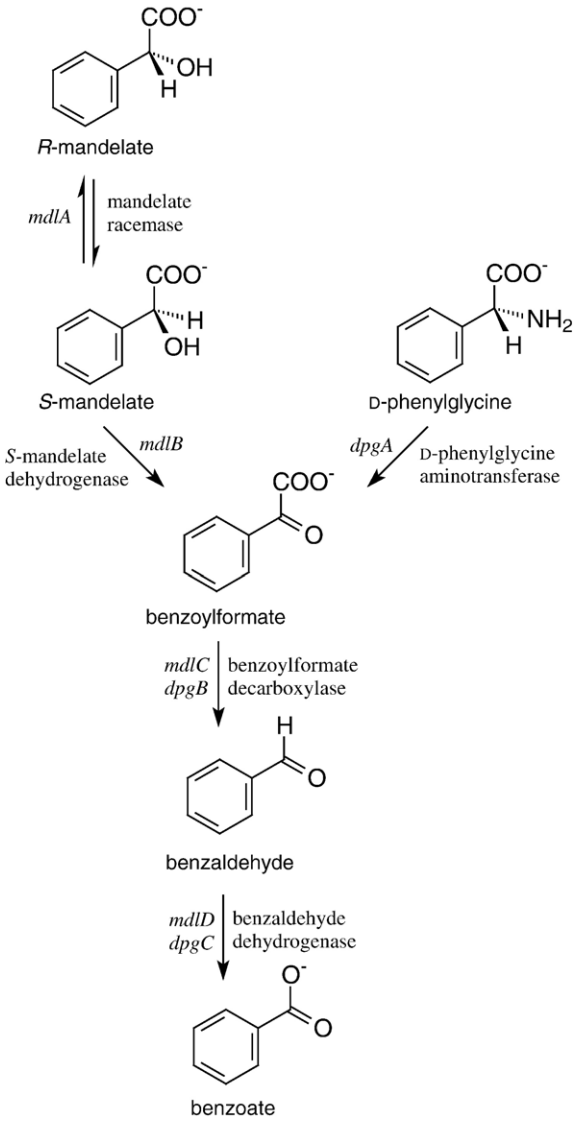

Fig. 1. The mandelate pathway in *P. putida* ATCC 12633 and the proposed pathway for D-phenylglycine degradation in *P. stutzeri* ST-201.

(D-PhgAT) in *Pseudomonas stutzeri* ST-201, a newly isolated soil bacterium found in Thailand [21]. Although *P. stutzeri* ST-201 had not been reported to possess BFDC activity, it had been shown to release both benzoylformate and benzoate into the culture medium during the early stages of D-phenylglycine degradation [21]. Therefore, it was reasonable to hypothesize that this strain could produce both BFDC and benzaldehyde dehydrogenase (BADH) for subsequent metabolism of benzoylformate and benzaldehyde, respectively. Here we confirm the presence of a BFDC in *P. stutzeri* strain ST-201 (*Ps*BFDC) and report the isolation of fragments of *P. stutzeri* ST-201 genomic DNA containing the genes encoding *Ps*BFDC (*dpgB)* and *Ps*BADH (*dpgC*). We describe the expression of *dpgB* and *dpgC* in *Escherichia coli* and the initial characterization of their gene products. Moreover, we suggest that these enzymes form part of a catabolic pathway, which we have termed the D-phenylglycine degradation pathway (Fig. 1).

2. Materials and methods

2.1. Materials

P. stutzeri ST-201 was available from a previous study [21]. *E. coli* strains, restriction enzymes, ligases, DNA polymerase and other molecular biology reagents were obtained from New England Biolabs, Promega, Stratagene or Novagen. All other chemicals were of the highest quality commercially available.

2.2. Screening for enzymes involved in mandelate and D-phenylglycine degradation

To verify the existence of enzymes catabolizing substrates of interest, *P. stutzeri* ST-201 was tested for growth on minimal medium (MM) agar containing (in 1 l): 15 g agar, 3.4 g KH_2PO_4, 3.6 g Na_2HPO_4, 0.2 g $MgSO_4$, 8 mg $CaCl_2$, 10 mg yeast extract and 1 ml trace metals solution [22]. The MM was supplemented, as appropriate, with the following carbon sources at a concentration of 10 mM: *R*-mandelate, *S*-mandelate, D-phenylglycine, benzoylformate or benzoate. For growth on benzaldehyde, a disk containing benzaldehyde (10 μl) was placed on the agar. With the exception of MM containing D-phenylglycine, 0.4 g NH_4NO_3 was included as the nitrogen source. The plates were examined for evidence of growth after incubation for 48 h at 30 °C.

To explore the induction of D-PhgAT and BFDC activity, *P. stutzeri* ST-201 was shaken in 200 ml Luria-Bertani (LB) medium at 30 °C until the culture reached an OD_{600} of 2.8. At that time the LB was exchanged for MM containing one of glucose, D-phenylglycine or benzoylformate (10 mM). Incubation was continued under the same conditions for a further 20–160 min with cell samples being harvested every 20 min. Enzyme activity in crude cell extracts was then determined using standard assays (below).

2.3. Purification of wt PsBFDC

P. stutzeri ST-201 was grown in LB (2 l) at 30 °C until the culture reached an OD_{600} ~2.8. At that time the LB was exchanged for MM containing 10 mM benzoylformate. Shaking continued at 30 °C for 9 h after which time the cells were harvested by centrifugation and the pellet resuspended in a buffer comprising 50 mM potassium phosphate, pH 6.0, 0.1 mM ThDP and 0.1 mM phenylmethylsulfonyl fluoride. Following sonication and centrifugation the cell-free extract (CFE) was subjected to stepwise ammonium sulfate fractionation. The ammonium sulfate fraction containing BFDC was dissolved in buffer A (25 mM potassium phosphate, pH 6.0, 0.1 mM ThDP, 0.1 mM $MgCl_2$, 10% glycerol) and applied to a Phenyl Sepharose FF column which had been equilibrated with buffer B (0.1 M sodium phosphate, pH 6.0 containing 0.1 M $(NH_4)_2SO_4$ and 0.1 mM ThDP). The BFDC was then eluted with buffer B at a flow rate of 2 ml min^{-1}. The active fractions were pooled, concentrated and exchanged into buffer C (25 mM Tris–HCl, pH 7.5, 0.1 mM ThDP) using a Centricon Plus-20 filtration unit (Amicon). The concentrate was loaded onto a Q Sepharose FF column equilibrated with buffer C, and the enzyme was eluted with buffer C containing NaCl (0.75 M). After the purity and molecular weight of the active fractions were checked by SDS-PAGE, a sample was blotted onto a polyvinylidine fluoride membrane and subjected to N-terminal sequencing (University of Newcastle, Australia).

2.4. Construction of subgenomic library and cloning of the dpgB gene

The degenerate forward primer, BFDC_F (Table 1), was designed based on the N-terminal amino acid sequence of *Ps*BFDC isolated in this work (above). The reverse primer, BFDC_R, was designed using the conserved amino acid sequences of BFDCs from *P. putida* (gi:3915757) and *P. aeruginosa* PAO1 (gi:15600094). With these primers a 1.28-kb DNA fragment containing part of the *dpgB* gene was amplified by PCR from the genomic DNA of *P. stutzeri* ST-201. The PCR products were cloned into pGEM-T Easy (Promega) and used to generate a digoxigenin-labeled *dpgB*-specific probe for Southern and colony hybridization.

Table 1
Primers used in this study

Primer	Sequence
BFDC_F[a]	5′-GGCATHGAYACCGTITTCGG-3′
BFDC_R	5′-TAGTTGGCCGAGCCGTCG-3′
BFDC_N[b]	5′-ATATCC**CATATG**GCATCGGTACACAGC-3′
BFDC_C[b]	5′-AAATC**AAGCTT**CACAGGCTGACCGTGCTGAC-3′
BFDC_X[c]	5′-GCACGGTCAGC**CTcgag**AGCTTGGTACCGAGCTCGG-3′
BADH_F[b]	5′-CCGAATAGAGGGATTG**CATATG**AATTATCTGTCCCC-3′
BADH_R[b]	5′-GCGCGCTCCGCGT**CTCGAG**TTACGGCACAATCC-3′

[a] Degenerate primer where H=A, C or T; Y=C or T; I=inosine.
[b] Introduced restriction sites are in bold.
[c] The new *Xho*I site is in bold and the lowercase letters indicate a base change from the wild-type sequence.

For subgenomic library construction, genomic DNA isolated from *P. stutzeri* ST-201 was subjected to digestion with various restriction enzymes, followed by agarose gel electrophoresis and Southern hybridization. Positive DNA fragments were eluted from the gel and ligated into pBluescript II SK which had been digested with the corresponding restriction enzyme(s). The ligation products were transformed into *E. coli* JM109 by electroporation and plated on LB agar containing 50 μg/ml ampicillin, 20 mM isopropyl-β-D-thiogalactopyranoside (IPTG) and 80 μg/ml 5-bromo-4-chloro-3-indolyl-β-D-galactopyranoside (X-gal). White colonies, containing a DNA insert, were screened by colony hybridization to identify individual colonies carrying a plasmid containing the *dpgB* gene. The two plasmids identified in this manner were designated pBCH1 and pBCH2.

2.5. DNA sequencing and gene analysis

The nucleotide sequences of both strands of the DNA fragment in pBCH1 and pBCH2 were determined at the National Science and Technology Development Agency, Thailand. The open reading frames (ORFs), DNA and protein alignment were analyzed using either VectorNTI (Invitrogen) or BioEdit (http://www.mbio.ncsu.edu/BioEdit/bioedit.html). The nucleotide and deduced amino acid sequences were compared to the sequences in the GenBank and SwissProt databases at the National Center for Biotechnology Information (Bethesda, MD) using the BLAST network server.

The nucleotide sequences determined in this work have been deposited under GeneBank accession no EF419244.

2.6. Expression of P. stutzeri dpgB gene in E. coli and purification of recombinant PsBFDC

The *dpgB* gene was PCR amplified using pBCH1 as the template. The forward and reverse primers, BFDC_N and BFDC_C (Table 1) introduced *Nde*I and *Hin*dIII sites, respectively. The PCR product was digested with *Nde*I and *Hin*dIII and ligated into pET17b. The resulting plasmid, pET17b*Ps*BFDC, was transformed into *E. coli* strain BL21(DE3). For expression of the recombinant *Ps*BFDC, the transformants were grown at 37 °C in LB to an A_{600} of 0.8 and induced by the addition of 0.4 mM IPTG. After a 6-h incubation the cells were harvested by centrifugation. Purification of the recombinant *Ps*BFDC was accomplished using the protocol described above for the wt enzyme. The purified enzyme, which showed a single band on SDS-PAGE, was stored at 4 °C in a buffer containing 50 mM phosphate, pH 6.0, 0.2 mM ThDP and 0.1 mM $MgCl_2$. The protein concentration was determined by the Bradford method using bovine serum albumin as the standard [23].

2.7. Expression and purification of histidine-tagged PsBFDC

Using pET17b*Ps*BFDC as the template, the QuikChange (Stratagene) methodology was employed to introduce an *Xho*I restriction site at the C-terminus of the *dpgB* gene. The sequence of the forward primer, BFDC_X, is shown in Table 1. The resultant plasmid was digested with *Nde*I and *Xho*I and the 1.6-kb fragment ligated into *Nde*I- and *Xho*I-digested pET24b, to provide a plasmid, denoted pET24b*Ps*BFDHis. The fidelity of the mutagenesis was confirmed by sequencing at the University of Michigan core facility.

pET24b*Ps*BFDHis was transformed into *E. coli* strain BL21(DE3)pLysS (Promega) and a single colony was used to inoculate 50 ml of LB broth containing kanamycin (50 μg/ml) and chloramphenicol (25 μg/ml). This culture was grown overnight at 37 °C and used to inoculate 1 l of fresh medium. The fresh culture was grown at 37 °C until OD_{600} reached 0.8. The cells were cooled to 25 °C, and the protein expression was induced by the addition of 1 mM IPTG. The cells were grown for an additional 12 h at 25 °C prior to harvesting by centrifugation. The cell pellet was resuspended in buffer D (50 mM potassium phosphate pH 8.0, 500 mM NaCl, 0.1 mM ThDP) containing 0.1 mM phenylmethanesulfonyl fluoride, disrupted by sonication and the cell debris was removed by centrifugation. The CFE was applied to a HIS-select™ Nickel Affinity column (Sigma) previously equilibrated in buffer D. After the column was washed with buffer D containing 20 mM imidazole, the enzyme was eluted with buffer D containing 250 mM imidazole. The fractions of highest purity, as judged by SDS-PAGE, were pooled and the buffer was exchanged for storage buffer (100 mM potassium phosphate buffer, pH 6.0, 1 mM $MgSO_4$, 0.5 mM ThDP, 10% glycerol) using Econo-Pac 10 DG desalting columns (Bio-Rad). The protein was concentrated using Amicon Ultra centrifugal filters (Millipore) before being stored at −20 °C. Protein concentrations were determined by either the Bradford [23] or a UV method [24].

2.8. Preparation and purification of histidine-tagged PsBADH

Based on the sequence of the open reading frame in pBCH2, two primers were designed to amplify the *dpgC* gene. The forward (BADH_F) and reverse (BADH_R) primers (Table 1) added *Nde*I and *Xho*I sites, respectively. Amplification was achieved with *PfuUltra* DNA polymerase (Stratagene), using pBCH2 as the template. The PCR product was purified, digested and ligated into pET19b (Novagen) previously digested with *Nde*I and *Xho*I. This construction added a 10× histidine tag to the N-terminus of the enzyme and generated the expression vector, pET19b*Ps*BADH-His. Once the fidelity of the amplification was verified by sequencing, the plasmid was transformed into *E. coli* strain BL21(DE3)pLysS (Promega) for expression.

Expression and preparation of a CFE of his-tagged *Ps*BADH were carried out as described for *Ps*BFDC-his. The extract was applied on HIS-Select™ Nickel Affinity column previously equilibrated in buffer E (50 mM potassium phosphate buffer, pH 8.0, 300 mM NaCl, 2 mM DTT) containing 10 mM imidazole. After washing with buffer E containing 40 mM imidazole, the enzyme was eluted in buffer E containing 250 mM imidazole. The fractions of highest purity were pooled and the buffer was exchanged for storage buffer (100 mM HEPES pH 7.5, 100 mM KCl, and 2 mM DTT) using Econo-Pac 10 DG desalting columns (Bio-Rad). The *Ps*BADH-his was then concentrated using Amicon Ultra centrifugal filters (Millipore) before being stored at −20 °C.

2.9. Measurement of enzyme activity

In crude cell extracts, D-PhgAT activity was determined using a spectrophotometric assay in which the rate of benzoylformate formation was measured by monitoring the increase in absorbance at 254 nm [25]. The assay was carried out in a buffer (1 ml) containing Tris–HCl (100 mM, pH 9.0), D-phenylglycine (1 mM), α-ketoglutarate (1 mM), pyridoxal-5′-phosphate (25 μM) and EDTA (25 mM). BFDC activity in crude cell extracts was determined using a continuous assay based on the decrease in absorbance at 334 nm as benzoylformate was converted to benzaldehyde [4]. The reaction mixture (1 ml) contained benzoylformate (8.33 mM) and ThDP (40 μM) in sodium phosphate buffer (66 mM, pH 6.0). Both assays were performed at 25 °C.

In addition to the direct method described for the induction studies, the decarboxylation of benzoylformate was also followed using a more sensitive coupled assay [9]. Here the assay was performed at the appropriate temperature in 100 mM potassium phosphate buffer pH 6.0, containing 1.0 mM $MgCl_2$, 0.5 mM ThDP, 0.3 mM NADH and 0.25 U/ml of horse liver alcohol dehydrogenase. The benzoylformate concentration was varied from 0.3 to 3× K_m and the reaction was initiated by the addition of BFDC. The decrease in absorbance at 340 nm was measured on a Cary 50 spectrophotometer (Varian) equipped with a temperature-controlled cell holder. Initial velocity data were

fitted to the Michaelis–Menten equation using the Enzyme Kinetics module of SigmaPlot® (SPSS Inc.). Kinetic parameters were determined per monomer using molecular masses of 56,302 for *Ps*BFDC or 57,367 for *Ps*BFDC-his.

Benzaldehyde dehydrogenase activity was monitored spectrophotometrically by observing the increase in A_{340} due to the reduction of NAD^+ [26]. Routine activity assays were carried out at 25 °C in a 1 ml reaction mixture containing 100 mM TAPS buffer, pH 8.5, 100 mM KCl, 1 mM DTT, 1 mM NAD^+ and 1 mM benzaldehyde. K_m(app) values for benzaldehyde were determined by fixing NAD^+ or $NADP^+$ at a concentration of 1 mM and varying the benzaldehyde concentration as required. For determination of the apparent K_m values for NAD^+ and $NADP^+$, benzaldehyde was maintained at a saturating concentration (1 mM) and the NAD^+ or $NADP^+$ concentration varied appropriately. Kinetic data were fitted to the Michaelis–Menten equation using the Enzyme Kinetics module of SigmaPlot® (SPSS Inc.). Kinetic parameters were determined per monomer using a molecular mass of 50278 Da for *Ps*BADH-his.

3. Results and discussion

3.1. Implication of a benzoylformate decarboxylase in D-phenylglycine degradation

With the exception of *R*- and *S*-mandelate, *P. stutzeri* ST-201 was able to grow on MM agar containing each of the tested carbon sources. The results demonstrated that the bacteria could produce enzymes capable of catabolizing D-phenylglycine, benzoylformate, benzaldehyde and benzoate. Further, the results showed that *P. stutzeri* ST-201 lacked, at the least, a *S*-mandelate dehydrogenase such as that found in the mandelate pathway of *P. putida* ATCC 12633 (Fig. 1, [3]). Therefore it was reasonable to assume that the benzoylformate found in cultures of *P. stutzeri* ST-201 grown on D-phenylglycine [21] was the product of the transamination of D-phenylglycine (Fig. 1).

In *P. putida* ATCC 12633 some of the enzymes of the mandelate pathway are coordinately regulated. BFDC activity, for example, can be induced by the addition of either *R*- or *S*-mandelate or benzoylformate (but not benzoate) to the culture medium [3]. In *P. stutzeri* ST-201 neither D-PhgAT nor BFDC activity was observed in MM containing glucose. However, when the culture medium was changed from LB to MM containing D-phenylglycine, D-PhgAT activity was detected after 40 min and was followed by BFDC activity which appeared after 100 min (Fig. 2A). Conversely, in MM with benzoylformate as sole carbon source there was no evidence for D-PhgAT activity but BFDC activity was observed after 60 min (Fig. 2B). Clearly, benzoylformate can induce only the expression of the BFDC gene whereas D-phenylglycine brings about an increase in the levels of both enzymes. What is not clear is whether this is because D-phenylglycine actually induces the genes for both enzymes or whether the gene for D-PhgAT is induced and the benzoylformate subsequently produced induces the BFDC gene. Based on the times at which the two enzyme activities are observed the latter is the most likely explanation. Regardless, the sequential expression of the enzymes substantiates the involvement of BFDC in the pathway in a step following D-phenylglycine degradation.

The decrease in the absorbance due to benzoylformate, as well as the presence of the characteristic odor of benzaldehyde, in the BFDC assays both pointed to the *P. stutzeri* ST-201 extracts having BFDC activity. Nevertheless, the presence of a

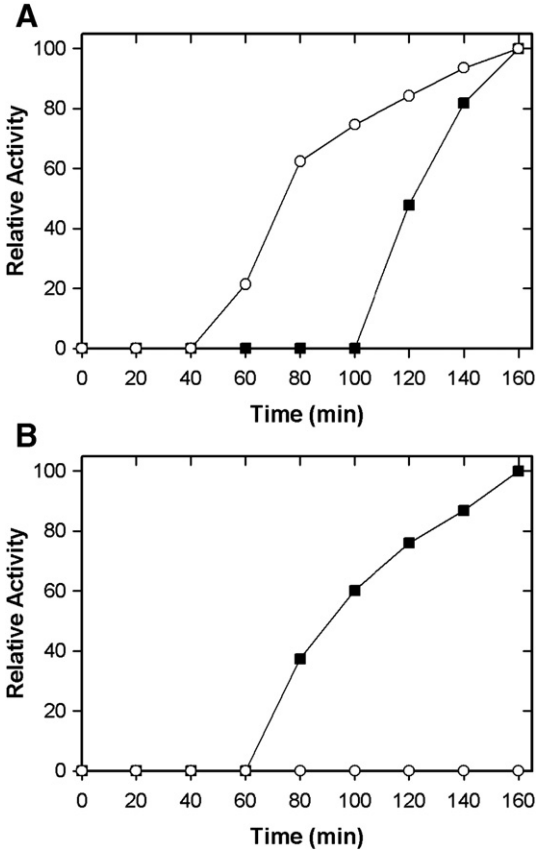

Fig. 2. Time course for the appearance of D-phenylglycine aminotransferase (○) and benzoylformate decarboxylase (■) activity. At $t=0$ the culture of *P. stutzeri* ST-201 was changed to a minimal medium containing either (A) D-phenylglycine or (B) benzoylformate at a concentration of 10 mM. Enzyme activity was measured as described in Materials and methods and normalized to activity at $t=160$ min.

*Ps*BFDC could only be confirmed by purification of the enzyme. This was achieved in a series of steps including ammonium sulfate fractionation, followed by hydrophobic and ion-exchange chromatography. SDS-PAGE analysis suggested a molecular weight of ~55 kDa. Sequencing of the purified enzyme provided an N-terminal sequence of ASVHSITYELLRRQGIDTVFGNP which was employed to generate primers (Table 1) for use in hybridization experiments.

3.2. Construction of subgenomic library and identification of the dpgB and dpgC genes

Southern hybridization of *P. stutzeri* ST-201 genomic DNA which had been digested with *Eco*RI and *Hin*dIII gave a positive band of ca. 5–7 kb. A subgenomic DNA library was constructed and, of 400 recombinant clones, one was positive to colony hybridization. That clone carried a plasmid with a 6-kb insert which was designated as pBCH1. Sequencing of pBCH1 revealed an open reading frame (ORF) of 1581 bp which was denoted *dpgB*, and which encoded a protein of 526 amino acids with a deduced molecular mass of 56 kDa. This was in good agreement with the 55 kDa observed on SDS-PAGE for the BFDC purified from induced *P. stutzeri* ST-201 cells. In addition, the deduced amino acid sequence of the N-terminal 23

amino acids of *dpgB* was identical to that of the native *Ps*BFDC lacking the N-terminal methionine.

BLASTp analysis of the deduced amino acid sequence of *dpgB* revealed significant homology to other bacterial benzoylformate decarboxylases, with the highest sequence identity being 91% to *Pp*BFDC (gi:3915757). Those active site residues implicated in the catalytic mechanism of *Pp*BFDC, including Ser26, Glu47, His70 and His281 [11], were all conserved. Analysis of the DNA sequence upstream of *dpgB* identified a putative ribosome binding site and −10 and −35 promoter regions. No ORFs were identified in the 300-bp sequence upstream from *dpgB* while downstream of the ORF a putative ρ-independent transcriptional terminator was also identified (data not shown). In addition a partial ORF was identified about 250 bp downstream of *dpgB* (Fig. 3A). Overall these results suggested that *dpgB* was transcribed monocistronically, unlike the gene encoding *Pp*BFDC which was arranged and transcribed in the *mdl*CBA operon (Fig. 3B) [8].

In addition to the *Eco*RI–*Hin*dIII digests described above, Southern hybridization of *P. stutzeri* ST-201 genomic DNA digested with *Pst*I also gave a positive band. Colony hybridization with a second subgenomic library identified a clone carrying a plasmid with a 4-kb insert. This plasmid was designated as pBCH2. Sequencing of pBCH2 identified a region which corresponded to part of the *dpgB* gene. However, this insert also carried the full-length ORF of 1311 bp downstream of *dpgB*. The ORF, denoted *dpgC*, was transcribed in the same direction as *dpg*B and encoded a protein of 436 amino acids with a deduced molecular mass of 47.7 kDa.

The evidence for BFDC activity coupled with the observations that *P. stutzeri* ST-201 was able to grow on benzaldehyde

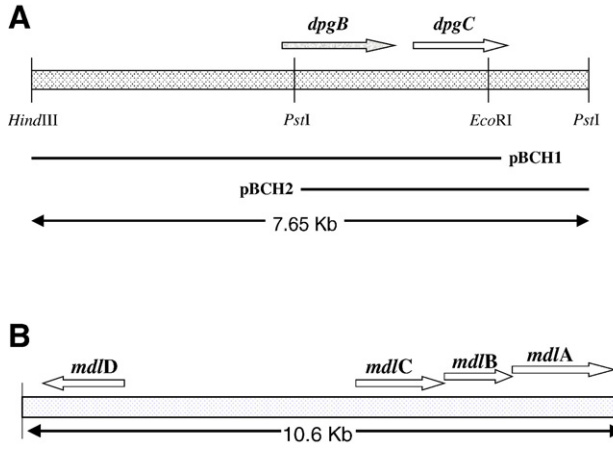

Fig. 3. (A) Restriction fragment of the genomic DNA from *P. stutzeri* ST-201 carrying the genes for benzoylformate decarboxylase (*dpgB*) and benzaldehyde dehydrogenase (*dpgC*). The fragment (7.65 kb) shown is the combination of two overlapping genomic DNA fragments contained in pBCH1 and pBCH2. The arrows show the position and orientation of the genes, and relevant restriction sites are indicated. The sequence of the combined fragment has been deposited under GeneBank accession no. EF419244. (B) Organization of the mandelate pathway genes based on GeneBank accession no. AY143338. Benzoylformate decarboxylase (*mdlC*), *S*-mandelate dehydrogenase (*mdlB*) and mandelate racemase (*mdlA*) make up the *mdlCBA* operon while benzaldehyde dehydrogenase (*mdlD*) is transcribed independently.

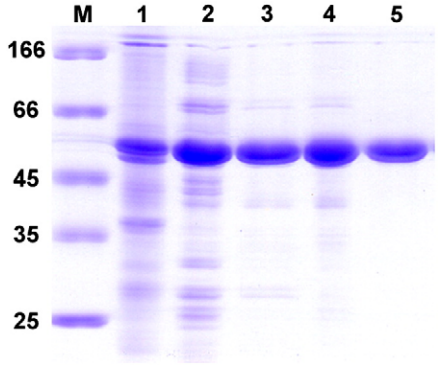

Fig. 4. SDS-PAGE analysis of the recombinant *Ps*BFDC during the purification process. Lanes: M, molecular mass standards (kDa); 1, crude cell lysate; 2, 45-65% ammonium sulfate fraction; 3, following phenyl sepharose chromatography; 4, following ultrafiltration; 5, following Q-Sepharose chromatography.

and that benzoate could be found in the culture medium suggested the likely presence of a BADH. Consequently, it was not surprising when a BLAST search of the full-length amino acid sequence indicated that the *dpgC* gene product was likely to be an aldehyde dehydrogenase, probably of the class 3 type. Dehydrogenases of this class are characterized by the ability to utilize both NAD^+ and $NADP^+$ [27]. The sequence was 86% identical to that of the BADH from *P. putida* ATCC 12633 [26]. The catalytic residues, including the catalytic thiol (Cys249) and the general base (Glu337), were conserved as was the aspartic acid residue (Asp253) that links conserved domains in class 3 aldehyde dehydrogenases [28]. *Ps*BADH also shared 30–40% sequence identity with other aldehyde dehydrogenases from pseudomonads, including the *p*-hydroxybenzaldehyde dehydrogenase from *P. putida* NCIMB 9866 [29]. However, although they are closely related phylogenetically, the other pseudomonad aldehyde dehydrogenases are not class 3 enzymes [27].

3.3. Expression and purification of recombinant PsBFDC

BFDC activity was found in the CFE from IPTG-induced *E. coli* BL21 (DE3) harboring the plasmid pET17b*Ps*BFDC. The majority of the BFDC activity precipitated at 45–65% ammonium sulfate saturation. As shown in Fig. 4, following hydrophobic interaction chromatography, ultrafiltration and ion-exchange chromatography, the enzyme ran as a single band by SDS-PAGE analysis.

The molecular mass of the recombinant enzyme, ~56 kDa, was in good agreement with the molecular mass calculated from the *dpgB* gene sequence. Gel-filtration experiments provided a native molecular mass of ~220 kDa (data not shown). This indicated that BFDC from *P. stutzeri* ST-201 associates as a homotetramer, a characteristic common in bacterial BFDCs [5,13]. The enzyme showed maximum activity at 35–50 °C and at pH 6.0 (data not shown) which was similar to results for the BFDCs from *N. crassa* [7] and *P. putida* [4], respectively.

Michaelis–Menten parameters were determined for *Ps*BFDC under optimal conditions (35 °C and pH 6.0, Table 2). The K_m value for benzoylformate of 0.69 mM was similar to

Table 2
Kinetic parameters for *Ps*BFDC [a]

Enzyme	Temperature (°C)	K_m (mM)	k_{cat} (s^{-1})	k_{cat}/K_m (s^{-1} M^{-1})
wt *Ps*BFDC	35	0.69±0.10	222±3	3.2×10^5
*Ps*BFDC-his	35	0.44±0.07	284±12	6.4×10^5
*Ps*BFDC-his	30	0.43±0.05	213±7	5.0×10^5
*Pp*BFDC-his [b]	30	0.54±0.05	342±13	6.3×10^5

[a] Experiments were carried out at pH 6.0 as described in Materials and methods.
[b] Data from Lingen et al. [17].

Table 3
Kinetic parameters for *Ps*BADH [a]

Variable substrate	Fixed substrate [b]	K_m (app) (μM)	k_{cat} (s^{-1})	k_{cat}/K_m (s^{-1} M^{-1})
Benzaldehyde	NAD^+	7.1±0.6	57±8	8.0×10^6
Benzaldehyde	$NADP^+$	6.9±0.4	6.4±0.4	9.3×10^5
NAD^+	Benzaldehyde	997±111	176±9	1.8×10^5
$NADP^+$	Benzaldehyde	6140±375	40±3	6.5×10^3

[a] Experiments were carried out at 25 °C and pH 8.5 as described in Materials and methods. The data are the mean of at least 3 individual experiments and are reported as ±S.D.
[b] Concentration of the fixed substrate was maintained at 1 mM.

that for *Pp*BFDC which was not surprising given that there is 91% sequence identity between the two enzymes, and those changes in sequence are located at some distance from the active site. However, at 222 s^{-1} the k_{cat} value for *Ps*BFDC was 35% lower than that of *Pp*BFDC even though the latter was determined at a lower temperature (30 °C). ThDP-dependent enzymes are often purified as his_6-tagged variants to avoid loss of activity during multi-step purifications [14,30]. So, to facilitate a more rapid purification, *Ps*BFDC was also prepared with a C-terminal histidine tag, and a homogenous preparation was obtained in a single step (Fig. 5A). This preparation showed an increase in k_{cat} to 284 s^{-1} and a decrease in K_m value to 0.43 mM. At 30 °C *Ps*BFDC had both K_m and k_{cat} values lower than those of its *P. putida* counterpart although the k_{cat}/K_m values were virtually identical (Table 2). Predictably, as suggested by the high sequence identity, preliminary experiments indicate that the substrate range for *Ps*BFDC is unlikely to be different from that of *Pp*BFDC (data not shown).

3.4. Cloning, expression, purification and characterization of benzaldehyde dehydrogenase

The X-ray structure of the class 3 aldehyde dehydrogenase from rat liver [31] shows that the C-terminal residues interact with other regions of the protein whereas the N-terminal residues are fully accessible. Based on these data a N-terminal histidine tag has been successfully employed in this laboratory to purify *Pp*BADH-his. The kinetic constants for this variant were essentially identical to those of the wt enzyme (C. Yeung and M. McLeish, unpublished results). Given the 86% sequence identity between *Pp*BADH and the putative *Ps*BADH it seemed reasonable to use a N-terminal histidine tag to facilitate the purification of the *dpgC* gene product. Accordingly the *dpgC* gene was amplified from pBCH2 and placed in the expression vector pET19b which adds an N-terminal His_{10}-tag. The enzyme was purified in a single step using a nickel affinity column. The purified protein showed a single band on SDS-PAGE with an estimated molecular mass consistent with that calculated from the gene sequence (Fig. 5B).

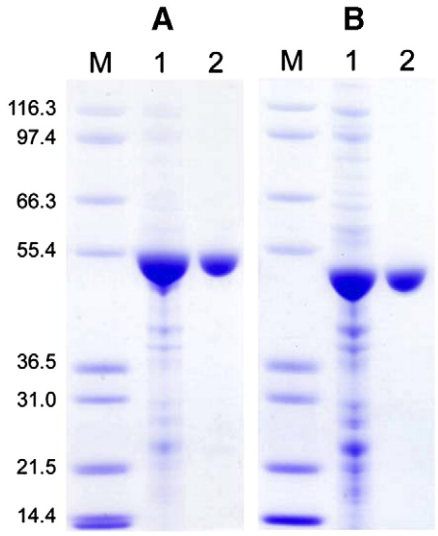

Fig. 5. Single step purification of (A) *Ps*BFDC-his and (B) *Ps*BADH-his. In each case the lanes are: M, molecular mass standards (kDa); 1, crude cell lysate; 2, after His-Select nickel affinity chromatography.

As predicted, the enzyme was able to oxidize benzaldehyde using either NAD^+ or $NADP^+$ as the cofactor. *Ps*BADH prefers NAD^+ over $NADP^+$ which is similar to both the rat aldehyde dehydrogenase [32] and *Pp*BADH [26]. The K_m(app) values for NAD^+ and $NADP^+$ were obtained at saturating benzaldehyde concentration and, therefore, are indicative of the true K_m values. However, for comparison with data for *Pp*BADH [26], K_m(app) values for benzaldehyde were obtained at 1 mM NAD(P)$^+$ which is less than saturating. As with *Pp*BADH, it was likely that benzaldehyde was the natural substrate for *Ps*BADH as its apparent K_m values were in the low micromolar range (Table 3). Overall, in keeping with their relative sequence identities, the kinetic properties of *Ps*BADH and *Pp*BADH are very similar.

4. Conclusions

We have shown that growth of *P. stutzeri* ST-201 on D-phenylglycine results initially in the induction of D-PhgAT and subsequently in the induction of BFDC. Conversely, benzoylformate is only able to induce BFDC. We have cloned and sequenced the *dpgB* and *dpgC* genes and characterized the gene products as a BFDC and a BADH, respectively. The two enzymes share a high degree of sequence identity with the homologous enzymes in the mandelate pathway of *P. putida*. Moreover, their kinetic parameters are similar, suggestive of comparable metabolic roles. It is possible that *Ps*BFDC and *Ps*BADH are components of the mandelate pathway yet *P. stutzeri* ST-201 is unable to utilize mandelate as a carbon

source. Further the genes are organized quite differently. In *P. putida* ATCC 12633, the gene encoding BFDC (*mdlC*) forms part of an operon with those encoding mandelate racemase (*mdlA*) and *S*-mandelate dehydrogenase (*mdlB*), while the BADH gene (*mdlD*) is located upstream of the *mdlCBA* operon and is transcribed in the opposite direction. In *P. stutzeri* ST-201, the BFDC gene (*dpgB*) is independently transcribed, and the BADH gene (*dpgC*) is located downstream of, and transcribed in the same direction as, *dpgB*. Taken together the data suggest that, in combination with D-phenylglycine aminotransferase, the two enzymes form a pathway for the degradation of D-phenylglycine with the product, benzoate, presumably entering the β-ketoadipate pathway [6]. Whether benzoate is initially converted to 4-hydroxybenzoate or to catechol, and whether the subsequent cleavage occurs by the ortho or meta pathway [6,33], is the subject of ongoing experiments.

Acknowledgements

This work is supported in part by the Commission on Higher Education and Faculty of Graduate Studies, Mahidol University, and by the Thailand Research Fund through the Royal Golden Jubilee Ph.D. Program (Grant No.PHD/0023/2548). The work was also supported by the National Science Foundation (EF 0425719).

References

[1] G.A. Sprenger, M. Pohl, Synthetic potential of thiamin diphosphate-dependent enzymes, J. Mol. Catal., B 6 (1999) 145–159.
[2] M.E. Hoey, C.A. Fewson, Is there a mandelate enzyme complex in *Acentobacter calcoaceticus* or *Pseudomonas putida*? J. Gen. Microbiol. 136 (1990) 219–226.
[3] G.D. Hegeman, Synthesis of the enzymes of the mandelate pathway by *Pseudomonas putida*: I. Synthesis of enzymes by the wild type, J. Bacteriol. 91 (1966) 1140–1154.
[4] G.D. Hegeman, Benzoylformate decarboxylase (*Pseudomonas putida*), Methods Enzymol. 17A (1970) 674–678.
[5] M.M. Barrowman, C.A. Fewson, Phenylglyoxylate decarboxylase and phenylpyruvate decarboxylase from *Acinetobacter calcoaceticus*, Curr. Microbiol. 12 (1985) 235–240.
[6] C.A. Fewson, Microbial metabolism of mandelate: a microcosm of diversity, FEMS Microbiol. Rev. 4 (1988) 85–110.
[7] D.N. Ramakrishna Rao, C.S. Vaidyanathan, Metabolism of mandelic acid by *Neurospora crassa*, Can. J. Microbiol. 23 (1977) 1496–1499.
[8] A.Y. Tsou, S.C. Ransom, J.A. Gerlt, D.D. Buechter, P.C. Babbitt, G.L. Kenyon, Mandelate pathway of *Pseudomonas putida*: sequence relationships involving mandelate racemase, (*S*)-mandelate dehydrogenase, and benzoylformate decarboxylase and expression of benzoylformate decarboxylase in *Escherichia coli*, Biochemistry 29 (1990) 9856–9862.
[9] P.M. Weiss, G.A. Garcia, G.L. Kenyon, W.W. Cleland, P.F. Cook, Kinetics and mechanism of benzoylformate decarboxylase using ^{13}C and solvent deuterium isotope effects on benzoylformate and benzoylformate analogues, Biochemistry 27 (1988) 2197–2205.
[10] E.A. Sergienko, J. Wang, L. Polovnikova, M.S. Hasson, M.J. McLeish, G.L. Kenyon, F. Jordan, Spectroscopic detection of transient thiamin diphosphate-bound intermediates on benzoylformate decarboxylase, Biochemistry 39 (2000) 13862–13869.
[11] E.S. Polovnikova, M.J. McLeish, E.A. Sergienko, J.T. Burgner, N.L. Anderson, A.K. Bera, F. Jordan, G.L. Kenyon, M.S. Hasson, Structural and kinetic analysis of catalysis by a thiamin diphosphate-dependent enzyme, benzoylformate decarboxylase, Biochemistry 42 (2003) 1820–1830.
[12] M.S. Hasson, A. Muscate, G.T.M. Henehan, P.F. Guidinger, G.A. Petsko, D. Ringe, G.L. Kenyon, Purification and crystallization of benzoylformate decarboxylase, Protein Sci. 4 (1995) 955–959.
[13] M.S. Hasson, A. Muscate, M.J. McLeish, L.S. Polovnikova, J.A. Gerlt, G.L. Kenyon, G.A. Petsko, D. Ringe, The crystal structure of benzoylformate decarboxylase at 1.6 Å resolution: diversity of catalytic residues in thiamin diphosphate-dependent enzymes, Biochemistry 37 (1998) 9918–9930.
[14] H. Iding, T. Dünnwald, L. Greiner, A. Liese, M. Müller, P. Siegert, J. Grötzinger, A.S. Demir, M. Pohl, Benzoylformate decarboxylase from *Pseudomonas putida* as stable catalyst for the synthesis of chiral 2-hydroxy ketones, Chem. Eur. J. 6 (2000) 1483–1495.
[15] T. Dünnwald, A.S. Demir, P. Siegert, M. Pohl, M. Müller, Enantioselective synthesis of (*S*)-2-hydroxypropanone derivatives by benzoylformate decarboxylase catalyzed C–C bond formation, Eur. J. Org. Chem. (2000) 2161–2170.
[16] P. Dünkelmann, D. Kolter-Jung, A. Nitsche, A.S. Demir, P. Siegert, B. Lingen, M. Baumann, M. Pohl, M. Müller, Development of a donor-acceptor concept for enzymatic cross-coupling reactions of aldehydes: the first asymmetric cross-benzoin condensation, J. Am. Chem. Soc. 124 (2002) 12084–12085.
[17] B. Lingen, J. Grötzinger, D. Kolter, M.R. Kula, M. Pohl, Improving the carboligase activity of benzoylformate decarboxylase from *Pseudomonas putida* by a combination of directed evolution and site-directed mutagenesis, Protein Eng. 15 (2002) 585–593.
[18] B. Lingen, D. Kolter-Jung, P. Dünkelmann, R. Feldmann, J. Grötzinger, M. Pohl, M. Müller, Alteration of the substrate specificity of benzoylformate decarboxylase from *Pseudomonas putida* by directed evolution, Chembiochem. 4 (2003) 721–726.
[19] P. Siegert, M.J. McLeish, M. Baumann, H. Iding, M.M. Kneen, G.L. Kenyon, M. Pohl, Exchanging the substrate specificities of pyruvate decarboxylase from *Zymomonas mobilis* and benzoylformate decarboxylase from *Pseudomonas putida*, Prot. Eng. Des. Sel. 18 (2005) 345–357.
[20] H. Henning, C. Leggewie, M. Pohl, M. Müller, T. Eggert, K.E. Jaeger, Identification of novel benzoylformate decarboxylases by growth selection, Appl. Environ. Microbiol. 72 (2006) 7510–7517.
[21] S. Wiyakrutta, V. Meevootisom, A stereo-inverting D-phenylglycine aminotransferase from *Pseudomonas stutzeri* ST-201: purification, characterization and application for D-phenylglycine synthesis, J. Biotechnol. 55 (1997) 193–203.
[22] J.D. Beggs, C.A. Fewson, Regulation of synthesis of benzyl alcohol dehydrogenase in *Acinetobacter calcoaceticus* NCIB8250, J. Gen. Microbiol. 103 (1977) 127–140.
[23] M.M. Bradford, A rapid and sensitive method for the quantitation of microgram quantities of protein utilizing the principle of protein-dye binding, Anal. Biochem. 72 (1976) 248–254.
[24] C.N. Pace, F. Vajdos, L. Fee, G. Grimsley, T. Gray, How to measure and predict the molar absorption coefficient of a protein, Protein Sci. 4 (1995) 2411–2423.
[25] T. Rojanarata, Genetic engineering of D-phenylglycine aminotransferase to facilitate immobilization and maximize catalytic performance, PhD thesis, Mahidol University, 2004.
[26] M.J. McLeish, M.M. Kneen, K.N. Gopalakrishna, C.W. Koo, P.C. Babbitt, J.A. Gerlt, G.L. Kenyon, Identification and characterization of a mandelamide hydrolase and an NAD(P)+-dependent benzaldehyde dehydrogenase from *Pseudomonas putida* ATCC 12633, J. Bacteriol. 185 (2003) 2451–2456.
[27] J. Perozich, H. Nicholas, B.C. Wang, R. Lindahl, J. Hempel, Relationships within the aldehyde dehydrogenase extended family, Protein Sci. 8 (1999) 137–146.
[28] J. Hempel, I. Kuo, J. Perozich, B.C. Wang, R. Lindahl, H. Nicholas, Aldehyde dehydrogenase. Maintaining critical active site geometry at motif 8 in the class 3 enzyme, Eur. J. Biochem. 268 (2001) 722–726.
[29] C.N. Cronin, J. Kim, J.H. Fuller, X. Zhang, W.S. McIntire, Organization and sequences of *p*-hydroxybenzaldehyde dehydrogenase and other plasmid-encoded genes for early enzymes of the *p*-cresol degradative

pathway in *Pseudomonas putida* NCIMB 9866 and 9869, DNA Seq. 10 (1999) 7–17.

[30] M. Pohl, P. Siegert, K. Mesch, H. Bruhn, J. Grötzinger, Active site mutants of pyruvate decarboxylase from *Zymomonas mobilis*—a site-directed mutagenesis study of L112, I472, I476, E473, and N482, Eur. J. Biochem. 257 (1998) 538–546.

[31] Z.J. Liu, Y.J. Sun, J. Rose, Y.J. Chung, C.D. Hsiao, W.R. Chang, I. Kuo, J. Perozich, R. Lindahl, J. Hempel, B.C. Wang, The first structure of an aldehyde dehydrogenase reveals novel interactions between NAD and the Rossmann fold, Nat. Struct. Biol. 4 (1997) 317–326.

[32] J. Perozich, I. Kuo, B.C. Wang, J.S. Boesch, R. Lindahl, J. Hempel, Shifting the NAD/NADP preference in class 3 aldehyde dehydrogenase, Eur. J. Biochem. 267 (2000) 6197–6203.

[33] C.E. Cowles, N.N. Nichols, C.S. Harwood, BenR, a XylS homologue, regulates three different pathways of aromatic acid degradation in *Pseudomonas putida*, J. Bacteriol. 182 (2000) 6339–6346.

BIOGRAPHY

NAME	Mr. Choedchai Saehuan
DATE OF BIRTH	May 14, 1967
PLACE OF BIRTH	Uttaradit, Thailand
INSTITUTIONS ATTENDED	Chiangmai University, 1985-1988: Bachelor of Science (Medical Technology) (First Class Honor) Mahidol University, 2000-2007: Doctor of Philosophy (Microbiology)
HOME -ADDRESS	202**,** Moo 3, Mahatart Road, Tumbol Naimuang, Amphur Pichai, Uttaradit, Thailand 53120
SCHOLARSHIPS	- Institutional Strengthening Programme, Faculty of Science, Mahidol University, 2000-2002 - Thesis Scholarship, The Commission on Higher Education and Faculty of Graduate Studies, Mahidol University, 2004 - Royal Golden Jubilee Ph.D. Programme, Thailand Research Fund, 2005-2007

PUBLICATION

1. Choedchai Saehuan, Theerasak Rojanarata, Suthep Wiyakrutta, Michael J. McLeish and Vithaya Meevootisom. Isolation and characterization of a benzoylformate decarboxylase and a $NAD^+/NADP^+$-dependent benzaldehyde dehydrogenase involved in D-phenylglycine metabolism in *Pseudomonas stutzeri* ST-201. Biochim Biophys Acta, 1770 (2007), 1585-1592.